Vol. 57 • No. 10
October 2014

Microwave Journal .com

mmWave Connected UAVs Enable Gigabit Mobile Network

MVP
NI
PXI SA

horizon house®
Founded in 1958


MCL B 744
ADP-2-10
MCL B 744
ADP-2-10
MCL B 744
ADP-2-10

Yeah, we do that.
TX
RX
Repeater Dilemma
that must be resolved.
Trying to send and
receive a small signal
among big interferers on
your repeater platform?
We should talk.
513.870.4087
mPG
POLE ZERO
A DOVER COMPANY
www.polezero.com

From Surface Mount Components
to Complex Testrack Assemblies
K&L
MICROWAVE
A DOVER COMPANY
In Touch with your Filtering Solutions
Microwave Products Group
BSC FILTERS • DOW-KEY MICROWAVE • K&L MICROWAVE • POLE/ZERO
www.klmicrowave.com • www.filterwizard.com • 410-749-2424 • sales@klmicrowave.com

The Future of Military Ka-band Is Here

Ground to Space & Everywhere Between

Teledyne Microwave Solutions **delivers the most comprehensive Ka-Band Microwave RF solutions.**

NEW!
Ka-band MIL-BUC & MIL-LNB

- *Suitable for terrestrial and airborne applications*
- *Interfaces directly to flat plate antenna or OMT*
- *Switch between any two 1 GHz Ka sub-bands (standard is 29-30 & 30-31GHz)*
- *Ultra-lightweight and power-efficient*
- *Hermetically sealed for high-reliability*

NEW!
500 Watt Ka-band TWTA

- *Integral BUC*
- *502W Peak Power*
- *IP/Serial M&C*
- *MIL & Commercial Bands*
- *Compact Size*
- *Built around Teledyne MEC-5530 TWT*

Ka-band Compact Outdoor SSPA

- *30-31 GHz*
- *Integral BUC*
- *Passes WGS certification*
- *Exported as EAR-99*

10 Watt Ka-band vBUC

- *8 watts Linear Power*
- *10 lbs*
- *IP/Serial/FSK M&C*
- *MIL & Commercial Bands*
- *Optional AC Power Supply*

TELEDYNE
MICROWAVE SOLUTIONS
Everywhere**you**look™

11361 Sunrise Park Drive
Rancho Cordova, CA 95742
T: 916.636.7423

teledynemicrowave.com
microwavesolutions@teledyne.com

Microwave Journal

CONTENTS

October 2014
Vol. 57 • No. 10
Government and Military Electronics
mwjournal.com

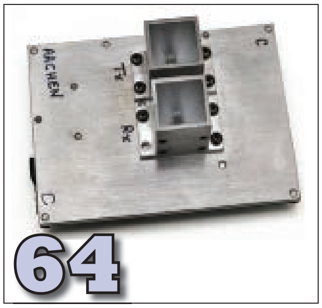

Cover Feature

MVP: Most Valuable Product

Technical Features

Special Report

AUGMENTED REALITY: HOW IT WORKS

STEP 1
Download the free Layar app from the iTunes (iOS) or Google Play (Android) store.

STEP 2
Launch the app to view enhanced content on any page with the layar logo.

STEP 3
Frame the entire page in the screen and tap to experience enhancements (tap screen again for full screen view).

Refer to page 176 for this month's participants

AR pages may expire after 60 days.

57 YEARS OF PUBLISHING EXCELLENCE

Microwave Journal CONTENTS

mwjournal.com

Product Features

Tech Briefs

Departments

Microwave Journal (USPS 396-250) (ISSN 0192-6225) is published monthly by Horizon House Publications Inc., 685 Canton St., Norwood, MA 02062. Periodicals postage paid at Norwood, MA 02062 and additional mailing offices.

POSTMASTER: Send address corrections to *Microwave Journal*, PO Box 3256, Northbrook, IL 60065-3256 or e-mail mwj@omeda.com. Subscription information: (847) 291-5216. This journal is issued without charge upon written request to qualified persons working in the RF & microwave industry. Other subscriptions are: domestic, $120.00 per year, two-year subscriptions, $185.00; foreign, $200.00 per year, two-year subscriptions, $370.00; back issues (if available) and single copies, $10.00 domestic and $20.00 foreign. Claims for missing issues must be filed within 90 days of date of issue for complimentary replacement.

STAFF

Publisher: Carl Sheffres
Editor: Patrick Hindle
Technical Editor: Gary Lerude
Managing Editor: Jennifer DiMarco
Associate Technical Editor: Cliff Drubin
Multimedia Staff Editors: Barbara Walsh and Leslie Nikou
Consulting Editor: Harlan Howe, Jr.
Consulting Editor: Frank Bashore
Consulting Editor: David Vye
Consulting Editor: Raymond Pengelly
Web Editor: Chris Stanfa
Client Services Manager: Kristen Anderson
Audience Development Manager: Carol Spach
Traffic Manager: Edward Kiessling
Director of Production & Distribution: Robert Bass
Art Director: Janice Levenson
Graphic Designer: Sachiko Stiglitz

EUROPE

International Editor: Richard Mumford
Office Manager: Nina Plesu

CORPORATE STAFF

CEO: William M. Bazzy
President: Ivar Bazzy
Vice President: Jared Bazzy

Executive Editorial Office

685 Canton Street, Norwood, MA 02062
Tel: (781) 769-9750
FAX: (781) 769-5037
e-mail: mwj@mwjournal.com

European Editorial Office

16 Sussex Street, London SW1V 4RW, England
Tel: Editorial: +44 207 596 8730 Sales: +44 207 596 8740
FAX: +44 207 596 8749

Subscription Services

Send subscription inquiries and address changes to:
Tel: (847) 291-5216
e-mail: mwj@omeda.com

BPA WORLDWIDE

www.mwjournal.com

Printed in the USA

Microwave Journal Online

Scan page using layar app

Visit us @ mwjournal.com

eLEARNING free webinars

VCO Fundamentals
Sponsored by: Mini-Circuits 10/7

Lightning and EMP Protection in Buildings
Presented by: CST 10/9

Simulation of Accelerator Components
Presented by: CST 10/16

Introduction to Radar
Sponsored by: Eastern OptX 10/21

Techniques for Characterizing Spurious Signals
Presented by: Keysight Technologies 10/21

Single Sweep 70 kHz to 145 GHz Broadband System and On-Wafer Measurements
Presented by: Anritsu 10/22

Designing Clean Mobile Electronic Devices – Mobile Phones and Automobile Systems
Presented by: CST 10/23

High Frequency Materials and Characterization up to Millimeter Wave Frequencies
Presented by: Rogers Corp. 10/23

Characterization and Test Challenges for MMPAs with ET & DPD
Presented by: Keysight Technologies 10/30

Power Delivery Network (PDN) Analysis
Presented by: CST 10/30

Web Survey

Will RF industry consolidation continue?

Look for our multiple choice survey online at mwjournal.com

August Survey

When do you think nano satellites will take flight?

This year [25 votes] (16%)

1-3 years [56 votes] (36%)

3-5 years [59 votes] (38%)

Not in my lifetime [14 votes] (9%)

Executive Interviews

Bob Bruggeworth, CEO of the recently combined **RFMD** and **TriQuint** company, **Qorvo**, discusses the company's strategy and goals going forward as they launch into a new identity. Read one of the first interviews from this newly formed entity.

Terry Jarnigan, CEO of **Pasternack**, discusses how the company's standard products have expanded well beyond cables and passive devices. He also highlights the company's other offerings such as applications assistance and superior customer service.

WHITE PAPERS

ar — 50S1G6AB Solid State Amplifier - 50 Watts CW, 1 to 6 GHz

RichardsonRFPD An Arrow Company / Arrow RF & Power — Overview of Microsemi's New Line of RF Monolithic Microwave Integrated Circuit Devices

.COM

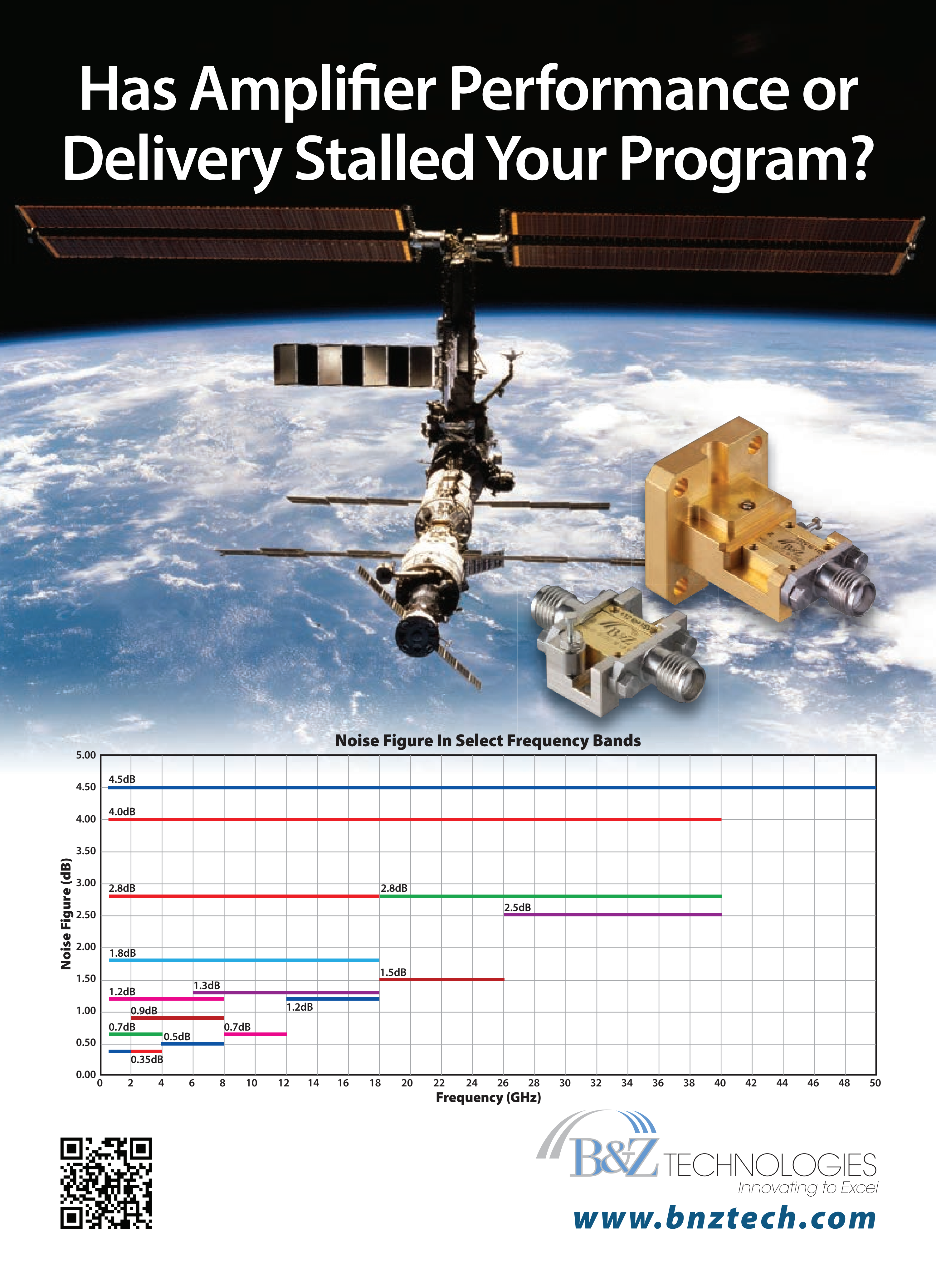

Has Amplifier Performance or Delivery Stalled Your Program?
Noise Figure In Select Frequency Bands
Noise Figure (dB)
5.00
4.50
4.00
3.50
3.00
2.50
2.00
1.50
1.00
0.50
0.00
4.5dB
4.0dB
2.8dB
2.8dB
2.5dB
1.8dB
1.5dB
1.3dB
1.2dB
1.2dB
0.9dB
0.7dB
0.7dB
0.5dB
0.35dB
0 2 4 6 8 10 12 14 16 18 20 22 24 26 28 30 32 34 36 38 40 42 44 46 48 50
Frequency (GHz)
B&Z TECHNOLOGIES
Innovating to Excel
www.bnztech.com

NOVEMBER 2014

SUNDAY	MONDAY	TUESDAY	WEDNESDAY	THURSDAY	FRIDAY	SATURDAY
26	27	28	29	30	31	1
2	3	4 **APMC 2014** **Asia-Pacific Microwave Conference** Sendai, Japan	5	6 **Webinar:** **EMC Simulation in Modern Electronics** Sponsored by CST **Webinar:** **MMIC Design Overview** Sponsored by AWR	7	8
9	10	11	12 **electronica 2014** München, Germany **Webinar:** **Passive Components** Sponsored by Mini-Circuits	13 **Webinar:** **Efficient Simulation of Optical Devices** Sponsored by CST **Webinar:** **Improving Microwave Circuits with High Thermal Conductivity (HTC) Materials** Sponsored by Rogers Corporation	14	15
16	17	18	19	20 **Webinar:** **3D EM Modeling of a DDR4 Memory Channel** Sponsored by CST	21	22
23	24	25 **Webinar:** **Modeling Material Properties Based on Measured Data** Sponsored by CST	26	27	28	29
30	1	2	3	4	5	6

Visit mwjournal.com/events

Coming**Events**

CALL FOR PAPERS

EDI CON 2015
October 31, 2014

IMS 2015
December 8, 2015

WAMICON 2015
January 5, 2015

mwjournal.com

OCTOBER

AMTA 2014
36th Antenna Measurement Techniques Association Meeting & Symposium
October 12–17, 2014 • Tucson, Ariz.
www.amta2014.org

ITC/USA 2014
October 20–23, 2014 • San Diego, Calif.
www.telemetry.org

MWP/APMP 2014
International Topical Meeting on Microwave Photonics (MWP)
9th Asia-Pacific Microwave Photonics Conference (APMP)
October 20–23, 2014 • Sapporo, Japan
www.mwp2014.com

IME/China 2014
9th International Conference & Exhibition on Microwave and Antenna
October 29–31, 2014 • Shanghai, China
www.imwexpo.com

NOVEMBER

APMC 2014
Asia-Pacific Microwave Conference
November 4–7, 2014 • Sendai, Japan
www.apmc2014.org

electronica 2014
November 11–14, 2014 • München, Germany
www.electronica.de

DECEMBER

Precise Time and Time Interval Systems and Applications
December 1–4, 2014 • Boston, Mass.
www.ion.org/ptti

ARFTG 84th Microwave Measurement Conference
December 2–5, 2014 • Boulder, Colo.
www.arftg.org

IMaRC 2014
IEEE MTT-S International Microwave and RF Conference
December 15–17, 2014 • Bangalor, India
www.imarc-ieee.org

JANUARY 2015

RWW 2015
Radio and Wireless Week
January 25–28, 2015 • San Diego, Calif.
www.radiowirelessweek.org

DesignCon
January 27–30, 2015 • Santa Clara, Calif.
www.designcon.com

MARCH

Mobile World Congress
March 2–5, 2015 • Barcelona, Spain
www.mobileworldcongress.com

Satellite 2015
March 16–19, 2015 • Washington, DC
www.satshow.com

APRIL

WAMICON 2015
IEEE Wireless and Microwave Technology Conference
April 13–15, 2015 • Cocoa Beach, Fla.
www.wamicon.org

EDI CON 2015
Electronic Design Innovation Conference
April 14–16, 2015 • Beijing, China
www.ediconchina.com

MAY

RFIC 2015
IEEE Radio Frequency Circuits Symposium
May 17–19, 2015 • Phoenix, Ariz.
www.rfic-ieee.org

IMS 2015
IEEE MTT-S International Microwave Symposium
May 17–22, 2015 • Phoenix, Ariz.
www.ims2015.org

85th ARFTG Microwave Measurement Symposium
May 22, 2015 • Phoenix, Ariz.
www.arftg.org

Cover Feature
Invited Paper

DARPA's Mobile Hotspot Program Drives E-Band Performance Benchmarks

Joe Chandler
Millitech (Smiths Microwave), Northampton, Mass.
R. William Steagall
L-3 Communication Systems-West, Salt Lake City, Utah

DARPA's Mobile Hotspots Program seeks to provide high-bandwidth communications for troops in remote forward operating locations. The program goal is to demonstrate a scalable, mobile, self-forming and managing network of millimeter-wave air-to-air and air-to-ground gigabit class data links. The concept as depicted in ***Figure 1*** is moving closer to a reality as the program progresses through Phase 2. It is a new, complex system that will maintain this network in the sky utilizing a fleet of small UAVs. Advanced millimeter-wave pointing, acquisition and tracking (PAT) technologies are needed to provide high connectivity among the UAVs and ultimately to the ground nodes.

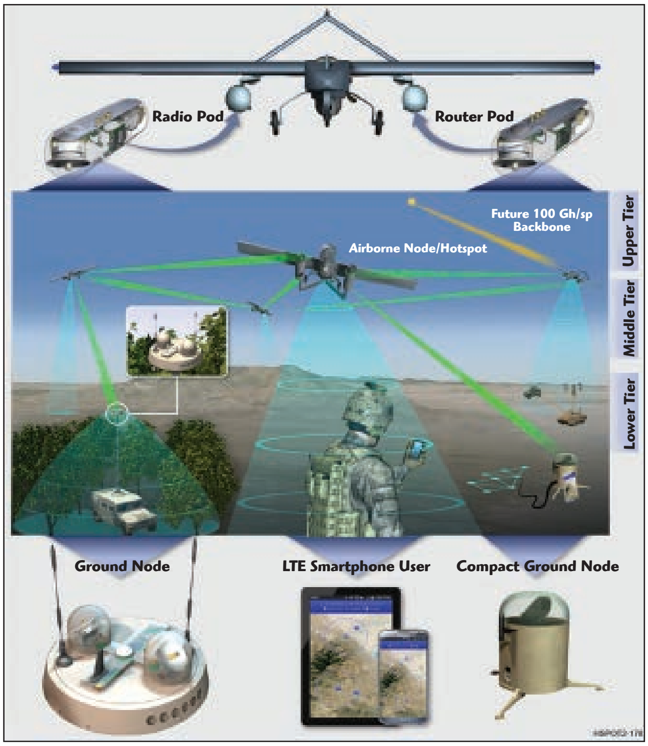

▲ *Fig. 1 MHS conceptual diagram.*

The Mobile Hotspot Program sought to capitalize on the technology base already initiated by the allocation of the E-Band spectrum for telecom use which included both maturing and emerging technologies. The prospect of a viable military application drew wide interest from industry. Phase 2 of the Mobile Hotspots Program is now underway to carry forward the successes of Phase 1. Among these successes are new performance benchmarks for the millimeter-wave elements.

Millitech is on a team led by L-3 Communication Systems - West. Key technology advances at E-Band, as demonstrated by Millitech, are directly related to the underlying Phase 1 technical advances of BAE Systems and HRL Laboratories for their respective LNAs and GaN power device capabilities. In addition to L-3 (team lead), Millitech, BAE Systems, and HRL, other members of the team include MaXentric Technologies LLC with responsibility for soft-

COAXIAL AND WAVEGUIDE SWITCHES

RLC has the exact solution you're looking for.

RLC Electronics manufactures a complete range of RF switches including coaxial in the frequency range from DC to 65 GHz and rectangular or double ridge waveguide. The operating modes on all designs are failsafe, latching and manual.

Control options are DC voltages as low as 5V, TTL, BCD, RS232, and RS422. All switches have excellent repeatability and lifetimes in excess of one million operations. Many types are QPL listed per MIL-DTL-3928.

- SPDT to SP12T
- Transfer
- Low VSWR
- High Isolation
- Low Insertion Loss
- High Power
- Low Passive Intermodulation
- Surface Mount Options

For more detailed information on coaxial and waveguide switches, visit our web site.

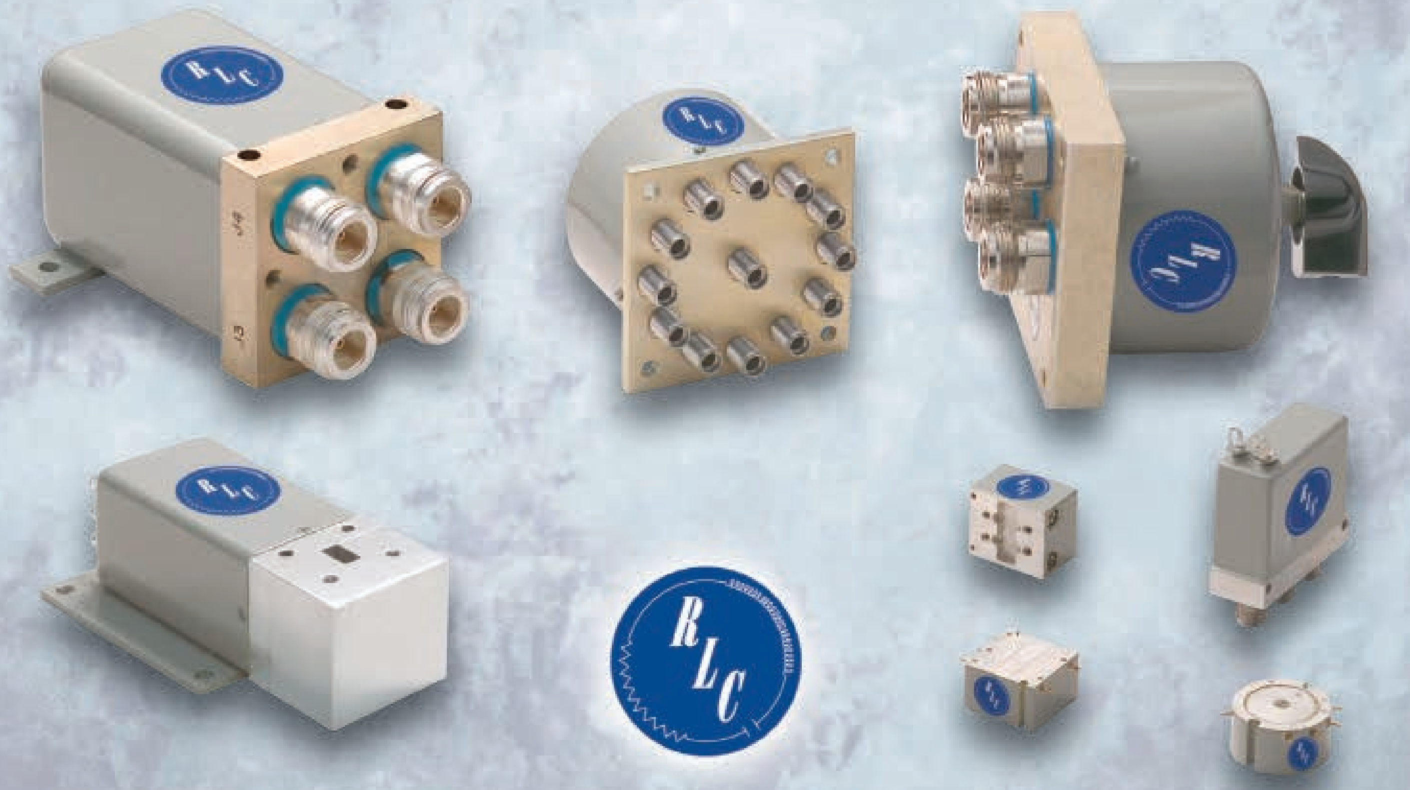

RLC ELECTRONICS, INC.

83 Radio Circle, Mount Kisco, New York 10549 • Tel: 914.241.1334 • Fax: 914.241.1753
E-mail: sales@rlcelectronics.com • www.rlcelectronics.com

ISO 9001:2000 CERTIFIED

VISA MasterCard

RLC is your complete microwave component source...
Switches, Filters, Power Dividers, Terminations, Attenuators, DC Blocks, Bias Tees & Detectors.

ware defined modem hardware (the waveform software itself is provided by L-3), IMSAR is managing the antenna pedestal, and Zivko Aeronautics Inc. is handling radomes and pod structures.

SYSTEM/SUBSYSTEM OVERVIEW

The Mobile Hotspots airborne segment (see ***Figure 2***), is being designed to operate on the SRQ-7 UAV platform commonly known as the Shadow. The Shadow is a “small” UAV which introduces a suite of advantages and disadvantages. The Shadow is easy to deploy and a much more cost effective choice for a platform than larger UAVs. The more UAVs or nodes introduced to the field, the more robust the network. However, the small size introduces challenges for size, weight and power (SWAP).

The key functional subsystems of the UAV mounted equipment are: the GPS & IMU, network router, discovery radio, LTE networking equipment and the millimeter-wave (mmWave) radios. These subsystems work together to enable the robust PAT function required by the highly directional mmWave radio links. Additionally, highly efficient power supplies and creative cooling techniques are also needed to realize the mission.

Essentially all of the Mobile Hotspot’s equipment in the L-3 design will be packaged into two underwing pods with the discovery and LTE antennas located at the wingtips and in the tail sections for isolation and spatial performance. Each pod contains several RF subsystems. Each pod contains two gimbaled mmWave radios, fore and aft; GPS antennas and IMUs; as well as associated power supplies. A total of four mmWave radios will provide the gigabit directional links with as wide an operating field-of-view (FOV) as possible. The remaining functions are split between pods, the primary network router in one and the discovery and LTE subsystems in the other – resulting in a good balance of weight and power between the two pods. Nominally, the mass of each pod is about 10 to 12 kg and each requires about 200 to 500 W depending on the operating mode. The size limitation of the pods is well established and realization is expected to be relatively low risk. Continued effort remains to contain the weight and power and drive the overall SWAP performance to provide operating margin to the Shadow.

In addition to the airborne equipment, there will be stationary ground-based nodes both mobile and compact deployable, as well as portable commercial LTE devices. The ground based nodes will be fully functional gigabit nodes similar in content to the

▲ *Fig. 2 Airborne equipment description.*

pods but also providing access in and out of the network.

NETWORKING OVERVIEW

Industry has invested significant resources in developing methods of creating networks and ways to get data to its intended destinations. These methods have been proven to be effective and reliable. However, traditional approaches assume links that are highly reliable and topologies that are relatively stable, such as fiber optic based connections. When attempting to apply these standard approaches to a wireless ad hoc airborne and ground-based backbone network, the links are not as reliable as wired solutions, and the topology is continuously changing – producing less than desirable results. A goal of the program is to add wedge solutions to industry standard networking protocol stacks to overcome these shortcomings and add additional features to account for the requirements of military users.

This challenging scenario requires development and implementation of many features and capabilities not only at the link level but with regard to routing and provisioning as well. These include methods of: correcting bit errors and accounting for missed packets before higher layer protocols become aware of them; allowing routes to change quickly and often in order for data packets to efficiently reach their destination; and tolerating and accounting for constantly changing links. Since the gigabit backbone depends on directional links that have limited angles of regard, where these directional links should be pointed and when they might be reaching limits of field of regard and range also needs to be managed. Optimizing how nodes are connected in order to make data transfers efficient and minimize hops, managing data flows to ensure the optimal performance to users and perhaps most importantly, supporting data from and to outside ports are all essential tools for success.

Implementation of Mobile Hotspots is a marvel when these demands on the management of the backbone network are fully appreciated, further recognizing that the network is autonomous and self-forming as new nodes are deployed or replaced. The ability to then tie in and extend the network with LTE will enable multiple "Hotspots" over 1,000 square miles of area to be connected within hours. For the user, these features create a virtual network with high availability that provides a broadband Internet-like experience, leveraging the millimeter-wave gigabit links as the core transport mechanism.

POINTING, ACQUISITION & TRACKING (PAT)

The ability to maintain highly directional mmWave links is the key to the success of the system. These paths must be reliable and stable to support gigabit links via antenna gains of nominally 40 dB and corresponding beamwidths of ~2 degrees. Supporting subsystems including the GPS/IMU and discovery radios contribute to achieving successful open loop link acquisition however, closed loop tracking is necessary to maintain robust links of this mobile environment. Each antenna is provisioned with tracking features to enable closed loop control.

mmWave RADIOS

The mmWave radios require state of the art performance to enable the envisioned capacity and range. Performance is dominated by the basic link budget elements: transmit power, receiver noise figure, data rate (bandwidth & SNR) and antenna gain. Millitech demonstrated under Phase 1 amplifier module output power and amplifier module noise figure performance values that are now the baseline going forward.

The original objective of the power amplifier was to demonstrate 10 W (20 W goal) in each of the two E-Band allocations, 71 to 76 and 81 to 86 GHz. Millitech proposed use of HRL's then in-process second generation GaN MMICs allowing for the potential to incorporate any suitable device should the opportunity arise. The approach was to design an integrated, highly efficient power combining scheme which we had been refined from spaceborne applications over recent years. Millitech had already demonstrated 0.7 dB of total loss divide and combined for an eight-way or 0.35 dB of combining loss (92 percent efficiency) Measured results are shown in ***Figure 3***.

The final results of this Phase 1 activity resulted in the power amplifier performance exceeding the requirement for both the lower and upper allocation and approaching the 20 W goal by delivering 17 W at 74 GHz with nearly 25 percent PAE (see ***Figure 4***). Note that the PAE figures include DC bias distribution. In addition to power and efficiency, size was another critical SWAP parameter. Each complete SSPA module was about the size of an iPhone with dimensions of 2.2" × 3.7" × 0.5" overall (<4.0 in^3) (see ***Figure 5***).

As part of Phase 1, BAE implemented their 50 nm mHEMT process in the design of a single LNA to cover both of the E-Band allocations. Millitech was enlisted by BAE to demonstrate the mounted-in-module performance.

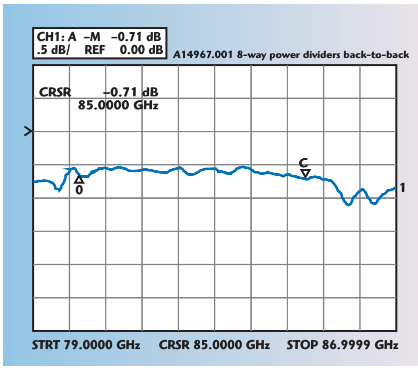

Fig. 3 Millitech back-to-back WR-12 combiner loss.

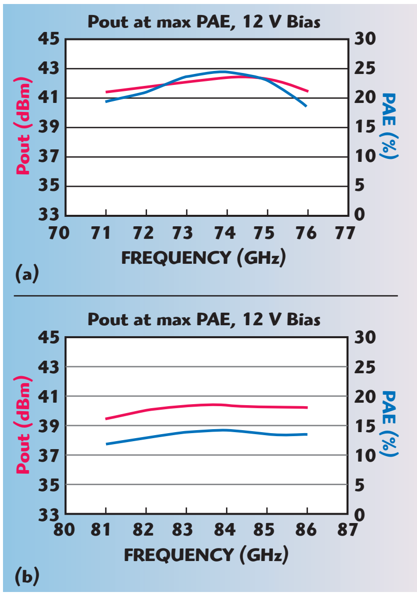

Fig. 4 Power amplifier results from Phase 1, lower E-Band (a) and upper E-Band (b).

Redefining RF and Microwave Instrumentation

with open software and modular hardware

Scan page using layar app

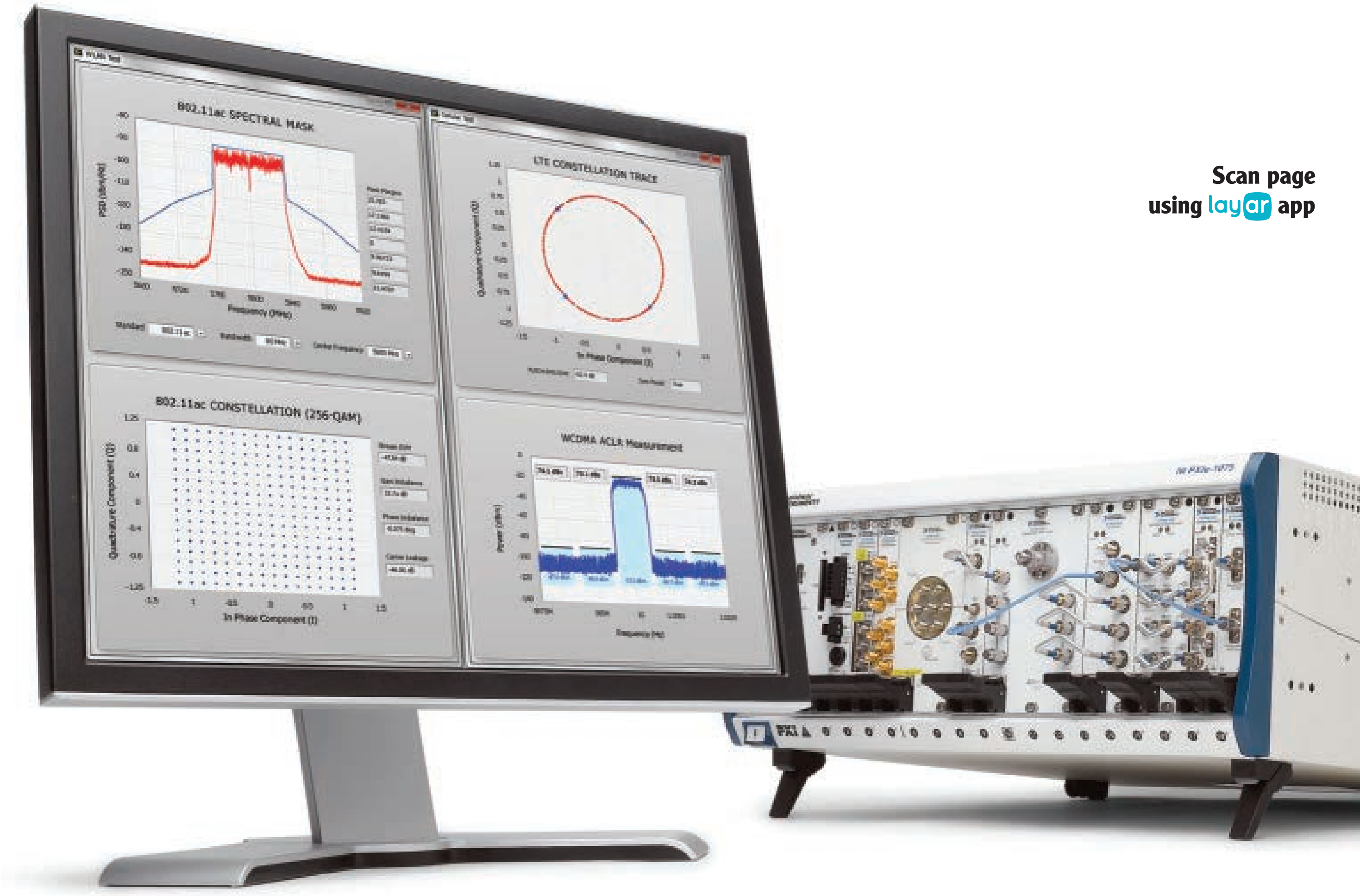

Achieve speed, accuracy, and flexibility in your RF and microwave test applications by combining National Instruments open software and modular hardware. Unlike rigid traditional instruments that quickly become obsolete by advancing technology, the system design software of NI LabVIEW coupled with NI PXI hardware puts the latest advances in PC buses, processors, and FPGAs at your fingertips.

WIRELESS TECHNOLOGIES

National Instruments supports a broad range of wireless standards including:

LTE
802.11a/b/g/n/ac
WCDMA/HSPA/HSPA+
GSM/EDGE
CDMA2000/EV-DO
Bluetooth

>> Learn more at ni.com/redefine

800 813 5078

NATIONAL INSTRUMENTS™

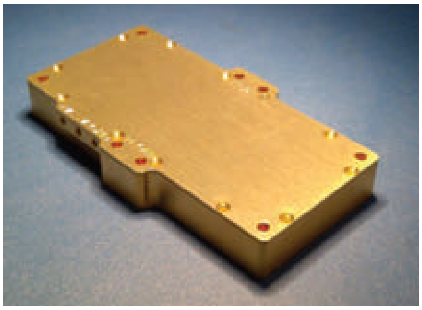

Fig. 5 *E-Band PA module from Phase 1.*

The results exceeded expectations, demonstrating the best seen MMIC based noise figures across very wide bandwidths. Nominally 2 dB noise figure was measured in each allocation at room temperature. A very flat gain response was measured to be below 2 dB in the 71 to 76 GHz allocation (see ***Figure 6***). Worth noting is that the noise figure and gain behaved well and were maintained down to 40 GHz.

These accomplishments represent new industry performance benchmarks for solid state power capability and noise figure. Millitech looks forward to repeating and even enhancing this performance during phase 2. This work in mmWave performance, fostered by DARPA, will also provide substantial benefit to commercial mmWave communications.

ANTENNA DESIGN

The antenna gain is the remaining millimeter-wave performance element to highlight. Given the effort put forth to achieve the power and noise figure capability described, it stands to reason that a conventionally efficient antenna would undermine the effort. A conventional Cassegrain topology and even low or no blockage apertures with Gaussian illumination would typically struggle to achieve 50 percent efficiency across the frequency of operation for Mobile Hotspots, particularly when the aperture size is less than 50λ.

The overlying challenge of fitting within the pod structure, further constrained by the swept volume of the gimbal for steering; maintaining low mass to reduce the burden of the steering mechanisms while maximizing the aperture size and efficiency resulted in Millitech and L-3 selecting a shaped optics reflector topology. Similar to a Cassegrain in appearance, but with vastly different optics, as shown in ***Figure 7***, it is commonly referred to as an Axial

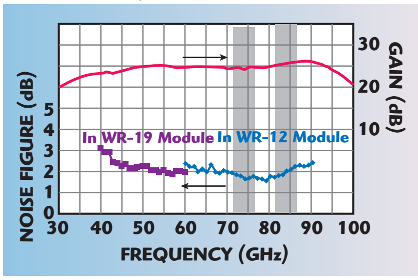

Fig. 6 *WR-12 LNA module results using mHEMT LNA.*

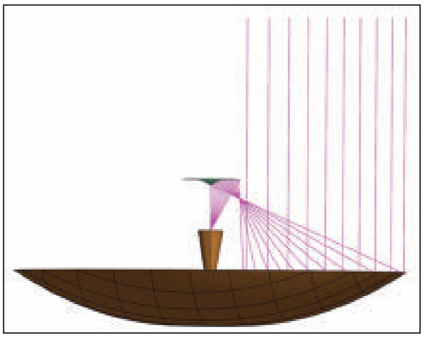

Fig. 7 *ADE ray trace.*

Displaced Ellipse (ADE). Through the use of today's standard for modelling techniques, Millitech is modelling 65 percent aperture efficiency relative to the diffraction limit for the antenna aperture including feed losses and all blockages which is consistent with results we have measured at other frequencies.

An ADE topology creates a focal ring in lieu of a typical focal point. The result is the peak illumination in a ring outside of the sub-reflector and very low illumination to the blocked areas. Additional losses of the polarizer and tracking features are minimized to less than 1 dB. Compiling an arbitrary link budget for the nominal performance benchmarks, it shows that in clear weather an air-to-air link can be made across 60 km as shown in ***Table 1***. A 60 km node separation is an indication of the scale of area coverage attainable by Mobile Hotspots.

TABLE I

REPRESENTATIVE LINK BUDGET AND RANGE

TTX Power	40 dBm
TX Antenna Gain	38 dB
FSL (1 km)	130 dB
Atmospheric Loss	0.25 dB/km
Noise Figure	3 dB
RX Antenna Gain	38 dB
Carrier BW	1 GHz
SNR min	15 dB
Clear weather link range	**~ 60 km**

FUTURE DEVELOPMENTS

There are other technology advancements being pursued by industry. Advances in SiGe and CMOS are being made at a great pace and the technology was successfully utilized for Phase 1 of the Mobile Hotspots. In time, most of the millimeter-wave and modem functionality is likely to be replaced by a few highly integrated, low cost chips. It is also likely that the power and low noise standards established by GaN and mHEMT technologies will prove dominant for several years to come.

While the ongoing technology advancement at E-Band was instrumental in Mobile Hotpots, the program will continue to advance the performance standards which will no doubt have a direct effect on the future capability of commercial E-Band telecom products and other millimeter-wave applications as well. It is very possible that a Mobile Hotpots like system will soon be available for disaster recovery or even large scale cultural events where the existing infrastructure may be in need of added capacity. ■

ACKNOWLEDGMENT

The author extends his gratitude and acknowledgment to the entire Mobile Hotpots team with particular thanks to Dr. Richard Ridgway, DARPA program manager, and the Millitech team whose dedication and expertise has made these millimeter-wave results possible. DARPA approved for public release, distribution unlimited.

Enabling wideband frequency agility

GaN and GaAs Solid-State Power Amplifiers for Multi-Function, Radar and EW System Design

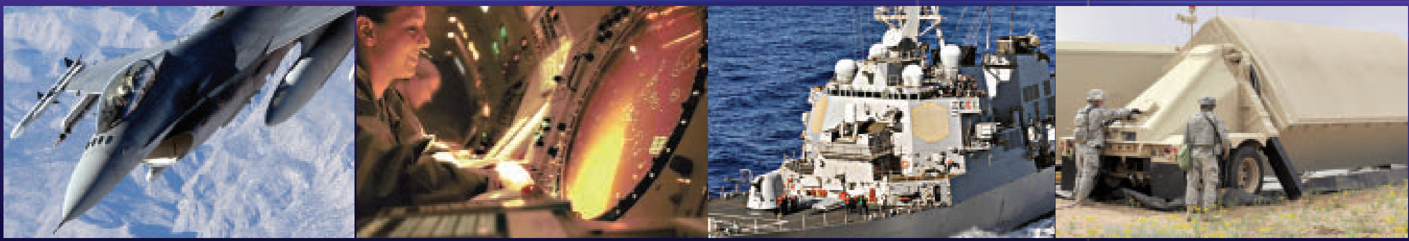

Whether your application is narrowband, wideband or ultra-wideband, operating in pulsed or CW mode, CTT's power amplifiers are an especially attractive choice for new multi-function frequency-agile systems that effectively conserve weight, space and power consumption.

The characteristics of the portion of the electromagnetic spectrum selected for any of these particular system designs are undoubtably the most important to the end user, as it has the greatest impact on the type of information required and received.

Engineered specifically to meet the stringent requirements imposed by many modern system designs, CTT's family of GaN and GaAs-based solid-state power amplifiers excel in a wide range of applications.

CTT has delivered production quantities of amplifiers with power levels from 10 through 200 Watts – and higher – for a variety of multi-function, radar and EW applications.

- AMDR • Shipboard Radar • AESA Radar
- VLO/FLO Threats • New Land Radar • EW • UAVs

More than thirty years ago CTT, Inc. made a strong commitment to serve the defense electronics market with a simple goal: quality, performance, reliability, service and on-time delivery of our products.

Give us a call to find out how our commitment can support your success.

It's that simple.

Microwave Technology Leadership

- ❖ **Power Amplifiers**
  - **NEW GaN and GaAs Models**
  - Radar Bands up to 400W
  - EW Bands up to 200W
  - Pulse and CW
  - Rack-Mount Configurations
- ❖ **Low-Noise Amplifiers**
- ❖ **Up and Downconverters**
- ❖ **Subsystems**
- ❖ **Custom Engineered Options**

nsai ISO 9001:2008 QUALITY

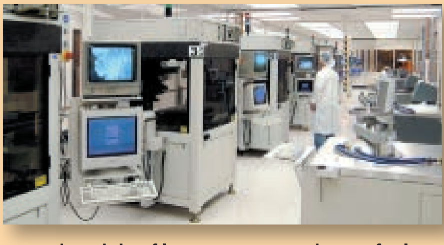

USA-based thin-film microwave production facility

CTT INC.

241 East Java Drive • Sunnyvale • California 94089 • Phone: 408-541-0596 • Fax: 408-541-0794
www.cttinc.com • E-mail: sales@cttinc.com

Scan page using layar app

765 MHz BW PXI Signal Analyzer

National Instruments
Austin, Texas

One of the requirements driving innovation in today's RF signal analyzers is the constant push for wider instantaneous bandwidth. From radar systems to spectrum monitoring to the next generation of wireless communications, engineers require more measurement bandwidth to analyze evolving types of signals. Although the design and manufacturing of extremely wide bandwidth RF signal analyzers was once cost-prohibitive, the increasing performance of off-the-shelf, analog-to-digital converters and advanced signal processing technologies like LabVIEW FPGA has allowed National Instruments to develop the widest bandwidth high performance RF signal analyzer currently on the market – the PXIe-5668R.

This RF signal analyzer offers 765 MHz of instantaneous bandwidth without compromising measurement speed or analog performance. The wide bandwidth of this high performance microwave signal analyzer is able to address applications such as radar test and spectrum monitoring – but with the dynamic range required for RFIC characterization and low-level spur sweeps.

One unique feature of this PXI signal analyzer is the inclusion of an onboard LabVIEW-programmable FPGA. By programming its Xilinx Kintex-7 FPGA, engineers are able to customize the behavior of the instrument by adding in-line signal processing routines or real-time control of a device under test.

ARCHITECTURE

The PXIe-5668R uses two distinct signal paths to deliver a combination of wide instantaneous bandwidth and best-in-class RF performance. In the low-band path below 3.6 GHz, the instrument uses a three-stage superheterodyne design with optional pre-amplification. In the high-band path, above 3.6 GHz, the instrument uses a two-stage design with a yttrium-iron-garnet (YIG)-tuned filter (YTF) for pre-selection.

In the low band of the PXIe-5668R (below 3.6 GHz), the instrument contains several features to improve measurement performance. ***Figure 1*** highlights a simplified block diagram. Notice that the 30 dB preamplifier can be engaged to reduce the instrument's inherent noise floor when measuring low-level signals.

Figure 1 also illustrates two high-pass filters before the first mixing stage. Engineers can engage these filters with a high-pass cutoff of 1350 and 2200 MHz to suppress fundamental frequency of common cellular communications bands around 1 GHz. With filters enabled, the instrument can more accurately measure second and third harmonics of devices, such as a power amplifier at approximately 2 and 3 GHz, respectively.

In the high band, above 3.6 GHz, a YTF function as a pre-selector for operation from 3.6 to 26.5 GHz, which is enabled by default for spectrum measurements. For extremely wideband vector signal analysis, one can disable the YTF to utilize the full 765 MHz of instrument bandwidth.

In conjunction with a 2 GS/s digitizer sample rate, the VSA's downconverter has a flexible IF structure that allows both high-end spectrum analysis and wideband vector signal analysis. For example, a narrow 300 kHz analog filter can be engaged to facilitate measurements requiring the highest dynamic range, such as two-tone intermodulation distortion (IMD) or ACLR. For vector signal analysis, the IF filtering can be entirely disabled to allow for bandwidths of up to either 320 or 765 MHz, depending on the center frequency.

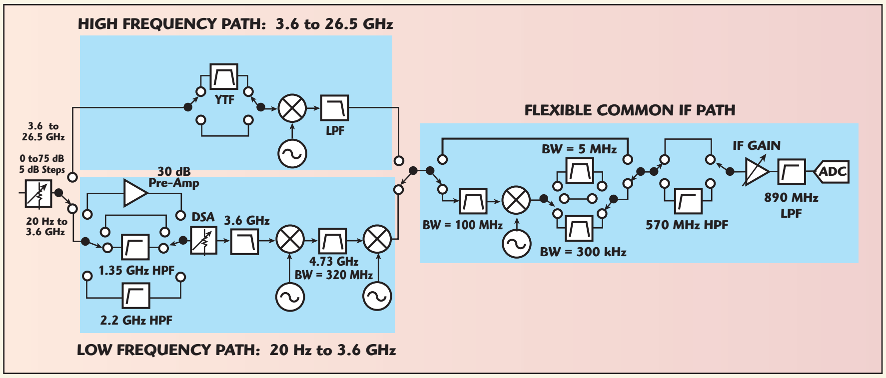

▲ *Fig. 1 Simplified block diagram of PXIe-5668R.*

RADAR DESIGN AND TEST

Engineers tasked with the design and test of advanced radar systems are utilizing increasingly wider signal bandwidths. In fact, typical radar signals such as the pulsed or modulated transmissions often require signal bandwidth that is much wider than what traditional RF signal analyzers can measure in a single acquisition.

In pulsed radar applications, fast switching pulsed signals produce extremely wide bandwidths. In order to accurately perform measurements such as rise-time, fall-time and pulse width, one must capture the full bandwidth of the signal – which includes a main lobe and several side lobes. Moreover, statistical properties of the pulse measurements, such as standard deviation, improve with increased bandwidth of the signal analyzer.

Historically, radar circuit designers have used the relationship "bandwidth = 0.35/pulse rise time" to determine the minimum bandwidth requirements of the radar receiver. This rule of thumb was to ensure that the bandwidth is sufficient for the rise time portion of the pulse to pass through the analog front end of the instrument without significant distortion. However, accurate measurement of radar pulse requires even wider bandwidth from the instrument. A general rule for performing advanced measurements on a pulse with rise time of x nanoseconds is that the VSA's instantaneous bandwidth must be 3/x. For example, to measure pulse rise times as low as 5 ns, the recommended instrument instantaneous bandwidth would be 3/(5 ns) or 600 MHz.

A second radar application that uses wide bandwidth is the use of Linear Frequency Modulated (LFM) Radar or Chirp Radars. In order to resolve two targets in space, radar engineers ideally need progressively narrow pulses. However, the amount of power one needs to generate on the target to get dissent distance/return is directly related to transmitted power. As the pulses get narrow (to gain resolution), engineers either have to generate unpractical peak power narrow pulses or give up range. LFM is an elegant answer to this problem and is a very similar concept to spread spectrum techniques in radios.

SPECTRUM MONITORING SIGNAL INTELLIGENCE

Another application that requires wide bandwidth measurement capabilities is spectrum monitoring and signal intelligence. In these applications, wide instantaneous bandwidth allows engineers to monitor multiple transmissions simultaneously with a single instrument. Using the onboard FPGA, the PXIe-5668R signal analyzer is able to perform real-time spectrum analysis without gaps in the time-domain record (see ***Figure 2***).

Real-time spectrum analysis allows engineers to analyze and view the most elusive signals. Such gap free spectral analysis is achieved through the use of a high performance FPGA computing up to 2 million overlapping FFT's per second. Spectral data is then visualized using both persistence and spectrogram displays.

ANALOG PERFORMANCE

In addition to extremely wide bandwidth, the analog performance of the PXIe-5668R enables engineers to more

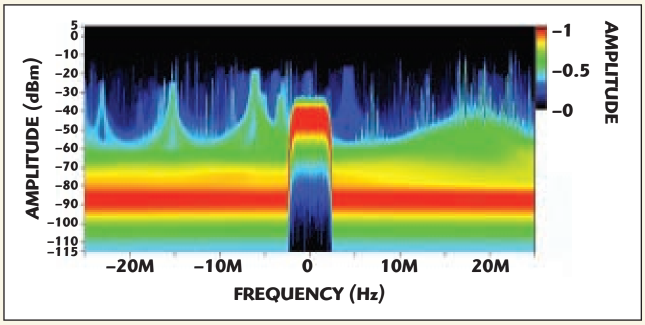

▲ *Fig. 2 The real-time spectrum analysis capability of the PXIe-5668R enables visualization tools such as the persistence display.*

accurately perform a wide range of RF measurements. In fact, the combination of low phase noise, low noise floor and high second and third order intercepts provides excellent dynamic range for applications ranging from adjacent channel leakage ratio (ACLR) measurements to spurs and harmonics measurements.

The dynamic range chart in ***Figure 3*** illustrates both the instruments' noise and linearity as a function of mixer level. The signal analyzer achieves an SFDR of up to 115 dB of SFDR in 1 Hz of bandwidth at 20 GHz.

IMD AND ACP MEASUREMENTS

A combination of a highly linear front end and low noise are critical for engineers performing measurements such as intermodulation distortion (IMD) and adjacent channel power

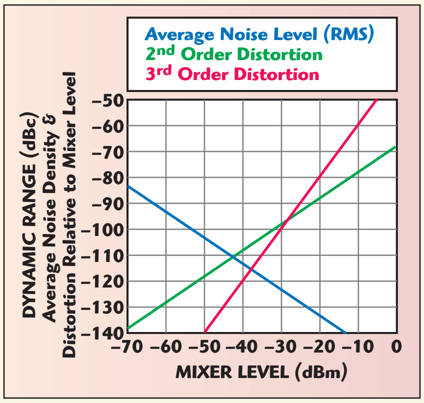

▲ *Fig. 3 PXIe-5668R dynamic range chart at 20 GHz.*

(ACP). In fact, the specification that best represents the ability of an instrument to perform these measurements is third-order intercept (TOI). The PXIe-5668R has a TOI specification of better than +23 dBm at 1 GHz with 0 dB of attenuation. As ***Figure 4*** illustrates, the instrument delivers nominal TOI performance of +25 dBm at 1 GHz.

Although the TOI specification of an RF signal analyzer is defined using 0 dB of attenuation by convention, an RF signal analyzer can measure TOI much higher than its specification. In practice, you can optimize measurement system linearity by switching the instrument's internal attenuation on the PXIe-5668R.

In addition to IMD measurements, the high dynamic range of the PXIe-5668R makes it ideal for spectrum measurements such as ACP and the related measurement, Adjacent Channel Leakage Ratio (ACLR). ***Figure 5*** illustrates an ACLR measurement of a W-CDMA signal and shows an inherent ACLR floor of ap-

CEL INTRODUCING **TOKYO KEIKI**

SERVING AEROSPACE & DEFENSE MARKETS

HIGH QUALITY CUSTOM RF PRODUCTS

JIS-Q9100 CERTIFIED FACTORY
(AS9100 U.S. EQUIVALENT)

ABOUT TOKYO KEIKI

TOKYO KEIKI is a well established medium sized Japanese company founded over 100 years ago with headquarters in Kamata, Tokyo. Their factory in Yaita, Japan is certified per the quality standard for Aerospace manufacturing, where microwave products are assembled and tested under a clean and controlled environment. Factory capabilities include thin-film processing, hermetic sealing, and environmental screening to produce high performance and reliable RF products.

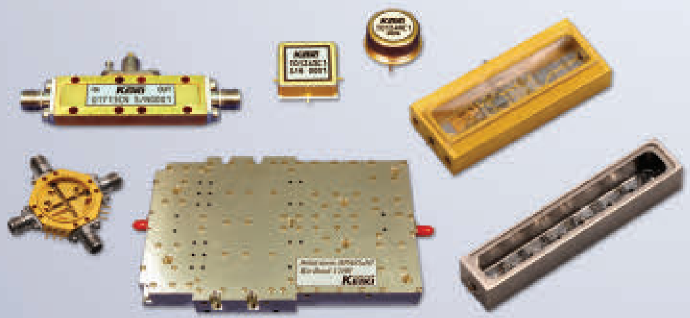

CUSTOM RF PRODUCTS

- Broadband VCOs
- PIN Diode Switches
- Wideband Filters
- Switched Filters Banks
- Broadband Amplifiers
- High Power Amplifiers
- Transceiver Sub-assmblies

CEL | TOKYO KEIKI

Scan code to learn more or visit:
www.cel.com/TK-MJ

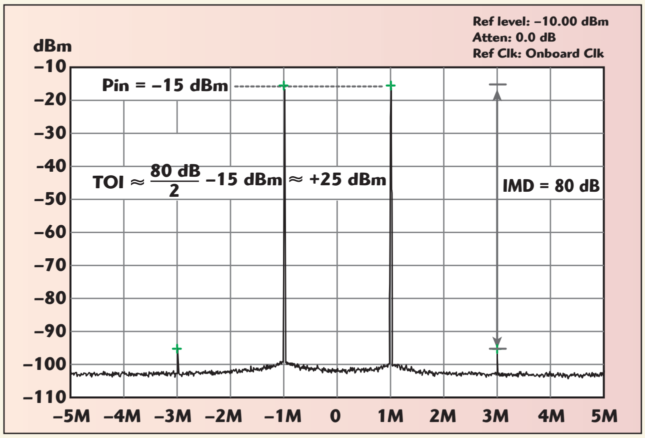

▲ *Fig. 4 PXIe-5668R Intermodulation Distortion Measurements.*

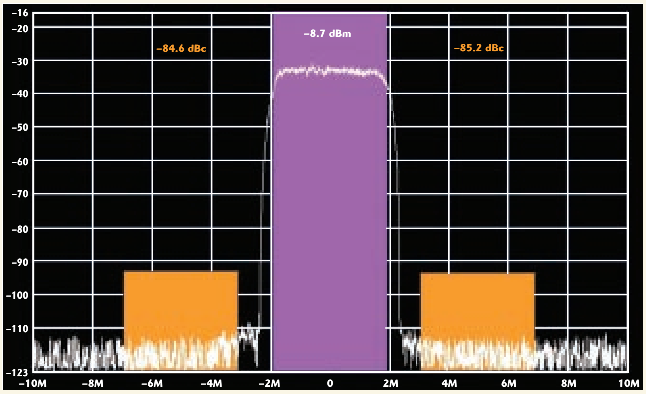

▲ *Fig. 5 PXIe-5668R W-CDMA ACLR performance at 468 MHz.*

proximately 85 dB.

NI wireless standards software toolkits software allows the PXIe-5668R to test devices using technologies including GSM/EDGE, UMTS/HSPA+, LTE/LTE Advanced, Bluetooth and 802.11a/b/g/n/p/ac.

MULTI-CHANNEL ANALYSIS

As a result of this instrument's modular architecture, additional downconverter and digitizer modules support multichannel receiver configurations. The PXIe-5668R VSA provides the ability to share the local oscillator and other timing signals across multiple modules and allows for phase-coherence between each RF channel. The phase-coherence of multichannel receivers is important in applications ranging from direction finding to beamforming and multiple input, multiple output (MIMO) device testing.

The PXIe-5668R is a high-performance 26.5 GHz VSA that is ideal for a wide range of applications. The combination of extremely wide bandwidth, excellent analog performance and ultimate flexibility empowers customers to solve challenging measurement applications ranging from ACLR measurements to radar verification and spectrum monitoring.

VENDORVIEW

National Instruments
Austin, Texas
www.ni.com/microwave

X-47B Achieves New Set of Firsts Aboard USS Theodore Roosevelt

VIEW VIDEO

The Navy's X-47B completed its final test aboard the USS Theodore Roosevelt (CVN 71) Aug. 24 and returned to its home base at Naval Air Station Patuxent River after eight days at sea. While underway, the X-47B flew in the carrier pattern with manned aircraft for the first time and conducted a total of five catapult launches, four arrestments and nine touch-and-go landings, including a night time shipboard flight deck handling evaluation.

"This is another detachment for the record books; all tests were safely and effectively executed," said Capt. Beau Duarte, Navy's Unmanned Carrier Aviation program manager. "We have set the bar for the future of unmanned carrier aviation."

Testing began Aug. 17 when the X-47B performed its initial cooperative launch and recovery cycle with an F/A-18. With its automatic wing-fold capability and new tailhook retract system, the X-47B met the program's objective to demonstrate that carrier-based manned and unmanned aircraft could maintain a 90 second aircraft launch and recovery interval. Throughout the week, the Navy/Northrop Grumman test team captured X-47B flying quality and recovery wind condition data to evaluate how the aircraft responds to wake turbulence during approach and landing. This data will be used to improve a simulation model for use with carrier-based aircraft.

"We have set the bar for the future of unmanned carrier aviation."

The team also evaluated how the unmanned aircraft performed during the first night time taxi and deck handling operations aboard a carrier. Since the shipboard environment presents different challenges at night, this test was an incremental step in developing the operational concept for more routine unmanned air system flight activity. "We conducted X-47B night flight deck operations to understand the human interface and suitability of the unmanned air vehicle and deck operator's handheld control unit in the night environment," said Barbara Weathers, X-47B Unmanned Combat Air System lead. "These lessons learned will help with the development of future unmanned platforms."

The Navy will continue to execute shore-based testing at Patuxent River to further the goal of seamless integration with manned aircraft and to refine best practices for the evaluation of future unmanned air systems.

Source: U.S. Navy Photo

Raytheon AI3 Missile Intercepts First Cruise Missile Target

Raytheon Co. and the U.S. Army achieved the first intercept of a cruise missile by the Accelerated Improved Intercept Initiative missile. An AI3 missile also destroyed an unmanned aerial system (UAS). Both intercepts occurred during the recent Black Dart demonstration – a U.S. military exercise held July 29 - August 11.

Fired from the Avenger launcher, AI3 missiles intercepted both targets at low altitude over water and in a high-clutter marine environment – capabilities made possible by upgrades to the missile's semi-active seeker and radar. The ability to defeat UAS and cruise missile threats is the key requirement of the U.S. Army's Indirect Fire Protection Capability (IFPC) Block 1. IFPC is a mobile, ground-based weapon system designed to acquire, track, engage and defeat UAS, cruise missiles, rockets, artillery and mortars.

"Raytheon's AI3 missile is breaking new ground with its destruction of these challenging targets that are real threats to today's warfighter."

"Raytheon's AI3 missile is breaking new ground with its destruction of these challenging targets that are real threats to today's warfighter," said Dr. Thomas R. Bussing, Raytheon Advanced Missile Systems vice president. "We've developed a missile that integrates easily into the Army's existing systems. It's affordable, the risk is low and we can get it in the field soon."

In preparation for the Black Dart event earlier this year, AI3 missiles destroyed a 240 mm rocket and a UAS at Yuma Proving Ground, Ariz.

GA-ASI Radar Shines During U.S. Navy Spearhead IIA Exercise

General Atomics Aeronautical Systems' Lynx® Multi-mode Radar successfully demonstrated the ability to support maritime operations in a littoral environment during the U.S. Navy Exercise Spearhead IIA exercise held off the coast of Key West, Fla., in June.

For More Information
Visit mwjournal.com for more defense news

Integrated aboard a Predator® B/MQ-9 Reaper surrogate (King Air 350), Lynx's synthetic aperture radar (SAR) and maritime wide-area search (MWAS) modes detected mine-like-objects and very small vessels, including fast boats, sailboats, and fishing boats. Concurrently, the King Air 350 data linked the Lynx and video data via the onboard L-3 Mini-T data link system to the Navy's Intelligence Carry-On Program (ICOP) data link system installed on the Joint High Speed Vessel (JHSV), with the ICOP system employing L-3's VideoScout®-CM2 video exploitation and management system.

"GA-ASI's main goal in supporting this exercise was to provide the ICOP system onboard the JHSV and deliver near-real-time, all-weather, day/night Lynx radar and electro-optical/Infrared (EO/IR) imagery on high-interest maritime targets," said Claudio Pereida, executive vice president, Mission Systems at GA-ASI. "We achieved several historical firsts, using the MQ-9 surrogate to provide the ICOP system with tactical Lynx Radar maritime data, demonstrating Reaper's continued operational relevancy via new Lynx capabilities, and successfully leveraging Reaper in support of the Air-Sea Battle Concept."

During the exercise, GA-ASI's Claw® sensor payload operation software cross-cued the Lynx imagery to the EO/IR sensor for visual target identification. The Lynx target data also was used to cross-cue other platform sensors used in Spearhead IIA. GA-ASI plans to continue integration and test coordination efforts to enhance surface vessels and shore C2 nodes receiving and conducting data exploitation capabilities of Lynx SAR and Moving Target Indicator (MTI) data further.

The Lynx Multi-mode Radar, upgraded to the two-channel Lynx Block 20A and in production, is capable of high-resolution video dismount detection and a 30-degree-per-second scan rate with algorithms optimized for detecting small vessels, including self-propelled semi-submersible (SPSS) vessels. The Lynx MWAS and dismount moving target indicator (DMTI) capabilities, along with a three-fold increase in the ground moving target indicator (GMTI) area coverage rate and a new SAR-aided alignment mode, have been incorporated into Lynx radars and are being deployed by U.S. customers.

The JHSV experiment campaign plan was directed by the Chief of Naval Operations (CNO) through U.S. Fleet Forces Command in an effort to evaluate new missions that could be supported by the JHSV, with an initial focus on options that involve little or no modification to the existing sea frame. In addition, the plan will inform the development of JHSV's concept of operations (CONOP) and assess how well the vessel could support other naval mission sets. The ICOP system onboard Navy vessels and now the JHSV offers a tremendous leap forward in providing an intelligence picture of the battlespace in terms of imagery processing, exploitation and dissemination.


Reactel, Incorporated
Reacting First to All Your Filter Needs.
REACTEL, INC.
Let our Engineers show you what we can do in tight spaces!
High Performance, Rugged Packaging, Small Size and Weight
Great things *can* come in small packages. Reactel filters are ideally suited for the demanding environments that unmanned vehicles encounter.
Many manufacturers rely on Reactel to provide units which are:
• High performance
• Lightweight
• Low profile
Contact a Reactel engineer with your filter or multiplexer requirements. We can create a unit which will be the perfect fit for your applications.
REACTEL, INC.
REACTEL, INC
Reactel is happy to introduce our Filter RFQ App available for Apple and Android devices.
8031 Cessna Avenue • Gaithersburg, Maryland 20879 • Phone: (301) 519-3660 • Fax: (301) 519-2447
For general inquiries, please email reactel@reactel.com • Follow us on Twitter: @reacteljim
Go online to www.reactel.com to download your Reactel catalog today.
FM Approvals
ISO 9001-2008 Registered
@reacteljim

EU MiWaveS Project Launched to Develop 5G Cellular Mobile Networks

A consortium of 15 leading telecommunications operators, vendors, research centres and academic institutions have launched Millimetre-Wave Small Cell Access and Backhauling (MiWaveS), a European collaborative project whose goal is to develop millimetre-wave (mmW) key radio technologies to provide multi-Gbps data rates to future 5th Generation cellular mobile networks users.

The global mobile data traffic is expected to increase by orders of magnitude in the next decade, driven by video streaming, web services, cloud computing and machine-to-machine applications. Data rates provided to mobile users are also expected to increase accordingly. The evolution of mobile networks towards these objectives is impeded by major bottlenecks, such as the scarcity of spectrum resources below 6 GHz leading to high interference levels, the public concern about microwave electromagnetic field (EMF) exposure in dense areas, the power consumption of the infrastructure, and the flexibility and robustness of the network.

MiWaveS is expected to have a major impact on the key enabling technologies for the next generation of heterogeneous wireless networks.

Dr. Laurent Dussopt, MiWaveS project manager and Leti research engineer, explained that "the flexible spectrum usage of the mmW frequency bands at 60 GHz and 71 to 86 GHz will enable data transmissions up to 10 Gbps for backhaul and 5 Gbps for mobile users access." He also indicated that "MiWaveS' objectives lead to significant challenges on the system architecture, networking functions and algorithms, radio and antenna technologies."

MiWaveS is expected to have a major impact on the key enabling technologies for the next generation of heterogeneous wireless networks. The deployment of mmW small cells in dense urban areas will not only improve the flexibility of the access infrastructure, but also the spectral and energy efficiency by low-power access points using mmW spectrum resources.

The MiWaveS project is partially funded by the European Commission's Seventh Framework Programme (FP7), within the Work Programme for Information and Communication Technologies under the objective "Network of the Future." This objective supports the development of future network infrastructures that allow the convergence and interoperability of heterogeneous mobile, wired and wireless broadband network technologies as enablers of the future Internet.

DOCOMO and Huawei Advance Standardization of LAA Technology

NTT DOCOMO Inc. and Huawei announced that their joint test has successfully demonstrated that LTE can be deployed over the 5 GHz unlicensed spectrum. In research carried out at a Huawei facility in Beijing since February 2014, the two companies have been conducting experiments of Licensed-Assisted Access (LAA), a technology that expands LTE-compatible spectrum to unlicensed spectrum bands, thereby providing complementary access for the LTE operator network. Currently, LTE's compatible spectrum bands are licensed between the 700 MHz and 2.5 GHz bands in Japan.

The indoor test found that LAA can work in 5 GHz bandwidth, leading to cell capacity of approximately 1.6 times greater than that of IEEE 802.11n, a standard specification for WLAN. This significant result was a positive indication that LAA can be utilized as an enhancement of LTE, and also LTE-Advanced, which DOCOMO plans to launch by March 2015. For example, higher-speed data communications and a higher cell capacity in dense traffic areas should be achievable by utilizing the 5 GHz spectrum for LTE and LTE-Advanced on a complementary basis in coexistence with wireless LAN.

"We are very pleased to have confirmed that LAA is a viable technology for LTE and future LTE-Advanced," said Seizo Onoe, executive vice president and chief technical officer at NTT DOCOMO. "We aim to contribute to the standardization of this technology, which inherits the highly advanced features of LTE, to further enhance the global user experience with wireless broadband."

"We are very pleased to have confirmed that LAA is a viable technology for LTE and future LTE-Advanced..."

The standardization of LAA, which shows great potential as a solution for extremely condensed data traffic, is likely to be discussed later this year by 3GPP, an industry initiative to drive standardization of key telecommunications technologies. DOCOMO will continue to pursue development of this advanced mobile technology while playing a leading role in its standardization.

Dstl Seeks Counter Terrorism and Security Suppliers

Following the successful pilot of a new commercial framework for research contracts known as Research Cloud (R-Cloud), the UK's Defence Science and Technology Laboratory (Dstl) is seeking suppliers within the area of Counter Terrorism and Security (CT&S). This is the second of nine capability areas to offer research opportunities through

For More Information Visit mwjournal.com for more international news

> "...broaden the supplier base..."

R-Cloud, which provides easy-to-use, direct access to current and future research requirements.

Suppliers working in the area of Counter Terrorism and Security have been asked to apply to be part of R-Cloud via the Defence Contracts Online (DCO) pre-qualification portal. Successful suppliers will be considered for future R-Cloud CT&S research contract opportunities with mini-competitions being run where suppliers will be invited to express interest and tender for different tasks.

Dstl's R-Cloud project manager, Neil Higson, said, "Dstl places a significant amount of research contracts every year with industry and academia. R-Cloud will eventually provide a commercial marketplace for research opportunities across the spectrum of Dstl's capability areas, with a contracting mechanism that will significantly help expedite the placement of research contracts and broaden the supplier base."

Thales Alenia Space Signs EGNOS Framework Contract with ESA

Thales Alenia Space has signed a new framework contract with the European Space Agency (ESA) concerning the European Geostationary Navigation Overlay Service (EGNOS) navigation system. The contract will enable ESA, delegated by the European Commission, to order work packages from Thales Alenia Space France for the period 2014-2017, to develop new versions of EGNOS V2. Designed to ensure the continuous improvement of EGNOS performance, these new versions will guarantee optimum service quality for users, while also addressing the need to manage obsolescence.

Thales Alenia Space is the prime contractor for EGNOS, which is designed to improve the positioning signals delivered by the GPS satellite navigation system. EGNOS was deployed in 2005, and has been operational since 2009 for open service. The system's Safety of Life service was officially declared operational in March 2011, allowing it to be used for aircraft landing and enabling precision approaches to European airports without ground guidance aids.

"The signature of this framework contract with ESA, in the presence of the European GNSS Agency (GSA), marks a decisive new step for Europe's EGNOS navigation system," noted Philippe Blatt, head of the Navigation business line at Thales Alenia Space France. "We are already the prime contractor for the Galileo Mission Segment (GMS), the Galileo Security Facility (GSF) and the Galileo system. This latest contract confirms Thales Alenia Space's position as the European leader in satellite navigation, a position we have held for over 20 years."

DC-12 GHz 1W Attenuators

only $18.95 ea. qty.1-9

Accurate attenuation over ultra-wide frequency range at low cost! Mini-Circuits' new FW-series fixed SMA attenuators cover your applications from DC – 12 GHz with a wide selection of attenuation values to meet your needs. All models offer excellent attenuation flatness versus frequency, low VSWR, and 1W input power handling, making them ideal, cost-saving solutions for impedance matching and signal level adjustment in a broad range of systems.

Built using Mini-Circuits rugged unibody construction with SMA(M) to SMA (F) connectors, FW-Series attenuators provide outstanding reliability in tough operating conditions. Just go to minicircuits.com for full specs and see how these attenuators can add performance and value to your design! They're available off the shelf for immediate shipment. Order today, and have them in hand as soon as tomorrow!

Model	ATTENUATION Nominal (dB)	ATTENUATION Flatness (dB)	VSWR (:1) Midband Typ.	Power (W)
FW-1+	1	±0.15	1.15	1.0
FW-2+	2	±0.15	1.15	1.0
FW-3+	3	±0.20	1.15	1.0
FW-4+	4	±0.20	1.15	1.0
FW-5+	5	±0.20	1.15	1.0
FW-6+	6	±0.25	1.15	1.0
FW-7+	7	±0.25	1.15	1.0
FW-8+	8	±0.30	1.15	1.0
FW-9+	9	±0.30	1.15	1.0
FW-10+	10	±0.30	1.15	1.0
FW-12+	12	±0.30	1.20	1.0
FW-15+	15	±0.35	1.20	1.0
FW-20+	20	±0.50	1.20	1.0

RoHS compliant.

Mini-Circuits®

www.minicircuits.com P.O. Box 350166, Brooklyn, NY 11235-0003 (718) 934-4500 sales@minicircuits.com

531 rev. orig.

Electronic Shelf Labels Revenue to Reach $2 Billion by 2019

Over the next five years electronic shelf labels (ESL) are set to grow beyond retail markets in legislated countries, with revenues increasing six fold to almost $2 billion by 2019.

In its latest report, "Next Gen Retail: Electronic Shelf Labels," ABI Research outlines how ESLs will be a key link in the retail technology chain, representing a great starting point when near field communication (NFC) or bluetooth low energy (BLE) is integrated. Retailer's attention has been caught by other technologies, but the ideal scenario and end game for most will be a tightly integrated system that consists of ESL, smartphone applications, BLE beacons, indoor location, mobile payments, digital coupons/loyalty, customer analytics, and omni-channel marketing and pricing. ESLs are a perfect starting point, bringing a return on investment to traditional brick and mortar bottlenecks, while also opening the door to next generation services and revenue opportunities.

ESLs will be a key link in the retail technology chain, representing a great starting point when near field communication (NFC) or bluetooth low energy (BLE) is integrated.

Senior analyst Patrick Connolly commented, "ESL, in combination with NFC and/or BLE solves ongoing retailer issues like out-of-stocks, check-out expenditure reduction, manual price coordination overheads elimination, inventory and store layout management, omnichannel consistency, and efficient price management of shrinkage/perishable goods, delivering an RoI within 18 months on these use cases alone. With integrated connectivity, it also brings future potential around dynamic pricing, positive showrooming, tightly integrated in-store advertising/redemption/loyalty, analytics, and pay-as-you-go shopping."

"Dynamic pricing can be a controversial topic, but many of the arguments against are naive or based on scenarios that are unlikely to occur in the brick and mortar space. The reality is it will give retailers far more control and flexibility, with the ability to reward loyal customers, dynamically match pricing to varying demand, while also meeting the needs of price sensitive customers," added Connolly.

Pricer and SES are the two major players in this space today, dominating traditional markets. In particular, SES has shown very strong growth over the last two years, with the recent imagotag acquisition giving it new capabilities. Displaydata (backed by Zebra Technologies) and Samsung are the clear emerging threats, with Altierre also achieving some success in its native U.S. market. There are also a number of localized start-ups such as Hanshow in China that will make this a very interesting market over the next five years.

The Internet of Things will Drive Wireless Connected Devices to 40.9 Billion in 2020

According to an updated market forecast from ABI Research, the installed base of active wireless connected devices will exceed 16 billion in 2014, about 20 percent more than in 2013. The number of devices will more than double from the current level, with 40.9 billion forecasted for 2020.

Principal analyst Aapo Markkanen comments, "The driving force behind the surge in connections is that usual buzzword suspect, the Internet of Things (IoT). If we look at this year's installed base, smartphones, PCs, and other 'hub' devices represent 44 percent of the active total, but by end-2020 their share is set to drop to 32 percent. In other words, 75 percent of the growth between today and the end of the decade will come from non-hub devices: sensor nodes and accessories."

From every technology supplier's strategic point of view, the critical question is how this plethora of IoT devices will ultimately be connected. Until recently, the choices that product OEMs have faced have been fairly straightforward, with cellular, Wi-Fi, Bluetooth, and others all generally addressing their relative comfort zones. Going forward, there will be increasing competition, making the strategic stakes for the suppliers much higher.

Practice director Dan Shey adds, "The recently introduced Thread protocol, spearheaded by Nest Labs, is the clearest example of this convergence. It is not only setting the bar higher for ZigBee in the 802.15.4 space, but also piling up pressure on Bluetooth suppliers to enable mesh networking. In the meantime, the LTE-MTC and LTE-M initiatives may well expand the market for cellular M2M, while startups like Electric Imp and Spark could do the same for Wi-Fi. And finally, we also shouldn't ignore what's going on with passive, proximity-based connectivity offered by RFID and NFC. For example, Thinfilm's plans with printed electronics warrant attention."

"75 percent of the growth between today and the end of the decade will come from non-hub devices: sensor nodes and accessories."

PXI Lowers Cost and Time to Market, First Choice in Test & Measurement Industry

Original equipment manufacturers (OEM) across industries are adopting PCI extensions for instrumentation (PXI)-based instrumentation as its measurement speed, small footprint, low power consumption, and flexibility reduce the time to market and overall cost of tests. In particular, companies in the wireless communications space are turning to these solutions to satisfy new test requirements for radio frequency (RF) wireless technologies. New analysis from Frost & Sullivan, "PXI Market to Change the Face of the Test and Measurement Industry," finds that the market earned revenues of $563.3 million in 2013 and estimates this to reach $1.75 billion by 2020.

"Besides the uptake in RF wireless communications, the global PXI market will get a leg up from new programs in aerospace and defense and integration of wireless technologies in the industrial and consumer electronics industries," said Frost & Sullivan test & measurement industry director Jessy Cavazos. "Additionally, it is finding opportunities in the semiconductor automatic test equipment market."

However, test engineers' trust in traditional box instruments they have used effectively for decades is slowing down the transition to PXI test systems. In due course, the emergence of a new generation of test engineers that is more comfortable with computers will mitigate this challenge.

> "Meanwhile, the more complex process of integrating PXI test systems, in comparison to rack-and-stack test systems, can be a challenge for customers..."

"Meanwhile, the more complex process of integrating PXI test systems, in comparison to rack-and-stack test systems, can be a challenge for customers," pointed out Cavazos. "To ease the process of integration, market participants across the globe are offering different levels of integration services and tools that enable customers to assemble PXI test systems quickly with minimal effort." Additionally, participants are offering subsystems, hardware/software bundles and box solutions that use PXI in their internal architecture to lessen the burden of integration on customers. Via organic means and partnerships, PXI manufacturers deliver multiple options ranging from individual components to fully integrated test systems. Furthermore, they are looking to expand the total addressable market by rolling out new PXI instruments with enhanced capabilities and increasing customer awareness of the benefits.

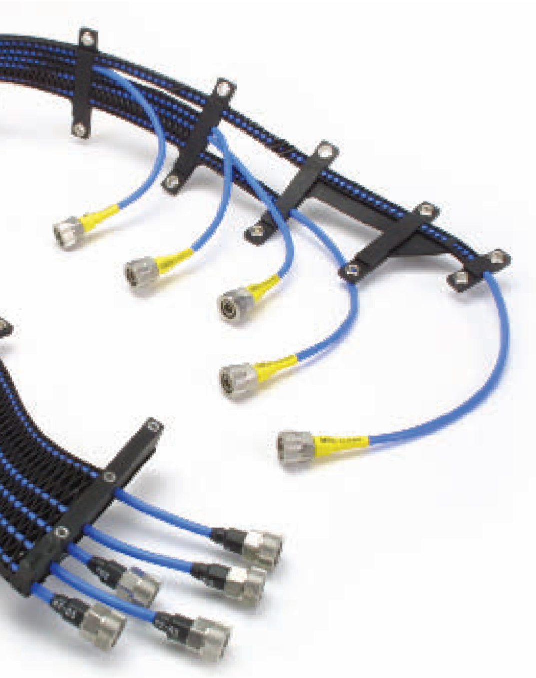

Around the **Circuit**

Barbara Walsh, Multimedia Staff Editor

MERGERS & ACQUISITIONS

Murata Electronics North America Inc. and **Peregrine Semiconductor Corp.** announced that they have entered into a definitive agreement under which Murata will acquire all outstanding shares of Peregrine not owned by Murata, for $12.50 per share in cash, or a total transaction value of $471 million ($465 million excluding Murata's existing holding). Upon closing of the transaction, Peregrine will become part of Murata's strategy to expand its core business. Peregrine will become a wholly owned subsidiary of Murata and continue with its current business model of solving the world's toughest RF challenges.

Infineon Technologies AG and **International Rectifier Corp.** announced that they have signed a definitive agreement under which Infineon will acquire International Rectifier for $40 per share in an all-cash transaction valued at approximately $3 billion. The acquisition combines two semiconductor companies with leadership positions in power management technology. By the integration of International Rectifier, Infineon complements its offerings and will be able to provide customers with an even broader range of innovative products and services. Infineon will also benefit significantly from greater economies of scale as well as a larger regional footprint.

TE Connectivity Ltd. announced that it has completed the acquisition of the **SEACON** group, a provider of underwater connector technology and systems. The SEACON group serves the military marine and sub-sea sectors for remotely operated vehicles (ROV)/autonomous underwater vehicles (AUV), oil and gas, environmental and oceanographic applications. The group will become part of TE's Industrial Solutions segment under the leadership of Terrence Curtin, president, Industrial Solutions, and will be integrated into the Aerospace, Defense and Marine business unit.

e2v technologies has agreed to acquire Seville-based Innovaciones Microelectronicas SL, trading as **AnaFocus**, a Spanish designer and developer of CMOS imaging sensors for up to €34.2 million. AnaFocus designs and develops high performance, high quality CMOS image-sensors and vision-systems for the industrial, professional, scientific, medical and high-end surveillance markets. AnaFocus will become an integral part of the machine vision business within e2v's fast-growing high performance imaging division, which grew by 26 percent last year and will fit well into the existing infrastructure of the division. The deal will accelerate e2v's CMOS development road-map and deepen the company's reach in the professional imaging markets.

COLLABORATIONS

Anritsu Corp. announced it has entered into a Manufacturing Test License (MTL) agreement with **Broadcom Corp.** Anritsu's modular MT8870A Universal Wireless Test Set enables cellular, wireless connectivity, location-based services (LBS) and other technologies to be tested in a single solution. The MTL agreement will allow Anritsu to provide certified calibration and verification test solutions to Broadcom WLAN and Bluetooth customers. The Broadcom® Manufacturing Test License agreement is a license and validation program, providing test equipment vendors with access to Broadcom WLAN and Bluetooth software tools as well as Broadcom technical support resources.

Isola Group S.a.r.l. announced a major qualification win in partnership with **KSG Leiterplatten GmbH** and **InnoSenT GmbH**. The joint conversion project among the three companies successfully tailored the dielectric properties of Isola's high performance I-Tera® MT laminate material to match the properties of an incumbent product. Isola's dielectric substrates will now be used on existing volume products produced by InnoSenT, and the printed circuit boards will be manufactured by KSG. The conversion to Isola's materials provides InnoSenT with higher performance material without modifying the metallization of the PCB.

ACHIEVEMENTS

Lockheed Martin's Dual Mode Laser Guided Bomb (DMLGB) was successfully employed during recent U.S. Marine Corps weapons and tactics instructor training. During the training exercises at Marine Corps Air Station Yuma in Ariz., AV-8B Harrier aircrews released 19 GBU-12F/B DMLGB weapons. The weapons were released in tactically representative engagements and used various targeting modes against fixed targets. All weapons performed successfully and met Marine Corps mission objectives. Lockheed Martin's DMLGB adds GPS/Inertial Navigation System (INS) guidance to standard laser-guided bomb weapons, allowing the U.S. Navy and Marine Corps to execute precision-strike missions against stationary and relocatable targets in all weather conditions.

The Rosetta comet chaser developed and built by **Airbus Defence and Space** for the European Space Agency (ESA) has arrived at its destination after flying for more than 10 years and travelling more than six billion kilometres. It is now ready to swivel into an orbit around the comet called 67P/Churyumov-Gerasimenko. The mission assigned to Rosetta and to the Philae lander that it is carrying, is to examine primary material from the nursery of the solar system 4.6 billion years ago over the next one and a half years. For planetary researchers, the Rosetta mission is akin to journeying back to the origins of the solar system.

Planar Monolithics Industries Inc. (PMI) announced that they have received their ISO 9001:2008 certification for their Quality Management System. With the recent successful completion of the audit at the El Dorado Hills, Calif. facility, now all three PMI facilities, including both facilities located in Frederick, Md. are ISO certified. ISO

For More Information For up-to-date news briefs, visit mwjournal.com

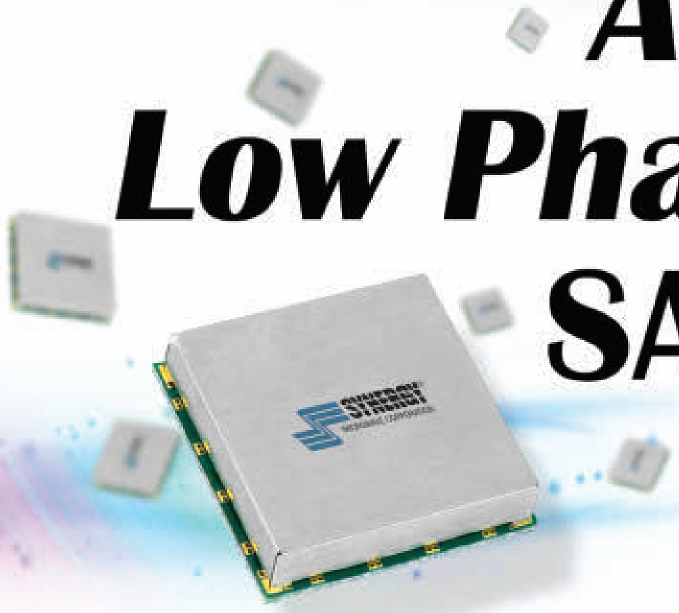

Around the **Circuit**

9001:2008 certification is a prestigious certification requiring companies to meet the complex and demanding documentation, quality system and continuous process improvement requirements of the aerospace, defense and commercial industries.

XMA Corp. announced that it has achieved AS9100 Rev C registration. This is the latest accomplishment for the XMA team as they work to maintain their position as a leader in the RF, microwave and millimeter wave industry. The certifying body, NSF, completed the AS9100 Revision C:2009 audit in May of 2014 and awarded the certificate in June after final ANSI-ASQ National Accreditation Board (ANAB) review. Additionally, this ensures XMA's compliance to ISO9001:2008.

DragonWave Inc. announced the completion of a series of extensive outdoor small cell backhaul propagation tests that have been conducted with a third party for street level characterization. This testing has validated and characterized non-line-of-sight (NLoS) paths at street level utilizing 60 GHz small cell backhaul deployment technologies. The exercise also validated and characterized the accuracy of NLOS path predictions in order to improve deployment and network planning. As a result, the testing characterized distance limitations that are experienced by street level line-of-sight (LOS) paths due to flat fading.

CONTRACTS

Boeing has received a contract from **NATO** worth approximately $250 million to install digital flight decks and avionics on 13 of the alliance's Airborne Warning and Control System (AWACS) aircraft, which are based on the Boeing 707 commercial airplane. The new technology ensures compliance with current and future air traffic control and navigation requirements, giving the aircraft broader access to airspace around the world. Additionally, the upgrade will result in a cost savings in personnel because the flight deck crew will be reduced from four to three. The modifications begin in 2016 and will be completed by 2018.

Waltham-based **Raytheon** will lead a team of Massachusetts-based companies that will convert Bay State tolling to an automatic system allowing drivers to pass through toll stations without slowing down. Raytheon, which has operations in central Mass., was awarded a $130 million contract to develop and install an All Electronic Tolling System (AETS) for the Massachusetts Department of Transportation (MassDOT). The system employs gantry-style structures that look like overhead signage, according to the company. MassDOT is pursuing the AETS as a means to reduce congestion, travel times and vehicle emissions created by existing toll plazas.

Harris Corp. has received a $15 million order to deliver its latest wideband handheld tactical radio to a country in the Middle East. Harris is supplying this nation with the RF-7850M handheld, a multi-band, multi-mission radio that provides advanced tactical communication capabilities. The radio offers a new embedded interface that gives users access to a library of applications that provide situational awareness, tactical messaging, file transferring and radio configuration support from a standard web browser. The interface is fully customizable through a software-development kit, simplifying the process of creating and distributing new applications.

Cubic Corp. announced it has been awarded a contract valued at $1.8 million from **Idaho National Laboratory** to perform phase one of a two-phase program to provide a common data link (CDL) for unmanned platforms, specifically Small Unmanned Aircraft Systems (SUAS). Idaho National Laboratory is a science-based applied engineering national laboratory dedicated to supporting the U.S. Department of Energy's missions in nuclear and energy research, science, and national defense. Phase one of the CDL for SUAS program requires the five selected companies, including Cubic, to complete a specified portion of the waveform development for a next-generation CDL known as Bandwidth Efficient Common Data Link (BE-CDL Rev B).

NuWaves Engineering announced that the company has been awarded a Phase I Small Business Innovation Research (SBIR) contract from the **U.S. Air Force Research Laboratory (AFRL)** to research and develop advanced RF cavity filters for use on Global Positioning System (GPS) III satellites. NuWaves worked with Exelis Geospatial Systems' Positioning, Navigation and Timing business located in Clifton, N.J., to propose an innovative method to dramatically reduce the size and weight of space-based diplexers, triplexers and quadruplexers – or "n-plexers" – for multicarrier RF combining by incorporating specialized inserts within the filter cavities. The proposed design also supports wider bandwidths and higher signal power levels than previous generation n-plexer solutions.

PEOPLE

Ethertronics Inc. announced the appointment of **Vahid Manian** as chief operating officer. In his new role with the company, Manian will be responsible for Ethertronics' Chip and Systems Divisions, and will lead all global manufacturing, supply chain, quality, sales, technology design, marketing and business development efforts. Manian joins Ethertronics from Entropic, where he served as senior vice president of global engineering and operations. A seasoned semiconductor executive with more than 30 years of proven business, technology and operations experience, Manian was responsible for Entropic's global engineering and operations organizations, including hardware and software product development, technical operations, quality and supply management.

M/A-COM Technology Solutions Holdings Inc. announced that **Thomas Hwang** has agreed to join the company as senior vice president of global sales. Hwang spent the last 10-plus years at Hittite Microwave Corp. in a variety of positions including VP of sales, and helped grow that company's annual revenues from $30 to $274 million prior to its acquisition by Analog Devices Inc., earlier this year.

Around the **Circuit**

PEOPLE

▲ Holger Stuehrmann

Southwest Microwave announced the appointment of **Holger Stuehrmann** as director of sales, Microwave Products Division (MPD). Stuehrmann brings more than 30 years of customer-centric focus, new product development success and operational performance improvement experience to Southwest Microwave. In this new role, he will assume management of MPD's worldwide sales and business generation activities. Stuehrmann joins Southwest Microwave from the STC Microwave Systems division of Crane Aerospace and Electronics, where he served as director of business development & sales and previously as business manager, Microwave Components.

▲ Hugh Baker-Smith

Nujira Ltd., a global envelope tracking (ET) chip company, has announced the appointment of **Hugh Baker-Smith** as vice president of sales, with a focus on driving sales of Nujira's Coolteq.L ET IC to leading smartphone vendors. The strategic hire underlines Nujira's focus on accelerating growth in Asia, driven by increased customer demand. Baker-Smith has an extensive track record in global electronic sales and will be focused on building up the sales channel and field support networks, utilizing his extensive experience in the global smartphone market to secure customers and drive revenue.

SV Microwave announced the addition of **Javier Merino** as western regional sales manager supporting new and existing commercial and military accounts. Merino joins SV with over 15 years of experience working in the semiconductor, aerospace and defense electronics, and RF industries. In his most recent sales management role at Lark Engineering, Merino was responsible for building and strengthening customer relationships while driving product and technology innovations.

▲ Judy Warner

eSurface® Technologies announced the appointment of **Judy Warner** to the eSurface Technologies Advisory Board, effective immediately. Warner is a seasoned veteran of the printed circuit board and electronics industry. She began her career in the early 80s at Details Inc., the company from which DDi was born. She was a top-performing sales professional for ElectroEtch Circuits, which was acquired by Tyco, then TTM. After a short time working for an independent sales rep firm, she opened her own company, Outsource Solutions, which offered fully integrated solutions, ranging from design to full turn-key product builds.

Isola Group S.a.r.l. announced that **Antonio "Tony" Caputo** has joined its Analytical Services Lab in Chandler, Ariz. Caputo's work at Isola will focus on research on the

▲ *Antonio Caputo*

chemical nature of Conductive Anodic Filament (CAF) failures – a failure mode in printed wiring boards (PWB) that occurs under conditions of high humidity and high voltage gradients. The ability to identify how CAF forms chemically and understand the fundamental reaction conditions that accelerate CAF formation will enable Isola to introduce new laminate systems that are more CAF resistant.

Indium Corp. announced that **Andy C. Mackie**, Ph.D., MSc, has been named president of the Empire Chapter of the International Microelectronics Assembly and Packaging Society (IMAPS). IMAPS is the world's largest society dedicated to the advancement and growth of microelectronics and electronics packaging technologies through professional education. Mackie's responsibilities as president include coordinating all activities for Empire Chapter members and organizing local technical meetings, tours and networking activities with the members, corporate members, and universities and labs in the region. The Empire Chapter hosts meetings throughout upstate N.Y., including Binghamton, Corning, Syracuse and Rochester.

REP APPOINTMENTS

Cree Inc., a global supplier of silicon carbide (SiC) and gallium nitride (GaN) wafers and devices, is enhancing its support of the European market by extending its partnership with **APC Novacom**. APC Novacom now stocks all Cree® RF devices that do not require an EU license, including GaN HEMT die, and actively supports Cree's European market through both volume distribution and small volume stock for network representatives.

Advanced Test Equipment Rentals (ATEC) announced an agreement with **Fluke Networks** to become a rental distributor of Fluke Networks products, bringing greater product availability to customers with immediate test equipment needs. ATEC will now carry the Versiv™ family of cable certification testers, which enable fast and accurate copper and fiber certification, as well as Optical Time Domain Reflectometer (OTDR) testing.

Anritsu Co. has expanded **RFMW**'s distribution territory for coaxial connectors and coaxial components. Along with the U.S., which RFMW has supported since 2008, the specialty electronics distribution company will now also market and sell Anritsu connectors and components in Canada, Mexico, as well as Central and South America. Anritsu is a leader in the design and production of precision microwave components and holds numerous connector design patents.

Florida's **Coaxial Components Corp.** has recently acquired new representation at the heart of one of the globe's major economies in Asia. **Anywave Technology**, specializing in the aerospace market in South Korea, will promote

and sell the Coaxicom product line of precision microwave components.

Dynawave, a designer and manufacturer of RF and microwave connectors, cable and cable assemblies, announced the appointment of **G Squared Technologies Inc.** as their new manufacturer's representative in the Mid-Atlantic region. G Squared will cover Md., Va., DC and Del. for the full range of Dynawave's products.

Intercept Technology Inc. announced its newest authorized reseller, **Shenzhen EDA Technologies Co. Ltd.** (EDATC). With over 12 years of experience selling and marketing EDA software, Shenzhen EDA Technologies joins the Intercept team in its continued efforts to bring more streamlined, global solutions to the Chinese market place. Intercept's EDA software solution provides users with scalable design and engineering software that can be tailored for simpler designs to the most complex PCB, RF, hybrid and mixed signal boards, panels and panel arrays.

Logus Microwave announced the addition of three new technical sales representatives for their waveguide and coaxial switch products. **T&E Repco** will cover Central and South Fla., **BWS Microwave Marketing** will cover North Fla., Ga., Tenn., S.C. and Ala.; and **G Squared Technologies** will cover Md., Va., DC, Del. and W. Va.

Richardson RFPD Inc. announced that it will globally distribute products from **Maxtena Inc.**, developer and producer for innovative wireless solutions, including GNSS, Iridium, Inmarsat and Thuraya satellites, and terrestrial M2M, MSS and LTE applications. Richardson RFPD will distribute Maxtena's line of reliable, rugged and compact helix antennas, microstrip antennas and combo antennas, as well as support customers with custom wireless solutions ranging from smart metering to 4G LTE. In other news, Richardson RFPD Inc. announced that it has completed an agreement with **Radius Power Inc.** to distribute EMI power line filters.

PLACES

ARC Technologies celebrated the grand opening of its new advanced manufacturing facility in Amesbury, Mass. Government officials and business partners joined the opening celebration and toured the manufacturing operations. Founded in 1989, the company services the conductive and microwave materials market, specializing in custom engineered products and solutions. Their new modern facility will help improve communications, simplify product flow and improve overall efficiency. ARC employs over 120 people.

USB & Ethernet Programmable

ATTENUATORS

0–30, 60, or 90 dB 1 MHz to 6 GHz from $395

Mini-Circuits programmable attenuators give you more options and more freedom with both USB and Ethernet control. Available in versions with maximum attenuation of 30, 60, and 90 dB with 0.25 dB attenuation steps, all models provide precise level control with accurate, repeatable performance for a wide range of test applications. Our unique designs maintain linear attenuation change per dB over the entire range of attenuation settings. Supplied with user-friendly GUI control software and everything you need for immediate use out-of-the-box, Mini-Circuits programmable attenuators offer a range of solutions to meet your needs and fit your budget. Visit minicircuits.com for detailed performance specs, great prices, and off-the-shelf availability!

RoHS compliant

	Models	Attenuation Range	Attenuation Accuracy	Step Size	USB Control	Ethernet Control	RS232 Control	Price $ ea.
	RUDAT-6000-30	0 – 30 dB	±0.75 dB	0.25 dB	✓	-	✓	$395
NEW	RCDAT-6000-30	0 – 30 dB	±0.75 dB	0.25 dB	✓	✓	-	$495
	RUDAT-6000-60	0 – 60 dB	±1.00 dB	0.25 dB	✓	-	✓	$625
	RUDAT-6000-90	0 – 90 dB	±1.70 dB	0.25 dB	✓	-	✓	$695
NEW	RCDAT-6000-60	0 – 60 dB	±0.30 dB	0.25 dB	✓	✓	-	$725
NEW	RCDAT-6000-90	0 – 90 dB	±0.40 dB	0.25 dB	✓	✓	-	$795

Mini-Circuits®

www.minicircuits.com P.O. Box 350166, Brooklyn, NY 11235-0003 (718) 934-4500 sales@minicircuits.com

523 Rev A

Measurement of an Active Radar Module in a Compact Antenna Test Range

Hammam Shakhtour
Institute of High Frequency Technology (IHF), Aachen, Germany
Dirk Heberling
IMST GmbH, Kamp-Lintfort, Germany
Karam Noujeim
Anritsu, Morgan Hill, Calif.
Ferdinand Gerhardes
Anritsu GmbH, München, Germany
Peter Knott
Fraunhofer Institute, Wachtberg, Germany

Due to their reciprocal nature, passive antennas can be completely characterized in transmit or receive mode. This is in contrast with active antennas where characterization is performed in one of two modes, with the other deemed not suitable due to non-reciprocity. This requires an antenna measurement facility be able to perform measurements in both transmit and receive modes. This article describes a measurement setup used to characterize an active radar module (ARM) in transmit mode and presents the results of these measurements, which were performed in the compact antenna test range at the Institute of High-Frequency Technology at the University of Aachen (RWTH), Aachen, Germany.

Active antennas have been attracting more interest for mobile communications (e.g., base stations) due to their flexibility and efficiency.[1] In contrast with passive antennas, the measurement of active antennas is more challenging. The term active antenna comes from the fact that active elements, such as transmitter power amplifiers (PA) and receiver low noise amplifiers (LNA), are part of the antenna. These active elements restrict antenna operation to either transmit or receive; thus, an active antenna must be characterized for either one or the other. Some active antennas are supplied with (so called) transmit/receive modules (Tx/Rx) to enable operation in both modes.[2] In this case, each mode is characterized separately.

Difficulties associated with active antenna measurements can depend upon several factors. First is the antenna type. It is particularly challenging to characterize antenna arrays that, apart from simply measuring the radiation pattern, need calibration.[3-5] Second is the measurement facility. This is challenging especially for spherical near field measurement facilities that require accurate phase and amplitude information to perform the near-to-far field transformation.[6] Third is the mode of operation (i.e., transmit or receive). Last is the availability of phase information. This is the case for applications where an entire system, including the Tx and Rx antennas, digital signal processing (DSP) modules, amplifiers and other components, are integrated onto a single chip, making

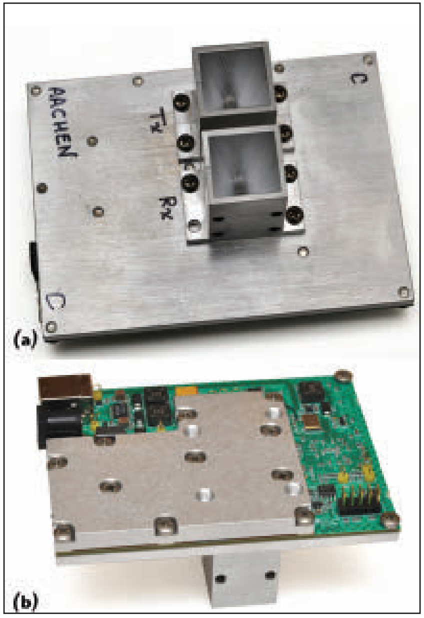

▲ *Fig. 1 Photos of the Anritsu active radar module (ARM); top view (a), bottom view (b).*

access to phase information very difficult, or impossible, unless taken into account in the early design stages.

This article presents the results of measurements run in the compact antenna test range (CATR) at the Institute of High Frequency Technology (IHF) in Aachen, Germany.[7] The device under test (DUT) is a prototype active radar module developed by Anristu®.

ACTIVE RADAR MODULE

The ARM is a stepped-frequency, continuous-wave (SFCW) radar. It consists of two beam-steerable dual-waveguide-fed horns, one used for transmission of CW signals, and the other for receiving signal reflections. The horns interface with nonlinear-transmission-line-based (NLTL) variable phase shifters,[8] samplers, frequency multipliers and supporting circuitry, resulting in a compact assembly that is controlled from a USB interface. It operates from 55 to 65 GHz. ***Figure 1a*** is a top view showing the Tx and Rx horn antennas. ***Figure 1b*** is a bottom view showing the printed circuit board, DC-power and USB connectors.

Figure 2 shows a block diagram of the SFCW ARM consisting of a sampling directional coupler and receiver, beam-steerable transmit and receive antennas, a CW stimulus source and USB control. The lower branch shows the antenna. One capability of SFCW radars is the measurement of distance from an object. This is done by sweeping the frequency of the CW transmitter over a given frequency range, measuring the reflection coefficient, and making use of a chirp-z transform to recover the roundtrip time delay from transmission to reception. The time delay determines the object's distance relative to the radar.[9,10] Another capability of this module is beam steering, achieved with the aid of variable phase shifters (VPS) integrated with a dual-waveguide-fed horn antenna. The introduction of a phase shift between the excitation signals enables main-beam steering, or scanning, by phasing one waveguide aperture with respect to the other. A 12 V power supply provides DC power, while module control and programming (e.g., setting the transmit frequency and phase shift necessary for main-beam scanning) are realized via a USB interface.

MEASUREMENT FACILITY

The module was measured in the CATR at the Institute of High Frequency Technology in Aachen (see

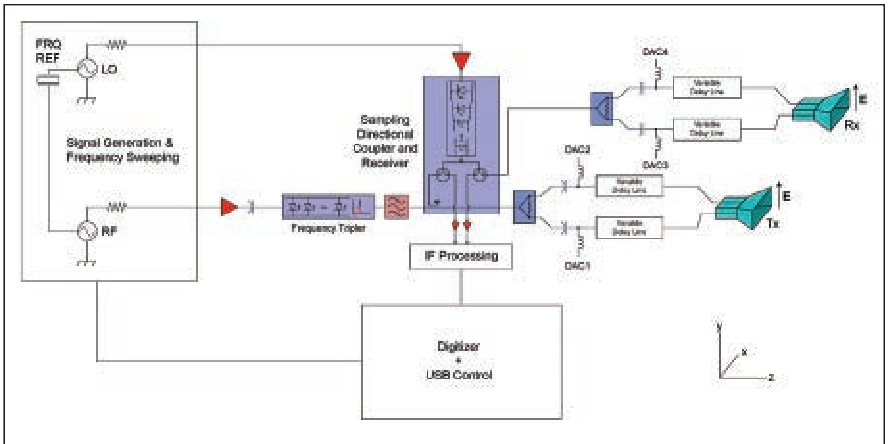

▲ *Fig. 2 Block diagram of the NLTL-based SFCW radar module.*

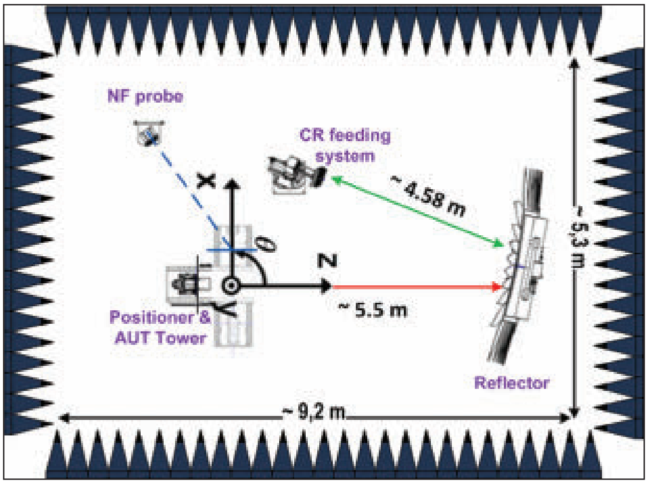

▲ *Fig. 3 Schematic showing the combined compact antenna test range and spherical near field antenna measurement facility at the IHF in Aachen, Germany.*

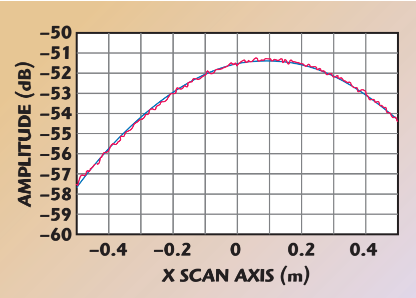

▲ *Fig. 4 H-plane Quiet Zone scan at 55 GHz.*

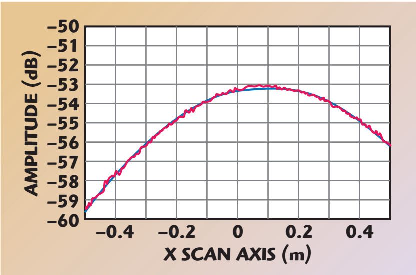

▲ *Fig. 5 H-plane Quiet Zone scan at 57 GHz.*

Figure 3). This is a combined compact antenna test range and spherical near field antenna measurement facility (CATR/SNF) with a frequency measurement capability from 800 MHz to 75 GHz. The SNF is used from 800 MHz up to 12 GHz, while the CATR covers the frequency range from 2 to 75 GHz.

A CATR is often operated in the transmit mode (i.e., the feed system illuminates a reflector creating a quasi plane wave region called the quiet zone (QZ)). The antenna under test (AUT) is situated in this region and its response to the stimulating field of the QZ is recorded. In this case, the AUT is characterized on receive. For the evaluation of this module, however, the CATR must also characterize the AUT in transmit.

Passivity of the system normally guarantees functionality, keeping in mind that the system is wavelength dependent.[11,12] It is important to realize that in a CATR, however, in order to operate in the dual-mode with minimal error, the AUT must create a plane wave at the reflector's surface that is, in turn, focused at the feed. The well-known criterion

$$r = 2D^2/\lambda \qquad (1)$$

where D is the maximum AUT size and λ is the operational wavelength, is a good approximation of the far field distance. This is the minimum separation between the AUT and the reflector required to ensure an approximate plane wave at the reflector's surface.[13] For the ARM, using the aperture plane of the horns as the phase center, this distance is 0.36 m at an operating frequency of 60 GHz. Given that the actual distance between the AUT positioner and the reflector is around 5.5 m, a plane wave condition at the reflector's surface is ensured. For this measurement an MI-Technology standard gain horn (SGH) model (MI-12-40)[14] is used as a receive feed.

The feed is connected to a Rohde & Schwarz two-port harmonic mixer. This mixer uses two parallel reverse-connected diodes, and requires no biasing.[15] The receiver is a Rohde & Schwarz FSP 40 spectrum analyzer containing a diplexer to separate the LO and IF signals which are fed on the same cable. The cable is short to preserve dynamic range by reducing high frequency signal losses.

MATLAB® is used to control the measurement process. Using visual basic scripting offered by the Active Cell software, the positioner, for example, is easily controlled using MATLAB. The spectrum analyzer is triggered by the positioning system

through the external triggering pin on its back panel (i.e., hardware triggering), ensuring correct sampling of the angular points.

MEASUREMENT RESULTS

Figures 4 and ***5*** show two plots for the QZ field acquired in the dual-mode, i.e., the ARM is in the transmit mode and moving across the QZ while the MI-12-40 SGH acts as a receive feed horn in the focal plane of the reflector. The red curves represent the actual measured QZ field, while the blue curves represent the second degree curve fitting polynomial. These help determine amplitude ripple and taper of the fields in the QZ and are, in turn, indicators of QZ quality at that specific frequency.[16]

Several observations are worth noting. First, the ripple effect is small while the taper effect is large. This is expected since the feed used is directive and very small compared to the reflector's size. Second, the amplitude difference between Figures 4 and 5 is due to the ARM, itself. Third, losses are mainly due to free-space and RF cable losses. The fourth and last observation is that there is a QZ center frequency shift, which is due to defocusing (i.e., defocusing from the optimum point, where the system is an offset-fed single reflector) of the feed that causes a reorientation (scanning) of the plane wave direction in the QZ. ***Figure 6*** illustrates this effect based on geometrical optics. The defocusing angle of the feed would in this case be around 1° ($\sin^{-1}$ of 0.1 m divided by 5.5 m – see Figures 3 and 4).

Figure 7 shows the H-plane pattern of the ARM at 55 GHz. This plot is taken for zero delay (i.e., both lines are fed in phase). The patterns are not symmetrical in shape, which indicates that the amplitudes of the excitation signals fed to the antenna are not equal, which is most likely due to asymmetry introduced during the assembly of the phase-shifter-to-horn transitions.

Figure 8 shows the pattern evolution at 55 GHz for a zero phase-shift voltage on line 1 and different phase-shift voltages on line 2. The figures show the scanning effect versus phase-shift voltage. For higher voltages, the ARM becomes insensitive as the phase shifter reaches saturation. To characterize the module from 60 to 65 GHz, an identical setup is used, employing an Anritsu signal analyzer

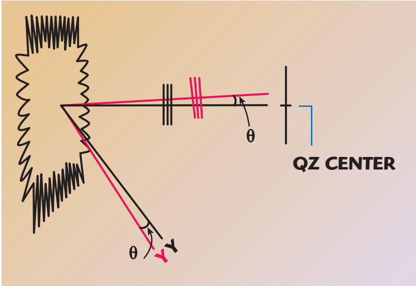

▲ *Fig. 6 Schematic showing the effect of feed defocus.*

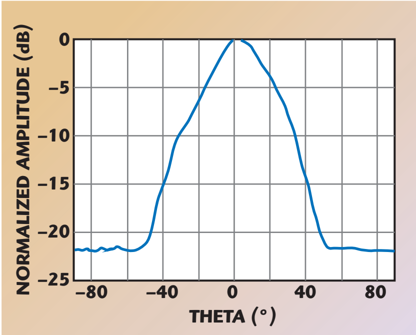

▲ *Fig. 7 H-plane pattern of the ARM at 55 GHz for zero delay.*

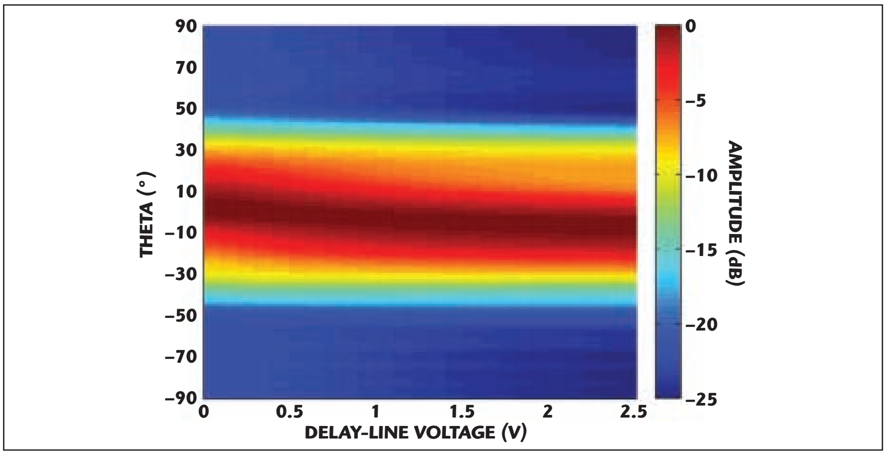

▲ *Fig. 8 H-plane patterns of the ARM at 55 GHz versus phase shift voltage setting.*

Keysight U2040 X-Series Wide Dynamic Range Power Sensors

The world's widest dynamic range: -70 to +26 dBm (96 dB)

Fast measurement speed: 10,000 readings-per-second

Choice of form factors: USB and LAN

Accuracy and repeatability across all common wireless signals

Internal zero and automatic calibration

Super fast. Super accurate. Super wide dynamic range.

Introducing a variety of power sensors that offer extremely high measurement speed and the world's widest dynamic range. Using Keysight BenchVue software for data capture/analysis, the sensors will allow you to obtain fast, accurate and repeatable measurements over a wide range of power levels. Choose from four USB models to test chipsets, radio systems, radar, mobile and handsets. Or choose the industry's first LAN and thermal vacuum-compliant power sensor for satellite testing.

HARDWARE + SOFTWARE + PEOPLE = INSIGHTS

USB LAN

Download an app note on fast, accurate power measurements for wireless test.
www.keysight.com/find/rfpowertips

USA: 800 829 4444
CAN: 877 894 4414

Scan to view video demo.

KEYSIGHT TECHNOLOGIES
Unlocking Measurement Insights

Agilent's Electronic Measurement Group has become **Keysight Technologies**.

(MS2830A)[17] with an external two-port harmonic mixer.

CONCLUSION

The process used to characterize a prototype active radar transmit module in a compact antenna test range is described. An active radar module, characterized over the frequency range of 55 to 65 GHz, is used to demonstrate measurements of pattern shaping and scanning depending on power and relative phase at its two apertures. ■

References

1. "Active Antenna Systems - A Step-Change in Base Station Site Performance," *Nokia Siemens Networks*, 2012.
2. S. Drabowitch, A. Papiernik, Hugh Griffiths, J. Encinas and B.L. Smith, *Modern Antennas*, 2nd edition, Springer, 2005.
3. P. Knott, T. Bertuch, H. Wilden, O. Peters, A.R. Brenner and I. Walterscheid, "SAR Experiments Using a Conformal Antenna Array Radar Demonstrator," *International Journal of Antennas and Propagation*, Vol. 2012, No. 142542.
4. T. Bertuch, P. Knott, H. Wilden and O. Peters, "Wide-Band Radar Front-End Calibration for Imaging SAR Experiments With Conformal Antenna Array," *Proceedings of the 5th European Conference on Antennas and Propagation*, April 2011, pp. 2610,2614.
5. W. Haselwander, M. Uhlmann, S. Wustefeld and M. Bock, "Measurement on an Active Phased Array Antenna on a Near-Field Range and an Anechoic Far-Field Chamber," *31st European Microwave Conference*, September 2001, pp. 1-5.
6. J.E. Hansen, "Spherical Near-Field Antenna Measurements," *Peter Peregrinus Ltd.*, London, UK, 1988.
7. www.ihf.rwth-aachen.de
8. K. Noujeim, J. Martens and T. Roberts, "White Paper - Frequency-Scalable Nonlinear-Transmission-Line-Based Vector Network Analyzers", *Anritsu*.
9. E.F. Knott, J.F. Shaeffer and M.T. Tully, *Radar Cross Section*, 2nd edition, SciTech Publishing Inc., Raleigh, NC, 2004.
10. M.I. Skolnik, *Radar Handbook*, 2nd edition, McGraw-Hill Inc., NY, 1990.
11. H. Shakhtour, R. Cornelius and D. Heberling, "Three Antenna Gain Determination Method in Compact Antenna Test Ranges," *Loughborough Antennas and Propagation Conference*, November 2013.
12. S. Brumley, "Extending the Low-Frequency Limits of the Compact-Range Reflector," *IEEE Antennas and Propagation Magazine*, Vol. 38, No. 3, June 1996, pp.81-85.
13. C.A. Balanis, *Antenna Theory: Analysis and Design*, 2nd edition, John Wiley & Sons, 1997.
14. www.mitechnologies.com/images/catalog/Antenna%20Solutions/MI-212_Family_of_Standard_Gain_Horns.pdf, accessed on 3 December, 2013.
15. "Harmonic Mixer, Operating Manual," Rohde & Schwarz Test and Measurement Division.
16. C.A. Balanis, *Modern Antenna Engineering*, John Wiley & Sons, 2008.
17. "MS2830A Operating Manual," www.anritsu.com/en-US/Products-Solutions/Products/MS2830A.aspx, accessed on 12 October 2013.

Hammam Shakhtour *received his B.Sc. degree in electrical engineering from Birzeit University, Birzeit, Palestine, in 2005 and his M.Sc. degree in electrical*

You're Covered!

New Hybrid Power Modules From 0.7 - 18 GHz

We have now complemented our previous line of 4-18 GHz Hybrid Power Modules (HPM's) to cover the entire 0.7 - 6 GHz frequency range in ONE amplifier module. These high gain 50 ohm module gain blocks provide up to 30 watts of Class A linear CW output power and up to 47 dB gain in a connectorized housing in applications where performance, size, and weight are critical. A higher power 50 watt Class AB configuration is also available when increased efficiency and lower cost is required while slightly sacrificing harmonic distortion. This design can meet the stringent requirements of today's military systems as well as being price competitive for wireless applications.

To obtain more detailed information on these and other narrow band custom modules and benchtop products call AR RF/Microwave Instrumentation at 215 723 8181 or visit us at www.arworld.us/covered.

www.arworld.us/covered

ISO 9001:2008 Certified

rf/microwave instrumentation

Other ar divisions: modular rf • receiver systems • ar europe

USA 215-723-8181. For an applications engineer, call 800-933-8181.

In Europe, call ar United Kingdom +44 1908 282766 • ar France +33147917530 • ar Deutschland +49 6101 80270 0 • ar Benelux +31 172 423000

www.arworld.us

engineering and information technologies from Karlsruhe Institute of Technology (KIT), Germany in 2009. He is currently at the Institute of High Frequency Technology (IHF), Aachen, Germany, working on near field measurement techniques for active antenna characterization as part of his Ph.D.

Dirk Heberling *studied electrical engineering and graduated from RWTH Aachen in 1987. He was employed as a scientist at the Institute for RF-Technologies, RWTH Aachen from 1987 to 1993. He received his Ph.D. (Dr.-Ing.) in 1993 for his thesis on conformal microstrip antennas. In 1993, Heberling joined IMST GmbH, Kamp-Lintfort to establish a new Antenna Section, and from 1995 to 2003 he was head of the Antennas Department, which was reorganized into the Department of Antennas and EMC in 1998. From 2003 to 2008, he took over the Department of Information and Communication Systems of IMST. He moved to RWTH Aachen in 2008 where he is currently head of the Institute and holder of the chair for High Frequency Technology.*

Karam Noujeim *received his graduate electrical engineering degrees in Canada starting with a master of engineering from McGill University in 1990, and an M.A.Sc. and Ph.D. from the University of Toronto in 1994 and 1998. In 2001, he was a visiting academic researcher at the Picosecond Electronics Laboratory, University of California, Santa Barbara. He was involved with the development of CAD tools for assessing the susceptibility of printed-circuit boards to electromagnetic interference (Bell-Northern Research, Ottawa, Jan. 1990 – Sept. 1992), and with the design of millimeter-wave components for LMDS (A divestiture of the Watkins-Johnson Company, Aug. 1998 – June 1999). In June 1999, he joined the Microwave Measurements Division of Anritsu Co. (formerly known as Wiltron), in Morgan Hill, Calif., as a senior microwave design engineer. In this role, Noujeim designed millimeter-wave transmitters, receivers and antennas for automotive-radar testing; NLTL-based directional samplers, harmonic generators, frequency-extension modules and sub-systems for a wide variety of measurement instruments; and high-sensitivity micro-machined thermal power sensors. He is currently a fellow hardware engineer and leads the technology group of Anritsu-USA's emerging business operations.*

Ferdinand Gerhardes *studied communication electronics with a focus on radar and navigation at University of Federal Armed Forces, Hamburg and finalized his Dipl.-Ing. Nachrichtentechnik in 1987. Until 1994 he served as an electronic warfare officer and entered industry at Fuba Hans Klobe & Co. For the last 20 years, Gerhardes has been engaged in the wireless industry, holding several marketing and sales positions.*

Peter Knott *received his Diplom-Ingenieur and Ph.D. degree from RWTH Aachen University, Germany, in 1994 and 2003. In 1994 he joined the Fraunhofer Institute for High Frequency Physics and Radar Techniques FHR (formerly FGAN e.V.) in Wachtberg, Germany. The focus of his work was design and development of antenna arrays and active antenna front ends as well as electromagnetic modelling and beamforming methods for conformal antenna arrays. Since 2005 Knott has been head of the Department Antenna Technology and Electromagnetic Modelling (AEM).*

MWJ REVIEW BOARD APPROVED

Compact Metamaterial Based Bandstop Filter

M. Palandöken
Gediz University, İzmir, Turkey
A. Sondas
Kocaeli University, Kocaeli, Turkey

A compact, highly selective, bandstop filter (BSF) is presented with numerical and experimental results. It is additionally modelled with lumped circuit elements in an equivalent circuit model (ECM) to describe resonator coupling and corresponding phase shift. The filter is composed of two electrically small metamaterial cells in the form of fractal resonators. The physical size of the main filtering section is as small as $\lambda_o/30 \times \lambda_o/14.64$, while the total size of the filter with the feed line sections is $\lambda_o/10.53 \times \lambda_o/6.6$. Measurements demonstrate frequency selectivity of 63.80 and 92.10 dB/GHz at the lower and upper frequency band edges, respectively. The passband insertion loss is better than 0.5 dB below 0.6 GHz and above 2 GHz, with a minimum insertion loss of 0.1 dB. The signal suppression level is greater than 20 dB in the frequency band of 1.50 to 1.56 GHz.

Metamaterials are artificially structured materials composed of periodically arranged unit cells in a host medium in order to produce specific electromagnetic behaviours not observed in nature. The controllable engineering of electromagnetic material parameters in microwave component design enables new microwave applications.[1-7] With the aim of miniaturization, alternative structures have been proposed,[8-12] one of which is exploited in the design of this microwave BSF.

A magnetic metamaterial-inspired BSF is introduced to illustrate filter performance enhancement in a compact size. Microwave BSFs are widely used in transceivers to reduce distortion by suppressing spurious signals. They are attractive because they have better rejection than bandpass filters as the resonators in BSFs resonate not in the passband, but in the rejection band. In addition, the use of artificial metamaterials with self-resonating electrically small cells results in compact filters with high selectivity.[13,14] Fractal resonators are used because they are self similar structures that fill any restricted area in a conformal manner while decreasing the resonant frequency.[15] Thus, the spiralling form of fractal curves is the next miniaturization step for compact microwave component design.[16]

FRACTAL RESONATOR AND BSF DESIGN

The geometry of the fractal spiral resonator is shown in ***Figure 1***. Each of the outer and inner fractal rings is the mirror image of the first order Hilbert fractal curve. These two concentric Hilbert fractal curves are then connected

at one end to obtain a fractal spiral resonator. The circled section is an extension of the inner Hilbert curve, increasing its resonant length to compensate for the increased inductive and capacitive coupling between different sections. Substrate material is standard 0.5 mm thick Arlon DiClad 880 with dielectric constant 2.2. The metallization is copper. The copper line width and minimum distance between any two lines are 0.3 mm. The other geometrical parameters are L1 = 2.5 mm, L2 = 0.7 mm and L3 = 1.5 mm. The electromagnetic properties of fractal resonators are investigated extensively by Palandoken and Henke.[16]

Results from the numerical model of the BSF along with the fabricated prototype are shown in ***Figure 2***. Two fractal resonators are connected asymmetrically along the y-axis through the feed line in order to have symmetrical return loss. The resonators are separated from each other with a gap of 0.4 mm. Each is connected directly with the feed line to increase the field coupling (see the red circles in ***Figure 2a***). To obtain low insertion loss in the passband, the two feed ports are connected through surrounding transmission line sections on the outer side of each resonator. The separation distance between the resonators and feed line sections is 0.3 mm. The filter width (W) and length (L) are 13.3 and 6.5 mm, respectively. The width of each metallic line is 0.3 mm except the width of the feed line, which is 1.5 mm to feed both resonators with 50 Ω line impedances at each port. The length of feed line sections at each port is 6 mm. The total size of the BSF is 18.5 mm.

The fractal resonators are fed directly through the feed line. The high impedance at the open end of each fractal resonator is then transformed into a low line impedance at the resonant frequency, as is the case for λ/4 resonators, in order to have high rejection in the stop band. In the passband, the incoming signal is transmitted with low insertion loss to the output port through the surrounding transmission line sections. The ECM of the BSF can therefore be derived as shown in ***Figure 3***.

The fractal spiral resonator (res1) can be modeled as a series resonant circuit with corresponding inductor (L1) and capacitor (C1) due to the λ/4 resonance at the stopband frequency.

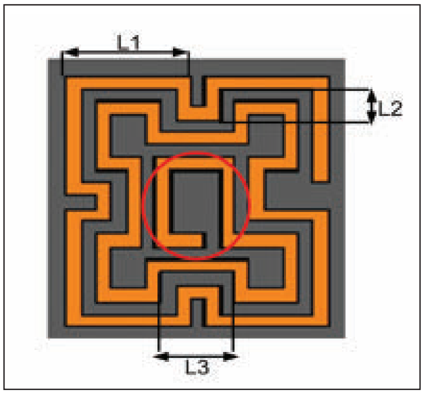

Fig. 1 Fractal spiral resonator geometry.

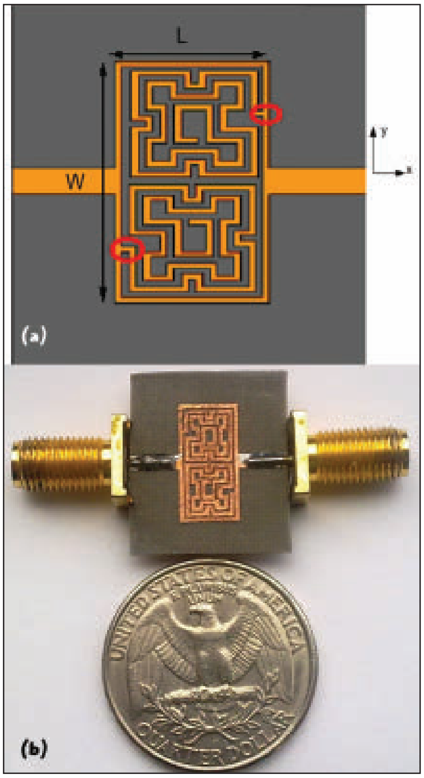

Fig. 2 Numerical model results (a) and BSF fabricated prototype (b).

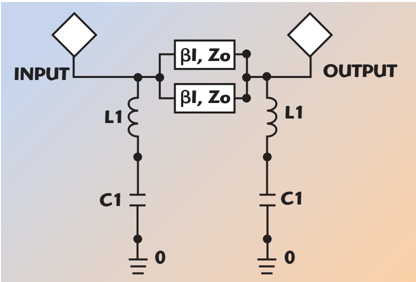

Fig. 3 BSF equivalent circuit model with distributed and lumped circuit elements.

The magnetic or electrical coupling between two fractal spiral resonators is negligibly small, as verified by numerical calculations with only one resonator and then with two resonators without any connecting transmission line sections. The surrounding transmission line sections are modeled as two parallel microstrip lines with electrical lengths of βl and line impedance Z_0. The input impedance of equivalent circuit is calculated as

$$Z_{in} = Z_{res1}Z_0\left(2Z_{res1}Z_2 + j\left(Z_{res1} + Z_2\right)Z_0 \tan\left(\beta 1\right)\right)/$$
$$Z_0\left(2Z_{res1}Z_2 + j\left(Z_{res1} + Z_2\right)Z_0 \tan\left(\beta 1\right)\right) +$$
$$Z_{res1}\left(2Z_0\left(Z_{res1} + Z_2\right) + j4Z_{res1}Z_2 \tan\left(\beta 1\right)\right) \qquad (1)$$

where Z_2 is the port impedance of second port, which is 50 Ω and

$$Z_{res1} = \frac{1 - \omega^2 L_1 C_1}{j\omega C_1} \qquad (2)$$

The input impedance is used to calculate the reflection and transmission parameters of the ECM. Ohmic losses are neglected for simplicity; however, these losses can be included in the formulation by substituting L and C with L^* and C^*, assuming that the R and Q values are known at a specific frequency.

$$L^* = L + \frac{R}{j\omega} = \frac{\left(jQ+1\right)}{j\omega}R$$
$$C^* = C + \frac{1}{j\omega R} = \frac{\left(jQ+1\right)}{j\omega R} \qquad (3)$$

The S-parameters are easily calculated from the Z-parameters of the symmetric equivalent RF circuit with only two unknown matrix elements, $Z_{11}=Z_{22}$ and $Z_{21}=Z_{12}$ for the lossy case. Z parameters are calculated as

$$Z_{11} = Z_{22} = Z_{res1}Z_0\left(2Z_{res1} + Z_0 \tanh\left(\gamma 1\right)\right)/ \qquad (4)$$
$$Z_0\left(2Z_{res1} + Z_0 \tanh\left(\gamma l\right)\right) + Z_{res1}\left(2Z_0 + 4Z_{res1} \tanh\left(\gamma l\right)\right)$$

$$Z_{12} = Z_{21} = Z_{res1}^2 Z_0\left(2Z_0 + 4Z_{res1} \tanh\left(\gamma 1\right)\right)/$$
$$\left(Z_0 \cosh\left(\gamma l\right)\right) +$$
$$Z_{res1} \sinh\left(\gamma l\right)\left(4Z_0Z_{res1} + \left(Z_0^2 + 4Z_{res1}^2\right)\tanh\left(\gamma l\right)\right)$$

γ =α + jβ, where β and α are propagation and attenuation constants, respectively.

Return and insertion losses of the BSF are numerically calculated to determine element values of the ECM as a first order approximation. The fabricated prototype is also measured to illustrate the filter performance experimentally and validate the design principle.

NUMERICAL AND EXPERIMENTAL RESULTS

Numerical analysis of the BSF is done using Ansoft HFSS, which is an FEM-based 3D EM full-wave simulation program. The results are experimentally verified with measurements from a Rohde & Schwarz ZVB8 Vector Network Analyzer. As shown in ***Figure 4***, the measured return loss is greater than 10 dB for frequencies lower than 0.8 GHz and higher than 2 GHz in the frequency band of 0.5 to 3 GHz, while the measured insertion loss is less than 0.5 dB in the passband. The measured rejection is greater than 20 dB in the frequency band of 1.5 to 1.56 GHz

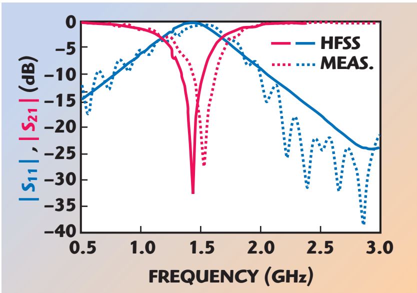

▲ *Fig. 4 Measured and numerically simulated reflection/transmission parameters.*

Planar Monolithics Industries, Inc.

Offering State-Of-The-Art RF and Microwave Components & Integrated Assemblies From DC to 40GHz

- Amplifiers
- Attenuators - Variable
- DLVA & ERDLVA & SDLVA's
- DTO's & Frequency Synthesizers
- Filters
- Form, Fit & Function Products
- IFM's & Frequency Discriminators
- Integrated MIC/MMIC Modules
- I/Q Vector Modulators
- Limiters & Detectors
- Log Amplifiers
- Pulse & Bi-Phase Modulators
- Phase Shifters
- Rack & Chassis Mount Products
- Receiver Front Ends & Transceivers
- Single Sideband Modulators
- SMT & QFN Products
- Solid-State Switches
- Switch Matrices
- Switch Filter Banks
- Threshold Detectors
- USB Products

ASSOCIATION OF OLD CROWS
Booth #711
October 6 - 9

WASHINGTON, D.C. ★ OCTOBER 6-9, 2014
51ST ANNUAL AOC INTERNATIONAL SYMPOSIUM CONVENTION

ANTENNA MEASUREMENT TECHNIQUES ASSOCIATION
AMTA 2014 TUCSON
Booth #30
Tucson, Arizona
October 12 - 17

100MHz to 18GHz Transceiver
3U Open VPX Architecture

Simplified Functional Block Diagram

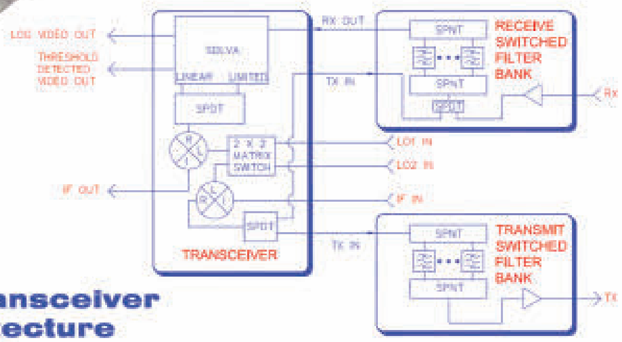

- 0.1 to 18.0 GHz Transceiver
- 3U Open VPX Architecture
- VITA 67 RF Interface
- Up to 4GHz Instantaneous Bandwidth
- Customizable Switched Filter Banks
- BIT Test Mode for Closed Loop Testing
- Linear & Limited RF, SDLVA Output Channels
- Log & Threshold Video SDLVA Output Channels
- Time Gated SDLVA's for Pulse Blanking
- CW Immunity
- Input Selection for Two Independent LO
- frequencies (4 to 20GHz)
- -80 to +10dBm Input Power Range
- IF Frequency of 100MHz to 4.0GHz
- LVDS Control Logic
- Ruggedized Construction for Military Applications
- 160mm x 100mm x 12HP per VITA 46 Standards (6.299" x 3.937" x 2.388")

West Coast Operation:
4921 Robert J. Mathews Pkwy, Suite 1
El Dorado Hills, CA 95762 USA
Tel: 916-542-1401 Fax: 916-265-2597
ISO9001:2008 REGISTERED
Email: sales@pmi-rf.com

East Coast Operation:
7311-F Grove Road
Frederick, MD 21704 USA
Tel: 301-662-5019 Fax: 301-662-1731
ISO9001:2008 REGISTERED
Website: www.pmi-rf.com

Hermetic Sealing, High Reliability to Mil-Std-883, Small Quantity Requirements accepted & we offer Custom designs too.

and 27.5 dB at 1.54 GHz. Numerical and experimental results agree well even though there are some ripples in the measured data as well as a small frequency shift between the numerical and experimental results due to fabrication, calibration and cabling-related errors.

The circuit element values of the ECM in Figure 3 are extracted by equations (1 through 4) and additional RF numerical simulations. They are tabulated in ***Table 1***, neglecting ohmic losses as a first order approximation. RF performance of the ECM with tabulated element values is also verified by the circuit simulator in Ansoft Designer. S-parameters calculated by ADS are shown in ***Figure 5***.

These results confirm the analytical formulation of the ECM. Figures 4 and 5 show that the ECM describes the frequency dependence of scattering parameters and the operation of the BSF quite well even though there are some discrepancies in the Q of the modelled and experimentally verified resonator designs. There are three main reasons for this. First, the capacitive and inductive coupling between fractal resonator and surrounding transmission line are neglected as a first order approximation. Second, the metallic loss, which degrades resonator Q, thereby affecting the resonant frequency and scattering parameters, is neglected for model simplicity. This is seen in higher return loss, lower insertion loss and higher Q calculated from the circuit model in comparison to calculations from the numerical model. Third, the circuit model is based on the calculation of circuit elements for a λ/4 resonator. This is not true for frequencies far from resonance, however, where the wave feature of the RF signal must be modelled by distributed circuit elements

TABLE I

EQUIVALENT CIRCUIT MODEL PARAMETERS

L_{res1}	12 nH
C_{res1}	1.2 pF
βl	5°
Z_0	70 Ω

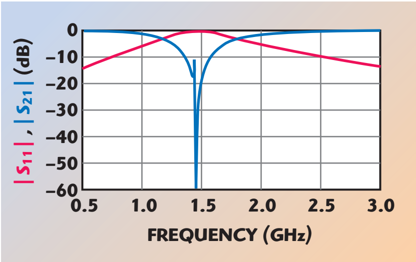

▲ *Fig. 5* $|S_{21}|$ *and* $|S_{11}|$ *of the ECM calculated by ADS.*

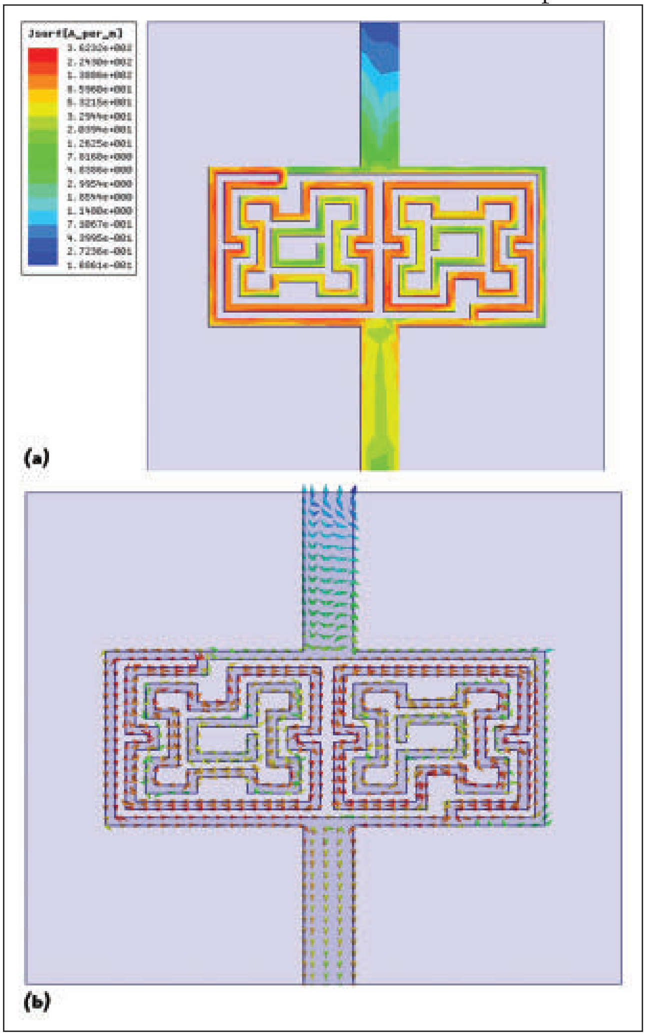

▲ *Fig. 6 BSF Resonant current distribution at the stopband frequency, magnitude (a) and direction (b).*


38GHz
60GHz
24GHz
79GHz

or additional reactive lumped elements in a more complex circuit model.

The operating principle of the BSF can be described with the help of the ECM in Figure 3. Transmission of the incoming signal is blocked in the stopband by the $\lambda/4$ spiral resonator. The electrical lengths and field coupling emerging from the surrounding transmission line cause the identical fractal resonators to split into two resonances. The resonant field distribution is shown in ***Figure 6***. As a result of the $\lambda/4$ resonance, the high impedance at the open end of each fractal resonator is transformed into a low impedance at the feed line with high reflection at the resonant frequency.

The frequency selectivity of the BSF is 63.8 and 92.1 dB/GHz at the lower and upper 3 dB frequency band edges. The measured resonant frequency is shifted from the calculated resonant frequency by 100 MHz. This is due mainly to fabrication-related geometrical differences and calibration imposed measurement deviations, which could be deduced from S_{11} and S_{21}. This filter has no matching network, which is advantageous in reducing its physical size. The physical size of the main filtering section is $\lambda_o/30 \times \lambda_o/14.64$ at 1.54 GHz, which is quite compact in comparison to the conventional stepped impedance or coupled line filters. The total size of the filter with the transmission line sections at input and output ports is $\lambda_o/10.53 \times \lambda_o/6.6$.

CONCLUSION

A compact, high selectivity BSF composed of two metamaterial cells of spiral fractal resonator is modelled with lumped and distributed circuit elements in an ECM to explain the functional description of spiral resonators and surrounding transmission line. The total physical dimensions of the BSF are $\lambda_o/10.53 \times \lambda_o/6.6$ with a very compact main filtering section of $\lambda_o/30 \times \lambda_o/14.64$. The insertion loss is better than 0.5 dB in the frequency band lower than 0.6 GHz and higher than 2 GHz with the minimum insertion loss of 0.1 dB. No matching network is required, which effectively reduces the total filter size. Insertion and return loss are numerically calculated and experimentally measured, showing good agreement with the ECM. Frequency selectivity of 63.8 and 92.10 dB/GHz at the lower and upper frequency band edges makes the filter quite suitable for use in modern communication and sensor applications.■

References

1. G.V. Eleftheriades and K.G. Balmain, *Negative Refraction Metamaterials: Fundamental Principles and Applications*, NJ, Wiley Interscience, 2005.
2. T. Kodera, D.L. Sounas and C. Caloz, "Magnetless Nonreciprocal Metamaterial (MNM) Technology: Application to Microwave Components," *IEEE Transactions on Microwave Theory and Techniques*, Vol. 61, No. 3, March 2013, pp. 1030-1042.
3. Y. Dong and T. Itoh, "Promising Future of Metamaterials," *IEEE Microwave Magazine*, Vol. 13, No. 2, March 2012, pp. 39-56.
4. W. Zhang, H. Chen and H.O. Moser, "Subwavelength Imaging in a Cylindrical Hyperlens Based on S-String Resonators," *Applied Physics Letters*, Vol. 98, No. 7, February 2011, pp. 073501-073501-3.
5. S. Yun, F. Namin, D.H. Werner, T.S. Mayer, C. Bungay, C. Rivero-Baleine and L. Zhang, "Demonstration of a Nearly Ideal Wavelength-Selective Optical Mirror Using a Metamaterial-Enabled Dielectric Coating," *Applied Physics Letters*, Vol. 102, No. 17, April 2013, pp. 171114–171114-5.
6. Z. Zhu, X. Zhang, J. Gu, R. Singh, Z. Tian, J. Han and W. Zhang, "A Metamaterial-Based Terahertz Low-Pass Filter With Low Insertion Loss and Sharp Rejection," *IEEE Transactions on Terahertz Science and Technology*, Vol. 3 , No. 6 , November 2013, pp. 832–837.
7. C.H. Liu and N. Behdad, "Tunneling and Filtering Characteristics of Cascaded-Negative Metamaterial Layers Sandwiched by Double Positive Layers," *Journal of Applied Physics*, Vol. 111, No. 1, January 2012, pp. 014906-014906-9.
8. Z. Wu, Y. Shim and M. Rais-Zadeh, "Miniaturized UWB Filters Integrated With Tunable Notch Filters Using a Silicon-Based Integrated Passive Device Technology," *IEEE Transactions on Microwave Theory and Techniques*, Vol. 60, No. 3, March 2012, pp. 518-527.
9. K. Mo, Q. Wang, D. Song and Y. Tan, "A Novel Compact Ridge Waveguide Band-Stop Filter for Harmonic Suppression," *International Workshop on Microwave and Millimeter Wave Circuits and System Technology*, April 2012, pp. 1–3.
10. J. De Dios Ruiz and J. Hinojosa, "Shunt Series LC Circuit for Compact Coplanar Waveguide Notch Filter Design," Microwaves, Antennas & Propagation, *IET*, Vol. 8, No. 2, January 2014, pp. 125-129.
11. M. Hayati and A. Abdipour, "Compact Microstrip Lowpass Filter With Sharp Roll-Off and Ultra-Wide Stop-Band," *Electronics Letters*, Vol. 49, No. 18, August 2013, pp. 1156-1160.
12. R. Habibi, C. Ghobadi, J. Nourinia, M. Ojaroudi and N. Ojaroudi, "Very Compact Broad Band-Stop Filter Using Periodic L-Shaped Stubs Based on Self-Complementary Structure for X-band Application," *Electronics Letters*, Vol. 48, No. 23, November 2012, pp. 1483-1484.
13. R. Marques, F. Martin and M. Sorolla, *Metamaterials with Negative Parameters: Theory, Design and Microwave Applications*, NJ, Wiley-Interscience, 2007.
14. C. Caloz and T. Itoh, *Electromagnetic Metamaterials: Transmission Line Theory and Microwave Applications*, NJ, Wiley-Interscience, 2007.
15. N. Engheta and R.W. Ziolkowski, *Electromagnetic Metamaterials: Physics and Engineering Explorations*, NJ, Wiley-IEEE Press, 2006.
16. M. Palandoken and H. Henke, "Fractal Spiral Resonator as Magnetic Metamaterial," *IEEE Applied Electromagnetics Conference*, December 2009, pp. 1-4.

Designing Multiconductor RF Backplane Connectors for Embedded Computing

Stephen Morley
TE Connectivity, Mount Joy, Pa.

The rapid advances in radio frequency (RF) technology after World War II provided the building blocks for the highly agile radar and high speed communications systems in use today. Innovations in RF signal processing, integrated electronics and miniaturization of interconnects have contributed to the evolution of radar from large and cumbersome narrow-bandwidth systems requiring mechanical articulation of the antennae to locate and track targets, to the active electronically scanned array (AESA) radar systems in use today. The AESA radar systems can form multiple beams on a single antenna panel, with the capability to track numerous targets simultaneously, providing a significant advantage to the modern warfighter on land, at sea and in the air.

Communications systems have also evolved to have greater bandwidth and range that enable the secure encrypted transmission of large packets of data. As open-architecture embedded systems grow smaller and more sophisticated, designers are looking for ways to package a larger number of interconnections into high-density arrays. The modularity of embedded systems and the need to integrate RF functionality offered the opportunity to create a separable RF daughtercard/backplane interface within the system architecture.

ORIGINS OF VITA 67

Before the arrival of open architecture VPX and the requirement for separable mixed signal connectivity at the backplane/daughtercard interface, there were no standards to ensure interoperability of RF, optical, signal and power. Providers of equipment either used front panel connectors or customized coaxial backplane configurations for analog, video and RF signals. Although many interconnect products were applied for this purpose – multi-sourced, interchangeable connectors were not common.

Systems integrators saw the need for separable, multiconductor, blind-mate RF connections at the daughtercard/backplane interface to simplify the routing of RF signals and eliminate the need for front panel RF cable jumpers. Jumpers present the inherent possibility of cross-connection and/or damaged connectors. A number of VITA 46 committee members recognized the need for a standardized framework for the application of multiple RF blindmate coaxial interconnects and established a working group within the VITA Standards Organization (VSO). Initially the RF effort was under a subcommittee, VITA 46.14; however, this effort was later broken out into a separate

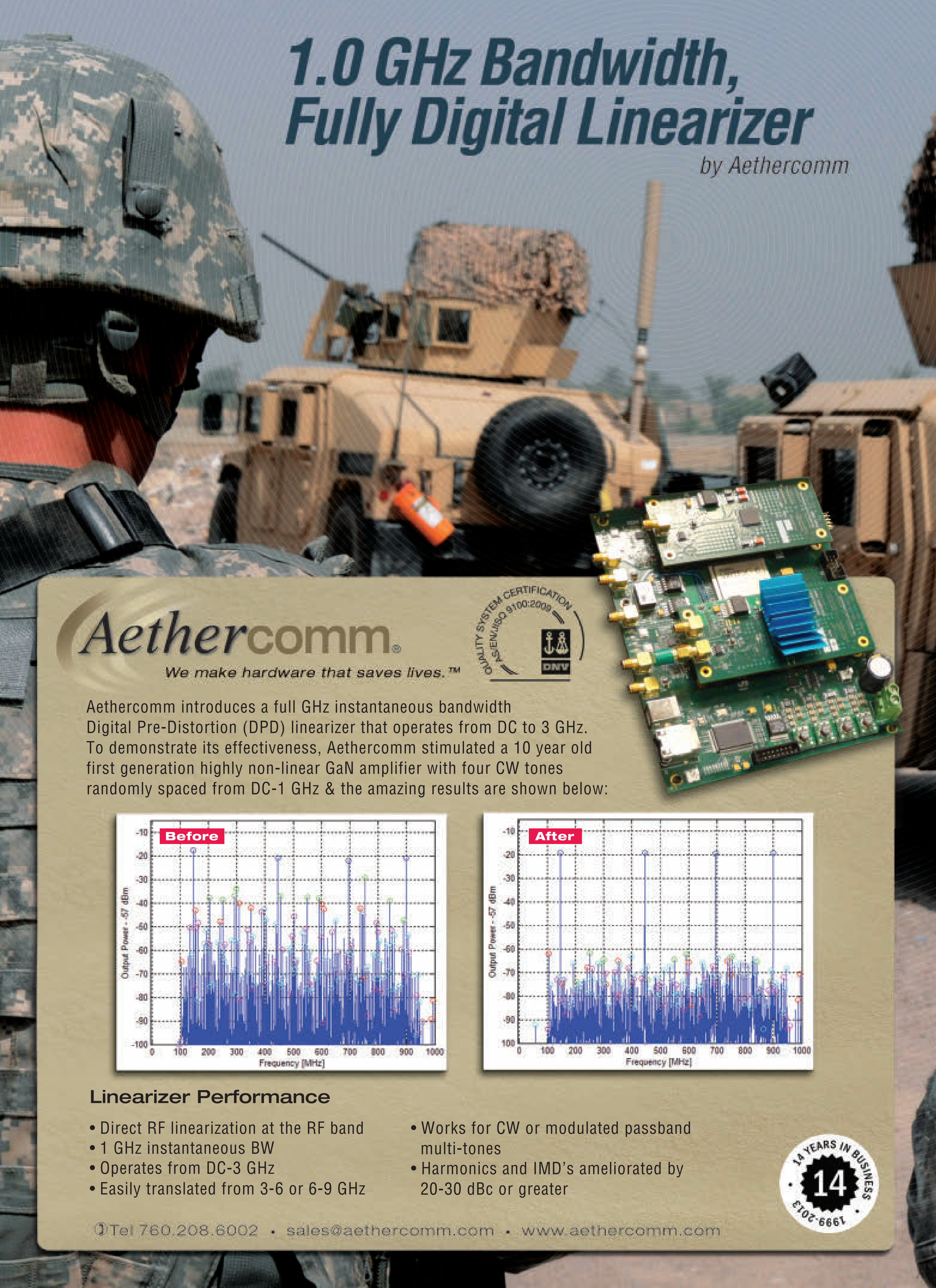
1.0 GHz Bandwidth,
Fully Digital Linearizer
by Aethercomm
Aethercomm®
We make hardware that saves lives.™
QUALITY SYSTEM CERTIFICATION AS/EN/ISO 9100:2009
DNV
Aethercomm introduces a full GHz instantaneous bandwidth Digital Pre-Distortion (DPD) linearizer that operates from DC to 3 GHz. To demonstrate its effectiveness, Aethercomm stimulated a 10 year old first generation highly non-linear GaN amplifier with four CW tones randomly spaced from DC-1 GHz & the amazing results are shown below:
Before
Output Power - -57 dBm
Frequency [MHz]
After
Output Power - -57 dBm
Frequency [MHz]
Linearizer Performance
• Direct RF linearization at the RF band
• 1 GHz instantaneous BW
• Operates from DC-3 GHz
• Easily translated from 3-6 or 6-9 GHz
• Works for CW or modulated passband multi-tones
• Harmonics and IMD's ameliorated by 20-30 dBc or greater
14 YEARS IN BUSINESS
14
1999-2013
Tel 760.208.6002 • sales@aethercomm.com • www.aethercomm.com

working group. The product of this working group is the "ANSI/VITA 67 Standard for Coaxial Interconnects on VPX."

CONTACT CHOICE AND SIZE REQUIREMENTS

The requirements of form, footprint and performance for the VITA 67 RF interconnect system were generated from customer input gathered through many voice-of-the-customer (VOC) interviews conducted with major military and aerospace integrators and subsystem suppliers.

With consideration that the RF interconnect structure must fit into existing VPX systems, ANSI/VITA 46 dictated the footprint for the RF modules. The RF modules are required to be a form fit to replace MULTIGIG RT 2 full- and half-size signal connector modules; the contact design must accommodate blind-mate application with total axial float of 2 mm and radial float of 0.25 mm. The connector pitch, which was driven by the requirement to accommodate small diameter (22 to 29 AWG) RF cables with low-transmission-loss characteristics is a compromise between density and performance. The SMPM series connector was chosen for this application because it best satisfies the density, performance, durability and blind-mate requirements. Three main factors favored the SMPM connector:

- Its interface configuration is standardized in MIL-STD-348.

▲ *Fig. 1 VITA 67 RF modules provide a standardized board-to-board interface.*

- The connector is 30 percent smaller than the SMP series, yet accommodates the same standard and low-loss 0.047" and 0.086" diameter flexible, conformable and semi-rigid cable sizes.
- Its size permits eight RF contacts to be easily arranged within the footprint of a full-size MULTIGIG RT 2 connector module.

While SMPM connectors have a maximum operating frequency of 65 GHz, the VITA 67 standard requires only a frequency range of DC to 26.5 GHz. This provides considerable capability to accommodate future requirements. ***Figure 1*** shows VITA 67 modules.

The application of connectors in a blind-mate configuration requires a design that allows sufficient axial and radial float to accommodate the variations in positional tolerances that are common in implementations of blind-mate interconnects. The design must incorporate features that provide accurate placement and critical contact alignment to achieve a proper and reliable connection and avoid damage due to stubbing.

The conventional solution for RF blind-mating is to use a pair of pin contact receptacles with a floating jack-to-jack "bullet" connector between them. This configuration has two separable interfaces per signal path. This approach, however, is problematic because of the dimensional variability where multiple interconnects are used. It is unlikely that all of the connectors will ever be fully mated, due to accumulation of axial tolerance variations. The mating uncertainty of this configuration results in degraded electrical performance caused by a "gap" that introduces an inductive response. This "gap" permits the bullet contact to move when subjected to vibration or mechanical shock and can result in the generation of microphonic noise. This condition is an unacceptable deficiency, considering the level of vibration and mechanical shock performance required by the ANSI/VITA 47 Environmental Specification.

The illustration in ***Figure 2*** shows the center connector stack at least material condition (LMC) flanked by two connector stacks at the maximum material condition (MMC), depicting a worst-case scenario where one of the three connector stacks is not fully mated. The jack-to-jack spring bullet is one solution to this tolerance problem; however, it has some signal integrity problems and is costly.


Expanding Portfolio Enabling The Internet of Things
72

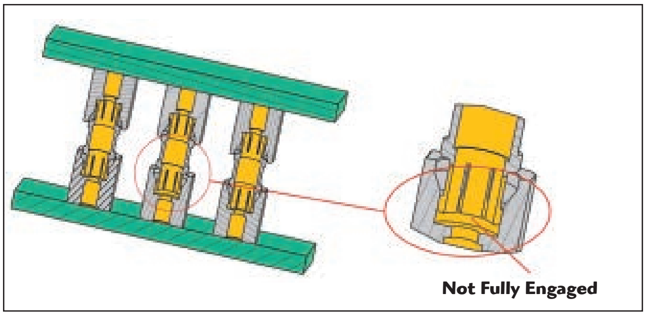

▲ *Fig. 2 Gap in mated connectors can degrade electrical performance.*

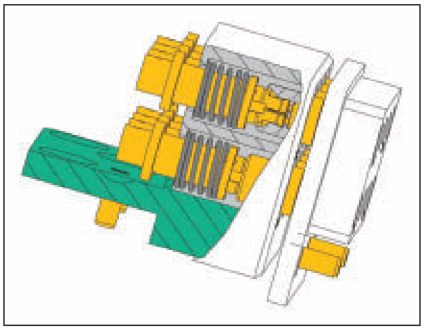

▲ *Fig. 3 VITA 67 mated pairs.*

VITA 67 RF modules use a two-connector SMPM configuration: a float-mounted cable jack and a fixed plug receptacle. The interfaces are in accordance with MIL-STD-348, except for a minor modification that increases the plug receptacle entrance diameter from a nominal 0.114" to 0.130" (2.9 to 3.3 mm) to provide a more generous capture range. Furthermore, the outer contact beams on the SMPM jack were analyzed using the ANSYS Workbench platform and configured to optimize contact durability when used in conjunction with a smoothbore receptacle. The SMPM cable jack is spring mounted to allow both axial and radial float. The spring force at preload is set to overcome the mating forces, and the force when fully mated is set high enough to maintain the fully mated condition under shock and vibration.

In the application of float-mounted connectors, the designer should consider that the attached cables contribute to the overall mass of the floating connector and therefore must be supported with an adequate strain relief mechanism. A cross-sectional view of an ANSI/ VITA 67.1 RF module mated pair is shown in ***Figure 3***.

Since the slotted outer conductor on the SMPM jack is a known path for RF leakage, features are required in the RF module design to mitigate cross-channel interference (isolation) and provide immunity from radiated susceptibility and emissions. This is accomplished in the VITA 67 RF module design by positioning the SMPM interface within a metal shell.

When the connectors are fully mated, this configuration benefits from the resulting two overlapping metal rings surrounding the slotted outer conductor of the jack (socket) connector. The overlapping rings improve the isolation between contacts (see ***Figure 4***).

The VITA 67 contacts are housed in robust stainless steel or aluminum modules that hold four (VITA 67.1) or eight (VITA 67.2) contacts. Contact spacing is 0.240" (6.1 mm), which represents a compromise in combining contact density and electrical isolation. The modules are configured to provide RFI/EMI shielding between the contacts and provide a high level of adjacent channel isolation of at least 100 dB up through 30 GHz. To put this in perspective, under similar conditions, the shielding effective-

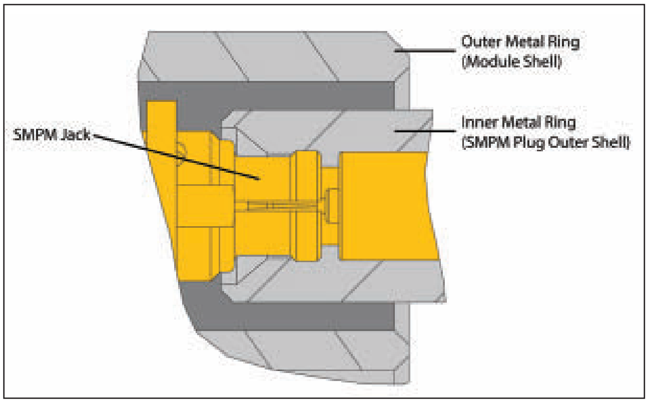

▲ *Fig. 4 Overlapping metal rings help increase cross-channel isolation.*

TABLE I VITA 67 ELECTRICAL REQUIREMENTS	
Operating Frequency Range	DC to 26.5 GHz
Flatness (Transmission Loss)	±1.0 dB, DC to 26.5 GHz
Transmission Loss	<0.12 dB
VSWR (Max.)	
Up to 10 GHz	1.15:1
10 to 26.5 GHz	1.25:1
26.5 to 40 GHz	1.35:1
DWV	
Isolation (Channel – Channel)	
3 to 30 MHz (HF)	>100 dBc
30 to 3 GHz (VHF/UHF)	>120 dBc
3 to 30 GHz (SHF)	>140 dBc
RF Power (CW Avg.)	
30 MHz to 30 GHz (VHF/UHF)	>20 dBc
3 to 30 MHz (HF)	>30 dBc
Temperature Range	-65° to +105°C

TABLE II
QUALIFICATION TEST REQUIREMENTS (SOURCE: TE CONNECTIVITY)

Electrical	Mechanical	Environmental
Contact Resistance	Durability	Thermal Shock (non-operating)
Reflection Coefficient (SWR)	Engagement & Disengagement Forces	Operating Temperature
Insulation Resistance	Vibration Class, V3	Corrosion Resistance
Dielectric Withstanding Voltage	Mechanical Shock, Class OS2	Humidity/Temperature Cycling
Transmission Loss		
Frequency Response		
Isolation		
Power Handling		

ness of typical cable assembly is 90 to 100 dB. The physical configuration, electrical performance and durability of the RF module-SMPM interconnect system contributes to the achievement of system performance that meets or exceeds the requirements of the VITA 67 specification.

The two module sizes provide application flexibility. Four-position modules (VITA 67.1) are intended for 3U VPX, in slots P2/J2. Suited for 6U systems, the eight-position modules (VITA 67.2) can be used in slots P5/J5 or P6/J6. Figure 3 shows the modules in a 6U system in slot P6/J6. The modules, of course, are not restricted only to VPX applications. The RF module profile is low enough to support a 0.8" card pitch, and the design has inspired many application specific spin-off configurations with RF contact counts from 1 to 24.

SMPM series RF connectors are available in vertical board-mount and edge-launch versions for application on the backplane and daughtercard. Cabled versions are also available for PCB-mounted applications. Cable designs are available for a wide range of standard cables that includes 0.047" (MIL-DTL-17/151), 0.086" RG-405 (M17/133) semi-rigid cables, conformable cables and flexible cables. There are also a number of high-performance, low-loss and phase-stable cables available for applications requiring these attributes.

Recently, applications have emerged that require low-transmission-loss versions of these small diameter cables. Traditionally, lower transmission loss was achieved by selecting a larger cable size; however, the SMPM series connectors' small size limits the maximum cable diameter that may be used. The solution is to look to technology for the answer. There are a number of outstanding sources for small-diameter, low-loss coaxial cables. These low-loss cables typically use a larger center conductor and an insulator

core of a material and configuration that permits a higher wave propagation velocity than standard cables with a solid insulation core.

Cable-mount backplane and daughtercard connectivity have several benefits over board mounting: the RF performance—i.e., transmission loss and reflection coefficient—achieved when using cables is superior and more predictable than that of in-board transmission line structures. The application of cables typically has a lower installed cost than multilayer RF circuit boards and are easily reconfigured, replaced or repaired. The downside of cable configured interconnects is overall packaging density is somewhat compromised.

SIGNAL INTEGRITY

Once the basic form factors are addressed, the electrical performance of the interfaces must be verified. Overall, this means ensuring signal integrity. Simply put, signal integrity is the preservation of electronic data routed through an electronic system for processing. If unintelligible upon receipt, system function will be impaired. The end user relies on and often takes for granted the effective functionality of electronic systems. The failure of mission-critical electronics in military, aerospace and avionics systems can have dire consequences. With the increasing complexity and density of electronic systems, there are a number of factors that contribute to signal integrity. For an RF interface, the challenge for the signal integrity engineer is to:

- Minimize attenuation and crosstalk
- Minimize degradation of the signal due to reflective, absorptive and resistive losses
- Isolate the signal from interference generated internally from external sources such as power supplies. External sources may be in close proximity or, worse, intentional interference from jammers.

Table 1 summarizes the electrical performance requirements for VITA 67 RF modules.

TESTING

Although the VITA 67 RF modules use SMPM series connectors, much consideration was given to the module design configuration to accommodate the requirements of ANSI/VITA 47-2005 (R2007), “Standard for Design and Construction, Safety, and Quality for Plug-In Units.” A comprehensive test plan, summarized in ***Table 2***, was developed to verify compliance to the specified requirements. A total of 21 VITA 67 RF modules were submitted in eight separate test groups and monitored for compliance to the VITA 67 specification.

Swept data was taken for the three frequency bands shown in ***Figure 5*** to verify cross-channel isolation at both the near and far ends. Figure 5 shows the results. In addition, the load on the target channel was removed and the change was noted to be minimal. In all testing, the specification limits were verified.

During vibration and mechanical shock testing, the test specimens were monitored for discontinuities of 10

WIN SEMICONDUCTORS

Leading Global Communications

PP25/-21 0.25μm Power pHEMT

- 0.25μm PHEMT process on 100μm substrates
- Power performance at 8V and 10GHz: >1W/mm, PAE 56%, 14dB Gain

PP25-21 (Class-AB) Tuned for Pout

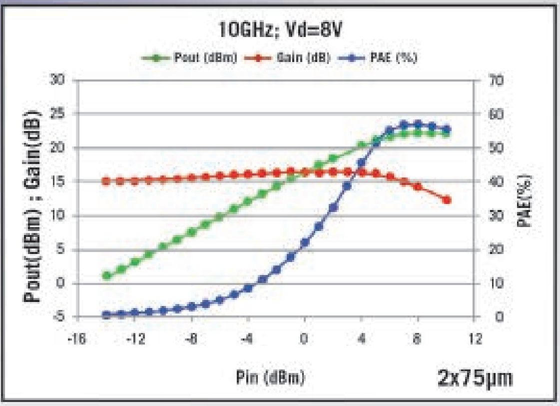

Gain (dB)	P1dB (dBm)	P1dB (mW/mm)	Psat (dBm)	Psat (mW/mm)	PAE Max(%)
15.0	22.1	1086	22.2	1114	56.8

2x75μm device @8V, 10GHz, 150 mA/mm

Summary of WIN mmWave pHEMT portfolio

	PP25-21	PP15-50/51	PL15-12	PP10-10/11
Gate length	0.25 μm	0.15 μm	0.15 μm	0.1 μm
Max Drain Bias	8 V	6 V	4 V	4 V
Idmax (Vg=0.5V)	490 mA/mm	620 mA/mm	525 mA/mm	760 mA/mm
Peak Gm	410 mS/mm	460 mS/mm	580 mS/mm	725 mS/mm
Vto	-1.15 V	-1.3 V	-0.7 V	-0.95 V
BVGD	20V(18V min)	16V(14V min)	9V(8V min)	10V(8V min)
f_T	65 GHz	90 GHz	100 GHz	130 GHz
f_{max}	190 GHz	185 GHz	150 GHz	180 GHz
Power Density (2x75μm)	1100 mW/mm @ 8V, 10GHz	870 mW/mm @ 6V, 29GHz	580 mW/mm @ 4V, 29GHz	860 mW/mm @ 4V, 29GHz (2x50μm)

WIN SEMICONDUCTORS CORP. Tel:+886-3-397-5999 Fax:+886-3-397-5069 http://www.winfoundry.com

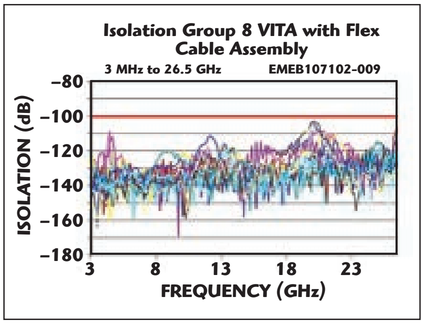

▲ *Fig. 5 Isolation test results.*

nanoseconds or greater using an energizing current of 100 mA. No discontinuities were detected.

VITA 67 RF modules were tested for power handling at 105°C, with RF CW power applied at 30 dBm from 3 to 30 MHz and at 20 dBm from 30 MHz to 26.5 GHz. The reflection coefficient (SWR) was monitored continuously and no significant variation was noted.

INTEGRATING VITA 67 INTO VPX AND APPLICATIONS

VITA 67 multi-position RF modules have been deployed globally in signals intelligence, radar, electronic warfare, and force protection applications. These applications cover the range of environments from naval systems to flight. With some applications using dozens of channels, installation and management of the RF modules and their cables become a new challenge. As with the VITA 66 fiber-optic modules, the interface includes a spring action to maintain engagement and help ensure high performance. This requires the integrators to provide secure injector/ejector and wedge-lock assemblies. Numerous companies have stepped into the VPX chassis space, and a wide variety of hardware catering to these new applications is now on the market.

Another packaging challenge brought about with the introduction of the VITA 67 modules is routing of cables for minimal loss, stability and ease of installation/repair. TE has developed a suite of solutions to assist in harness management, ranging from conformable strain reliefs to lightweight structures with integrated cable management features. These advances have made the integration and deployment of VITA 67 technology very convenient and have hastened the global adoption.

As users gain experience with VITA 67 modules, they are looking toward newer configurations that will offer advanced performance in several areas:

- Higher densities, with pitches under 0.10"
- Higher frequencies 50 to 65 GHz
- Direct board attachment
- More reliable blind-mating (non-stubbing)

As is the trend in electronics and electronic interconnects, evolution is a constant.■

Stephen Morley *is a product development engineer for TE Connectivity, Global Aerospace, Defense & Marine. He has more than 30 years experience designing, testing and analyzing microwave and radio frequency connectors, cable assemblies and components. Connect with Stephen at www.designsmarterfaster.com.*

Try NI AWR Design Environment Today!


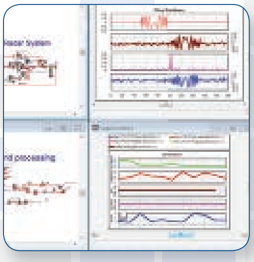
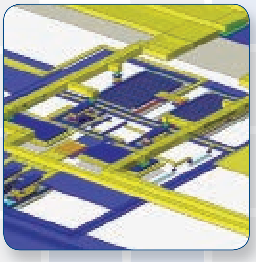
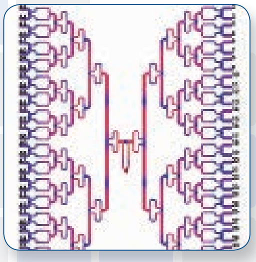
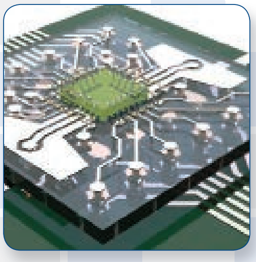

Microwave Office | Visual System Simulator | Analog Office | AXIEM | Analyst

Try NI AWR Design Environment

today and see for yourself how easy and effective it is to streamline your design process, improve end product performance, and accelerate time to market for MMICs, RFICs, RF PCBs, microwave modules, 3D/planar passive interconnects, antennas, communication systems, and more.

>> Learn more at ni.com/awr

NI AWR Design Environment consists of a comprehensive software product portfolio that offers a variety of high-frequency design tools that embrace system simulation, circuit simulation, and electromagnetic analysis.

- Microwave Office for MMIC, module, and RF PCB design
- Visual System Simulator for RF/comms. systems design
- Analog Office for analog and RFIC design
- AXIEM for 3D planar electromagnetic analysis
- Analyst for 3D FEM EM simulation and analysis

Visit **awrcorp.com/whatsnew** for a complete list of features found in the current version of NI AWR Design Environment.

MWJ REVIEW BOARD APPROVED

Wideband Balun-LNA with Noise Cancellation in 0.13 µm CMOS

Benqing Guo and Shiquan An
No.38 Research Institute of CETC, Hefei, China
Guoning Yang
Qualcomm Atheros Co. Ltd., Shanghai, China

A wideband common-gate (CG) and common-source (CS) CMOS balun-LNA with noise cancellation uses cross-coupled feedback between the CG input transistor and the cascode transistor of the CS input stage to increase LNA input transconductance. Fabricated using a 0.13 µm RF CMOS process, the LNA achieves a flat voltage gain of 18 dB, a NF of 2.7 to 3.2 dB, and an IIP3 of -4.5 to -7.4 dBm over a 3 dB band from 0.1 to 4.4 GHz. It consumes only 4.1 mA from a 1 V supply and occupies an area of 520 × 490 µm². This LNA has the merits of lower power consumption and lower supply voltage when compared to other reported wideband LNAs. It has comparable gain with negligible additional NF degradation.

With the wide variety of communication protocols in use today such as digital TV, WiMax and Bluetooth, a software-defined radio (SDR) accommodating multiple radio standards is more desirable than ever before.[1] This has motivated an increasing interest in wideband receiver techniques.[2]

The design of a key building block in a wideband receiving front end, the low noise amplifier (LNA), involves a compromise of noise figure (NF), bandwidth and power consumption. Two commonly adopted CMOS wideband LNA topologies are the capacitance cross-coupled (CCC) LNA[3] and the common-gate (CG) and common-source (CS) LNA.[4] The CCC LNA, however, requires an off-chip balun for single to differential input conversion. For wideband operation, an off-chip passive balun typically has high loss that degrades overall receiver NF.

In most cases, to receive single-ended signals from antennas and drive following differential mixers, a balun-LNA combining the active balun and the LNA into a single circuit becomes a more attractive option.[5] This makes the CG-CS LNA with an inherit balun function highly desirable, where wideband input matching, good voltage gain and possibly high linearity can be achieved simultaneously.[4,6] Nevertheless, to obtain low NF, a large amount of power must be consumed in its CS stage. This article describes an improved wideband CG-CS balun-LNA with noise cancellation. The CCC technique and bulk effect are adopted to boost the transconductance of the CG stage and the cascode transistor of the CS stage, both of which are beneficial for low noise and low power. Additional noise deterioration ascribed to the two techniques is negligible.

Need a Standard or Custom Filter? Anatech Has the Answer

That's because we design and manufacture every filter we sell. And with 25 years of filter design and manufacturing experience and a library of more than 5,000 designs, we can modify standard designs when others cannot.

- Change connector type
- Change the center frequency
- Widen or narrow the filter's bandwidth
- Achieve sharper transition from passband to stopband
- Modify or reduce the filter's footprint
- Weatherproof the filter for outdoor use
- Add hardware for every type of mounting
- Suggest design options that achieve desired performance at lower cost and reduced size
- …and many more options as well.

Seen our new Web site?

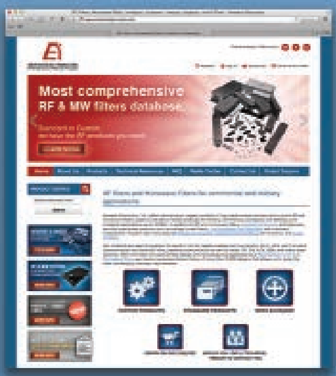

It makes finding a standard filter or specifying a custom one easier than ever!

ANATECH ELECTRONICS INC
RF & Microwave Filters & Related Products

Bring us your challenge, we'll provide the solution!

Call us at (973) 772-4242
Send us an email at sales@anatechelectronics.com
www.anatechelectronics.com

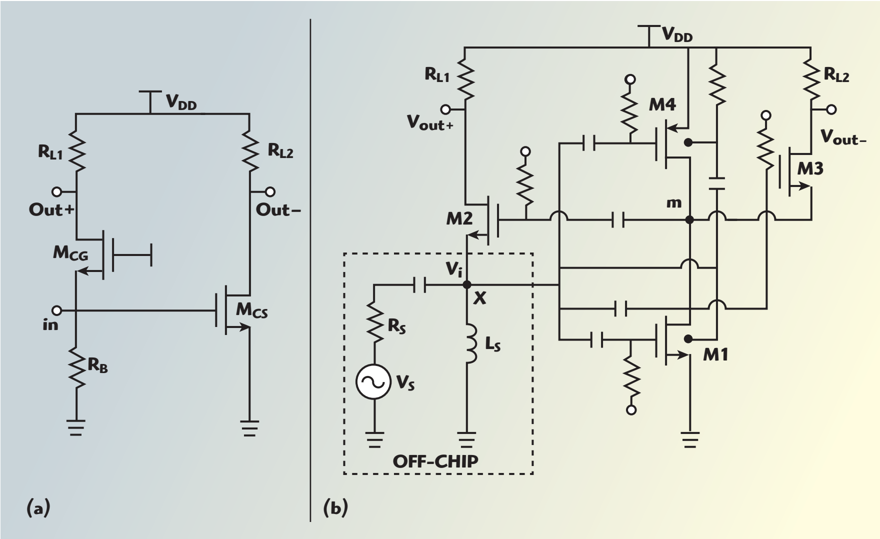

▲ *Fig. 1 Conventional CG-CS LNA (a) and CG-CS LNA with CCC feedback (b).*

LNA CIRCUIT

Figure 1a shows a conventional CMOS CG-CS LNA consisting of the CG input stage (M_{CG}) and the CS input stage (M_{CS}).[4] Thermal noise cancellation for M_{CG} and differential balanced gain can be guaranteed simultaneously by setting $g_{mCG}R_{L1}=g_{mCS}R_{L2}$, where g_{mCG} and g_{mCS} are the transconductance of M_{CG} and M_{CS}, respectively. To acquire overall low noise, g_{mCS} is often 3 to 5 times g_{mCG}. Consequently, the power consumption of the CS stage always occupies a majority of that of the whole LNA. To alleviate this, an inverting amplifier CS stage including the stacked NMOS and PMOS is used to increase the transconductance of CS stage under fixed power consumption. In addition, a feedback path is added from the drain of M_{CS} to the gate of M_{CG}, boosting the transconductance of M_{CG} and reducing power consumption.[6]

Figure 1b shows the design of a CMOS CG-CS LNA, consisting of the CG input stage (M2), the stacked CS input stage (M1, M4), and the cascode stage (M3). The CG input stage achieves the input impedance matching. The cascode M3 is designed mainly to reduce the Miller effect of the parasitic gate-drain overlap capacitance in the stacked CS input transistors. It also helps increase the output impedance and improves input–output isolation. CCC feedback is added between M2 and M3 to boost their transconductance. A bulk couple technique is adopted at the CS input transistors to further enhance effective transconductance. This is beneficial for the low noise and low power of the CS stage. The source choke inductor Ls and the equivalent parasitic capacitance observed at node x, are resonated for input matching to provide an overall low input reflection coefficient within the bandwidth.

Through small-signal analysis, the voltage gain of the proposed LNA, can be derived as

$$A_V \frac{V_{out+} - V_{out-}}{V_i} = \left(1 + A_{bst}\right)\left(g_{m3}R_{L2} + g_{m2}R_{L1}\right) \qquad (1)$$

where the g_m-boosting coefficient A_{bst} equals $(g_{m1}+g_{mb1}+g_{m4}+g_{mb4})/g_{m3}$. Parameters g_{mi}, g_{mbi}, R_{L1}, and R_{L2} are the gate transconductance and bulk transconductance of FETs and the load resistors of the CG and CS stages. For the balanced differential outputs, the relationship $g_{m3}R_{L2}=g_{m2}R_{L1}$ must be met. This is also the noise cancellation condition of M2 under the input impedance matching condition $Rs=1/_{gm2}(1+A_{bst})$. According to Wang et al.,[6] the gain is increased with the bulk effect of CS input transistors being utilized. Due to the feedback path from V_i to the gate of M3, g_{m3} is also incorporated into equation 1 to further boost the gain of the LNA. Generally, it can be appreciated that the incorporated transconductance of the cascode transistor by the cross-coupled feedback and the bulk effect of the CS input transistors, maintains a comparable transconductance of the CS stage but with reduced bias current. This is the main advantage of the topology.

After derivations with the input impedance matching condition, the noise factor expression of the LNA yields:

$$F = 1 + \frac{\gamma_1}{\alpha_1} \qquad (2)$$

$$\frac{g_{m1}}{\left(g_{m1} + g_{mb1} + g_{m4} + g_{mb4} + g_{m3}/2\right)^2 R_S} +$$

$$\frac{\gamma_4}{\alpha_4}\frac{g_{m4}}{\left(g_{ml} + g_{mbl} + g_{m4} + g_{mb4} + g_{m3}/2\right)^2} +$$

$$\frac{R_S}{R_{L1}} + \frac{1}{R_S g_{m3}^2 \left(1 + A_{bst}\right)^2 R_{L2}} + \frac{\gamma_3}{\alpha_3} \cdot$$

$$\frac{g_{m3}}{R_s\left(1 + A_{bst}\right)^2 \left(2\left(g_{ml} + g_{mb1} + g_{m4} + g_{mb4}\right) + g_{m3}\right)^2}$$

where α and γ are the bias-dependent parameters. The second and third expressions are from the noise of M1 and M4. The fourth and fifth expressions are from the loads of R_{L1} and R_{L2}. The last is from M3. Due to the feedback path from Rs to the gate of M3, it is no longer an ideal cascode transistor (i.e., contributing no noise).[7] The noise derivation equation 2, however, shows that the noise contribution of M3 is far smaller than that of M1 by a factor of $g_{m3}/4g_{m1}(1+A_{bst})^2$ (0.01 in the design). Thus, the additional degradation in NF can be negligible. Moreover, compared to that reported by Wang et al.,[6] thanks to the bulk effect of the CS input transistors and g_{m3} being incorporated into the transconductance of CS stage, the noise of M1 and M4 can still be effectively inhibited but with reduced bias currents.

According to equation 2, as A_{bst} increases, NF decreases; however, with increased frequency things become complex. A large A_{bst} generates a low frequency pole at node m as shown in Figure 1b and introduces an additional phase shift in the CS stage. The differential phase shift between the CG and CS stages has an adverse impact on the noise cancellation of M2, because an ideal cancellation requires that the differential voltages of V_{out+} and V_{out-} have exactly

the same magnitudes and opposite phases. In other words, the imbalanced phase shift caused by a large A_{bst} could increase the overall NF and reduce the bandwidth.

Due to large parasitic effects in stacked transistors, the bandwidth of the LNA is limited mainly by the pole in the CS stage signal path. This path must be examined carefully. Using small signal methods to analyze the circuit of Figure 1b, one can determine that the bandwidth at node m is the same as that reported by Wang et al.[6] Meanwhile, for node x, the bandwidth yields:

$$\omega_x = \frac{1}{R_s\left(\begin{array}{l}C_{gsM1}+C_{gsM4}+\left(1+A_{NEG}\right)\cdot\\ \left(C_{gdM1}+C_{gdM4}\right)+C_{bsM1}+C_{sbM4}\end{array}\right)} \quad (3)$$

where C_{gsM1}, C_{gsM4}, C_{gdM1}, C_{gdM4}, C_{bsM1}, and C_{sbM4} are the gate source capacitance, gate drain capacitance, and source bulk capacitance of M1 and M4, respectively. The utilization of the bulk effect, introduces parasitic capacitances C_{bsM1} and C_{sbM4}, but this does not constitute a limitation since all of these parasitic capacitances can be resonated with off-chip inductor Ls.

MEASUREMENT RESULTS

The LNA core circuit is implemented using standard 0.13 µm RF CMOS technology. ***Figure 2*** is a micrograph of the LNA, which occupies 520 × 490 µm² including the probing pads. With a single 1 V power supply, transistors M1 and M2 are biased at 3.68 and 0.45 mA, respectively, while parameter A_{bst} is taken as 2.5. R_{L1} and R_{L2} are set to 250 and 100 Ω, respectively. Two source-follower buffers are added after the outputs of the LNA to drive 50 Ω loads. An external passive balun is also used at the outputs of the buffers for a test target.

Figure 3 shows the measured and simulated input reflection coefficients. Owing to the inherent wideband input match of the common-gate topology, $|S_{11}|$ is below -10 dB across a wide frequency range of 0.1 to 5 GHz. ***Figure 4*** shows $|S_{21}|$, demonstrating a flat gain of 18 dB over a 3 dB frequency band from 0.1 to 4.4 GHz. ***Figure 5*** compares both the measured and simulated NFs. The measured result shows a maximum noise figure NF_{max} of 3.2 dB at 4.4 GHz and an average NF of 2.7 dB. Although it is about 0.7 dB higher than the simulated NF, the

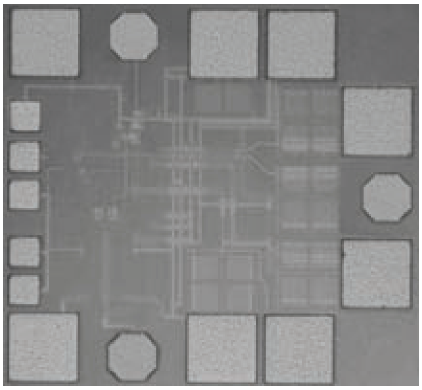

Fig. 2 Chip micrograph.

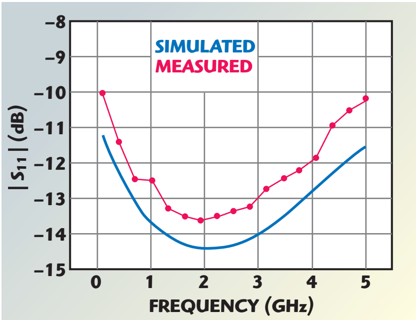

Fig. 3 Measured and simulated $|S_{11}|$.

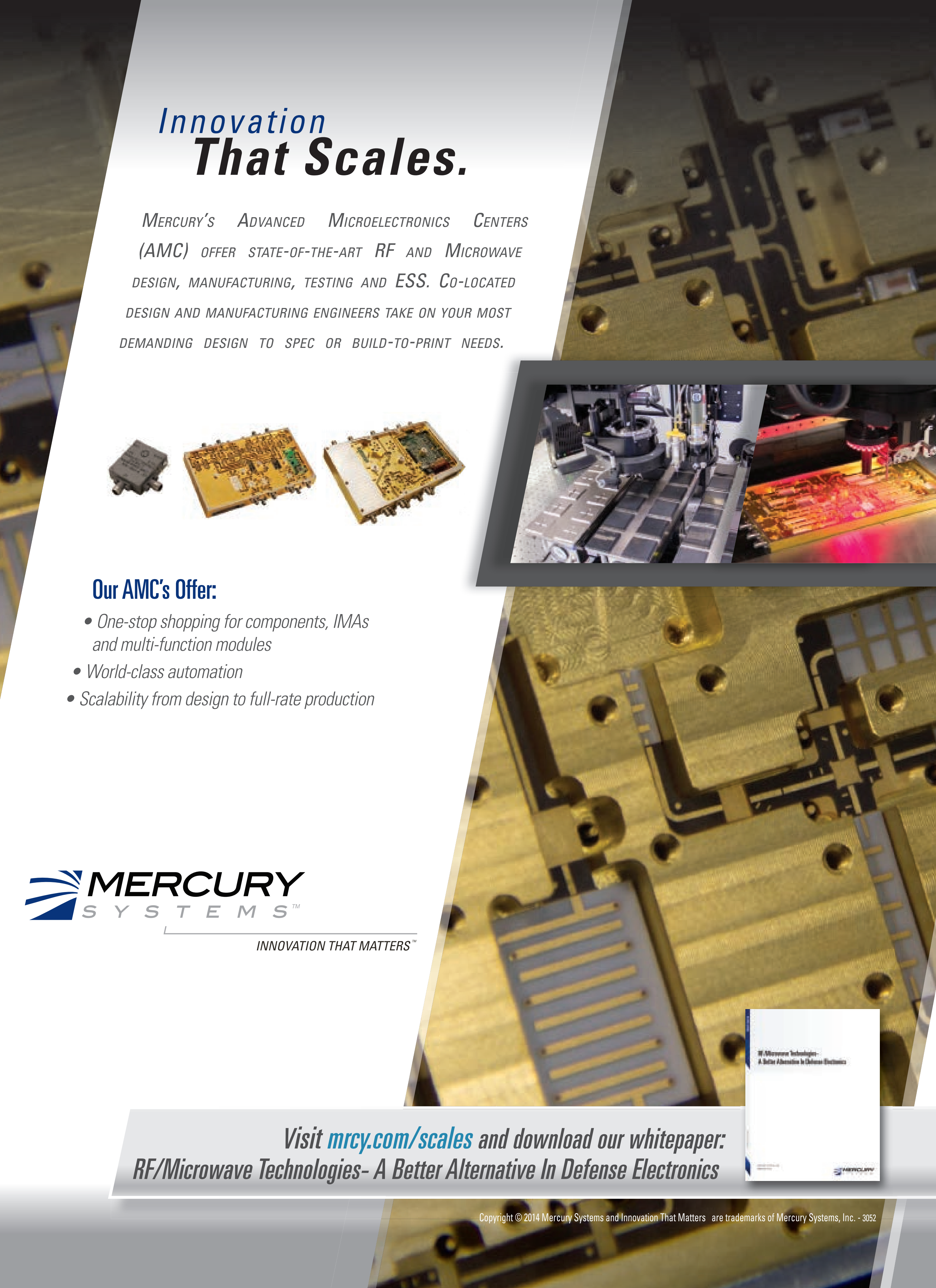
Innovation
That Scales.
Mercury's Advanced Microelectronics Centers (AMC) offer state-of-the-art RF and Microwave design, manufacturing, testing and ESS. Co-located design and manufacturing engineers take on your most demanding design to spec or build-to-print needs.
Our AMC's Offer:
• One-stop shopping for components, IMAs and multi-function modules
• World-class automation
• Scalability from design to full-rate production
MERCURY
SYSTEMS™
INNOVATION THAT MATTERS™
Visit mrcy.com/scales and download our whitepaper:
RF/Microwave Technologies- A Better Alternative In Defense Electronics
Copyright © 2014 Mercury Systems and Innovation That Matters are trademarks of Mercury Systems, Inc. - 3052

shape and the flatness of the measured curve are almost the same, which we believe to reflect the actual NF of the LNA. In contrast to the bias current of 5.7 mA, reported by Wang et al.,[6] this is accomplished with a bias current of 4.1 mA due to the incorporated transconductance of the cascode transistor and the bulk effect of the CS input transistors. Gain and noise performance is achieved with comparable CS input transistor transconductance but with reduced bias current.

The high order distortion generated by M2 is cancelled in accordance with the noise cancellation principle described by Blaakmeer et al.[4] Thus, LNA linearity is dominated mainly by the voltage to current conversion transistors M1 and M4 of the CS input stage. By adjusting the bias and size of M4 to cancel the second-order nonlinearity of M1 with only minor impact on the third-order nonlinearity, an optimized IP3 is achieved.[6] The input third-order intercept point (IIP3) of the LNA is measured at 1, 2 and 3 GHz with a two tone of 5 MHz spacing. In ***Figure 6***, the measured IIP3 drops from -4.5 to -7.4 dBm when the frequency is increased from 1 to 3 GHz. This can be ascribed to the fact that as the frequency increases, the distortion cancellation of the LNA is deteriorated by the large phase shift of the CS stage.

Measured performance of the LNA is summarized in ***Table 1***. Other recently published wideband LNAs are also included for comparison with a figure of merit (FOM) defined by equation 4.[10] The LNA achieves comparable NF and gain with lower power consumption, and has the highest FOM among these designs.

$$\text{FOM} = \frac{\text{BW(GHz)Gain(lin)IIP3(mW)}}{\text{Pdc(mW)}\left[\text{NF(lin)}-1\right]} \quad (4)$$

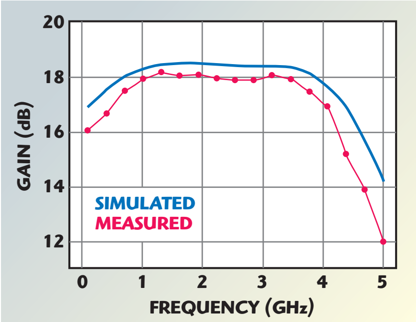

▲ *Fig. 4 Measured and simulated gain.*

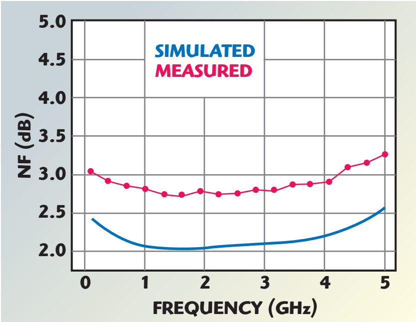

▲ *Fig. 5 Measured and simulated NF.*

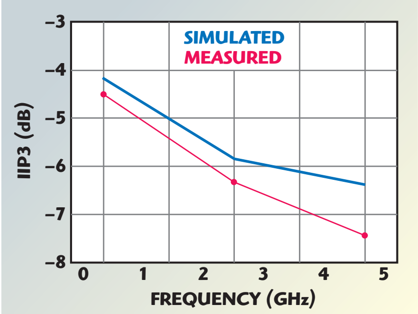

▲ *Fig. 6 Measured and simulated IIP3 within the band.*

TABLE I

SUMMARY OF THE ELECTRICAL RESULTS AND COMPARISONS

Reference	4.	6.	8.	9.	This Work
BW (GHz)	0.2 to 5.2	0.2 to 3.8	0.32 to 1	0.1 to 2.1	0.1 to 4.4
Gain (dB)	15.6	19	23.5	18.3	18
NF_{max} (dB)	3.5	3.4	2.7	2.7	3.2
IIP3 (dBm)	0	-4.2	0	-7	-4.5
Power (mW)	21	5.7	15.3	14	4.1
FOM	7	16	12	2	22
Technology	65 nm	0.13 μm	0.18 μm	0.13 μm	0.13 μm

CONCLUSION

An improved wideband noise cancelling balun-LNA in common-gate and common-source topology is described. Cross-coupled feedback and the bulk effect are adopted to increase the input transconductance of the LNA. Gain and noise performance comparable to other reported LNAs are achieved with reduced bias current. Fabricated in a 0.13 μm RF CMOS process, the LNA achieves a flat voltage gain of 18 dB, a NF of 2.7 to 3.2 dB and an IIP3 of -4.5 to -7.4 dB over a 3 dB frequency band from 0.1 to 4.4 GHz. It consumes only 4.1 mA from a 1 V supply, which is quite suitable for low voltage and low power applications.■

ACKNOWLEDGMENT

This work was supported by the National Natural Science Foundation of China (No. 60901019).

References

1. F.M. Ghannouchi, "Software-Defined Radio Transmitters for Advanced Wireless and Satellite Communications Systems," *Microwave Journal*, Vol. 51, No. 5, May 2008, pp. 202-216.
2. C.X. Chen, M.A. Do, K.S. Yeo, C.C. Boon and W.M. Lim, "A Low-Power Multi-Channel UWB Single Chip Transceiver With Pulse Detectors," *Microwave Journal*, Vol. 55, No. 10, October 2012, pp. 104-122.
3. W. Zhuo, X. Li, S. Shekhar, S.H.K Embabi, J.P. de Gyvez, D.J. Allstot and E. Sanchez-Sinencio, "A Capacitor Cross-Coupled Common-Gate Low-Noise Amplifier," *IEEE Transactions on Circuits and Systems II: Express Briefs*, Vol. 52, No. 12, December 2005, pp. 875-879.
4. S.C. Blaakmeer, E.A.M. Klumperink, D.M.W. Leenaerts and B. Nauta, "Wideband Balun-LNA With Simultaneous Output Balancing, Noise-Canceling and Distortion-Canceling," *IEEE Journal of Solid-State Circuits*, Vol. 43, No. 6, June 2008, pp. 1341-1350.
5. B. Guoand and G. Wen, "Periodic Time-Varying Noise in Current-Commutating CMOS Mixers," *Progress in Electromagnetic Research*, Vol. 117, June 2011, pp. 283-298.
6. H. Wang, L. Zhang and Z. Yu, "A Wideband Inductorless LNA With Local Feedback and Noise Cancelling for Low-Power Low-Voltage Applications," *IEEE Transactions on Circuits and Systems I: Regular Papers*, Vol. 57, No. 8, August 2010, pp. 1993-2005.
7. X. Fan, H. Zhang and E. Sánchez-Sinencio, "A Noise Reduction and Linearity Improvement Technique for a Differential Cascode LNA," *IEEE Journal of Solid-State Circuits*, Vol. 43, No. 3, March 2008, pp. 588-599.
8. M. Moezzi and M.S. Bakhtiar, "Wideband LNA Using Active Inductor With Multiple Feed-Forward Noise Reduction Paths," *IEEE Transactions on Microwave Theory and Techniques*, Vol. 60, No. 4, April 2012, pp. 1069-1078.
9. Z. Li, L. Chen, Z. Wang, C. Wu, J. Cao, M. Zhang, C. Wang, Y. Liu and Z. Wang, "Low-Noise and High-Gain Wideband LNA With gm-Boosting Technique," *Electronics Letters*, Vol. 49, No. 18, August 2013, pp. 1126-1128.
10. H. Zhang, X. Fan and E. Sánchez-Sinencio, "A Low-Power, Linearized, Ultra-Wideband LNA Design Technique," *IEEE Journal of Solid-State Circuits*, Vol. 44, No. 2, February 2009, pp. 320-330.

Extending the Quiet Zone Using an RF Lens on a Conical Tapered Chamber to 18 GHz

V. Rodriguez
ETS-Lindgren L.P., Cedar Park, Texas
S. Matitsine
Matsing Pte. Ltd. and Temasek Laboratories, National University of Singapore
T.T. Chia
DSO National Laboratories and Temasek Laboratories, National University of Singapore
P. Lagoiski, L. Matytsine and M. Matytsine
Matsing Pte. Ltd.
P.K. Tan
Temasek Laboratories, National University of Singapore

A tapered chamber is traditionally constructed using a square based pyramidal shaped taper that transitions to an octagon and then finally into a cylindrical launch section. This approach is related to the manufacturability of different absorber cuts. In this article, we introduce a chamber where the conical shape of the launch continues throughout the entire length of the tapered chamber. The results of free space VSWR measurements at different frequencies over a 1.5 m diameter quiet zone (QZ) are presented. The conical taper appears to have a better illumination wave front than the traditional approach and better QZ VSWR levels even at frequencies above 2 GHz.

▲ *Fig. 1 A typical tapered anechoic chamber.*

▲ *Fig. 2 Shaping from square to octagonal cross-section at the feed.*

As with all antenna chambers, when the frequency increases, the usable or far field illuminated QZ is reduced. At a 12 m distance from the feed to the turntable, the quiet zone at 8 GHz is reduced to 45 cm. A solution to extend the quiet zone at high frequencies employs a large dielectric lens installed in front of the turntable to improve the phase distribution of the field. A lightweight, broadband lens with a diameter of 2 m was developed and weighs just 35 kg with a focal length of 10 m. With the lens installed, the usable far field QZ is increased, allowing electrically larger antennas to be measured in the chamber. The use of the lens can also be applied to traditional square cross-section tapered chambers.

BACKGROUND

Tapered anechoic chambers have been around for almost 50 years,[1,2] introduced to address issues present in rectangular chambers at frequencies below 500 MHz.[3,4] At lower frequencies, high gain antennas used in an antenna measurement range become physically large and can be difficult to handle inside an anechoic chamber, so less directive antennas are used. These radiate more energy to the side walls, ceiling and floor of the chamber forcing it to grow in size in order to accommodate thicker absorbers needed to reduce reflections. Tapered anechoic chambers were introduced to solve this low frequency problem. Instead of trying to eliminate specular reflections in

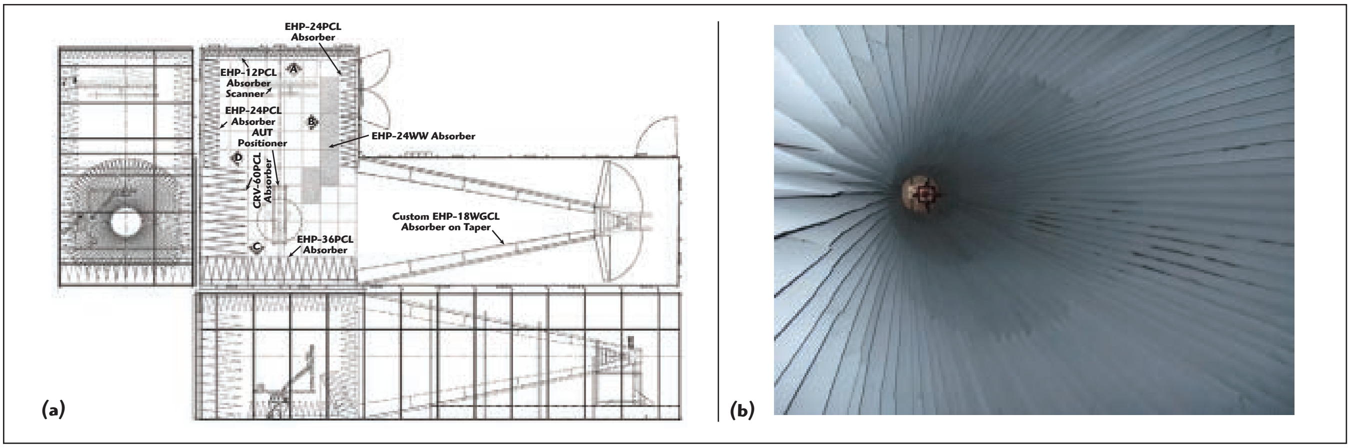

▲ *Fig. 3 The conical tapered anechoic range plan and elevation (a), and a picture of the taper section (b).*

the quiet zone, the specular area is brought closer to the measuring antenna and the specular reflections are used to create a QZ illumination.[2,5] Traditionally, tapered anechoic chambers were built having a square based pyramid as the taper (see ***Figures 1*** and **2**). To better accommodate different feed antennas, the square section may be gradually transformed to a cylindrical cross section taper. These changes in cross section require a lot of special cuts of absorber to make the transition from the conical section to the square section as smooth as possible and to create the illumination in the QZ.[2-5]

The design presented in this article introduces a conical taper (see ***Figure 3***). The entire tapered structure maintains a constant angle and a circular cross section. The tapered section is about 10 m in total length. Results for the free-space VSWR[6] are presented and compared with similar chambers employing a traditional design. To improve performance at high frequencies a dielectric lens is used to create a plane wave behavior.[7]

MEASURED RESULTS

The chamber QZ is scanned using free space VSWR tests[6] at a series of frequencies from 200 MHz to 18 GHz. The chamber is lined with 60" (152 cm) curvilinear absorbers on the back (i.e., receive) wall and a combination of 24" (61 cm) pyramidal absorbers and 36" (91.44 cm) on the sidewalls, floor and ceiling. The tapered section has a specially cut wedge material that lines the tapered section from the feed location to the QZ area. The wedges range from 18" (45.72 cm) at the QZ end to 8" (20.32 cm). ***Figure 4*** shows a picture of the conical treatment. The tapered section is built inside an RF

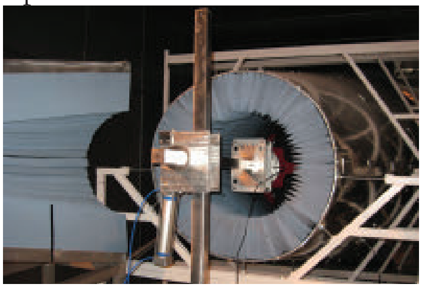

▲ *Fig. 4 The tapered section as seen from the feed location.*

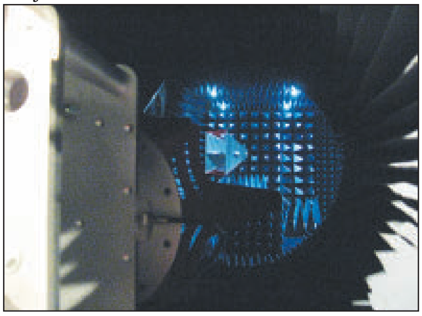

▲ *Fig. 5 The scanning antenna at the QZ viewed from a point right behind the source antenna at the apex of the taper.*

Performance is its middle name.

KEYSIGHT M9393A PXIe PERFORMANCE VECTOR SIGNAL ANALYZER

Introducing the world's fastest, 27 GHz high performance PXIe vector signal analyzer (VSA), the realization of Keysight's microwave measurement expertise in PXI. The M9393A integrates core signal analysis capabilities and proven measurement software with modular hardware speed and accuracy. So you can tailor your system to fit specific needs today and tomorrow. Deploy the M9393A and acquire the performance edge in PXI.

M9393A PXIe performance VSA	
Frequency Range	9 kHz to 27 GHz
Analysis Bandwidth	Up to 160 MHz
Frequency Tuning	150 µs
Amplitude Accuracy	± 0.15 dB

Download new app note on innovative techniques for noise, image and spur suppression.
www.keysight.com/find/M9393APXI

USA: 800 829 4444   CAN: 877 894 4414

KEYSIGHT TECHNOLOGIES

Unlocking Measurement Insights

Agilent's Electronic Measurement Group has become **Keysight Technologies**.

shielded room to avoid outside interference during measurements.

The source antenna is an ETS-Lindgren model 3164-06 dual linearly polarized open boundary quad-ridge horn,[8] rated from 300 MHz to 6 GHz. In this application, the antenna is used from 200 MHz with attenuators at the feed to reduce the effects of the high VSWR. The QZ is scanned with an ETS-Lindgren model 3106B dual ridge horn. The scanning antenna and source antenna are shown in ***Figure 5***.

Figure 6 shows reflectivity levels of the QZ versus direction for horizontal and vertical polarizations. Results are shown for 200, 400, 800 and 1,000 MHz. All of these results are measured with the source antenna at a fixed position in the apex of the taper. The antenna is commonly moved as frequency changes to maintain the phase center close to the reflections and maintain a QZ illumination free of ripples.[3,4]

For frequencies above 2 GHz, an ETS-Lindgren 3164-05 dual linearly polarized open boundary quad-ridge horn, rated from 2 to 18 GHz, is used. For scanning the QZ, a series of standard gain horns are used with gains ranging from 10 to 20 dBi. Additionally, since a smaller horn is used as the source, it is positioned inside an extension of the conical taper. Figure 4 shows one of the two halves that make up this high frequency extension.

Figure 7 shows the results of the scans at high frequencies. As discussed by Rodriguez and Hansen,[5] tapered chambers are better suited for low frequencies and care must be taken to properly position the source antenna. However, it is possible to use them at these high frequencies once the chamber is characterized.

COMPARISON WITH TRADITIONAL CHAMBERS

Comparison with traditional chambers is difficult. There are no two identical chambers that have the exact same absorber treatment with the exception of the taper geometry. A qualitative comparison, however, suggests some advantages. With traditional chambers, antennas with gains of 16 dBi and

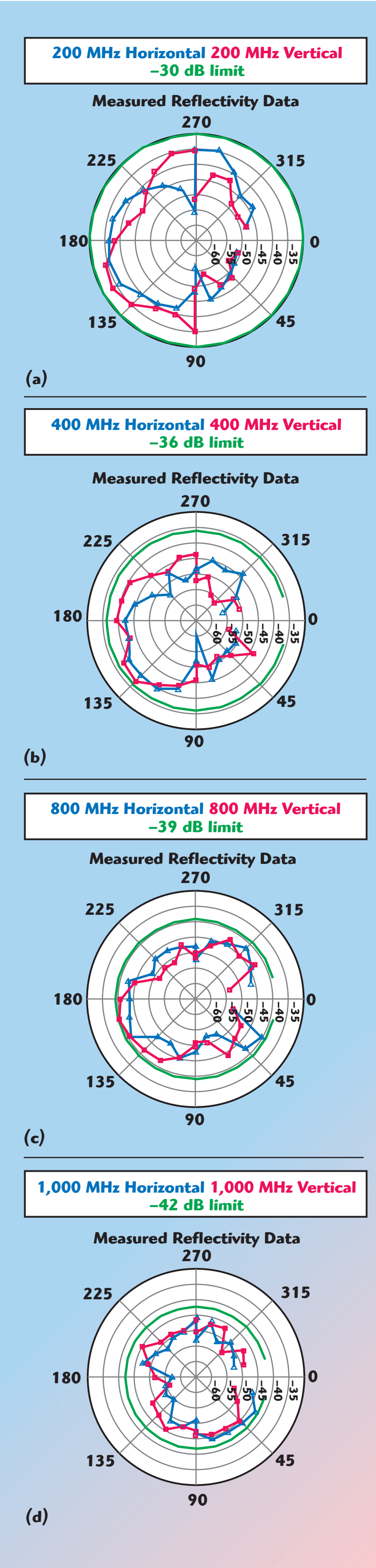

▲ *Fig. 6 Reflectivity results for the conical tapered chamber at 200 (a), 400 (b), 800 MHz (c) and 1 GHz (d).*

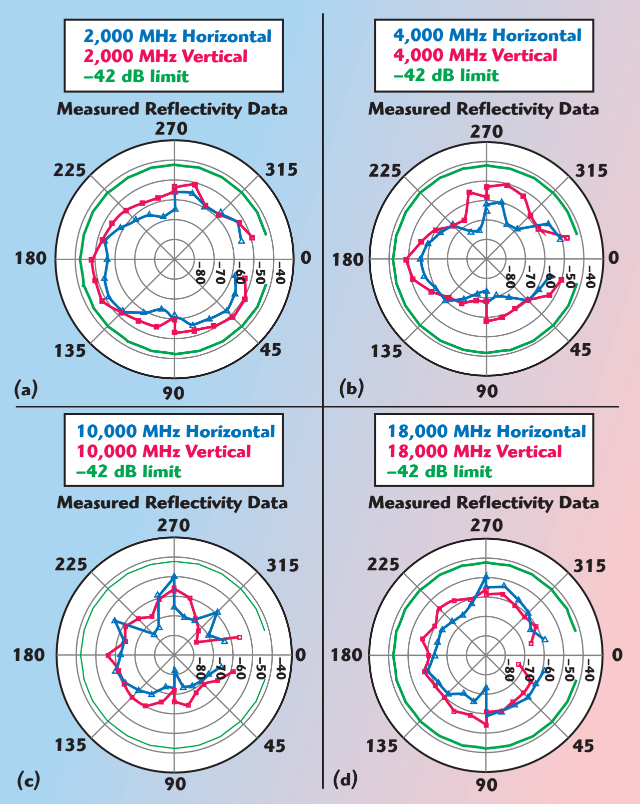

▲ *Fig. 7 Reflectivity levels in the QZ versus angle at 2 (a), 4 (b), 10 (c), and 18 GHz (d).*

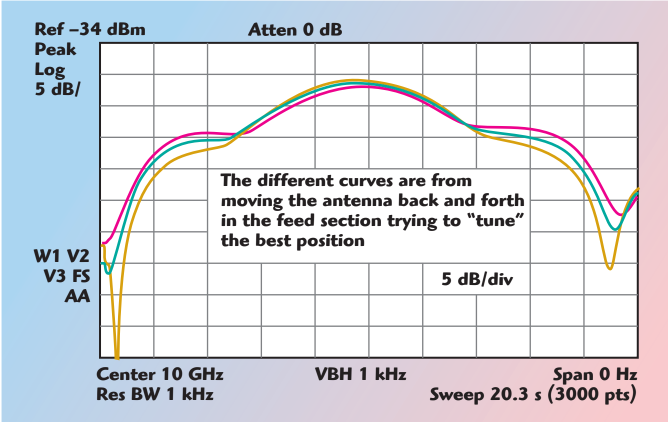

▲ *Fig. 8 Data for a transverse scan of a traditional chamber using the same horn used in the conical design.*

above are required to achieve adequate illumination in the QZ. It appears that one of the features of the conical taper is that lower gain antennas can be used. At 10 GHz, the source antenna has a directivity of 12 dBi,[8] whereas the conical quad ridge horn used in many traditional tapered anechoic chambers has a directivity of 14 dBi. The open boundary ridge horn is successfully used in the conical chamber design; however, when used in a traditional chamber, a smooth amplitude taper is not achieved (see ***Figure 8***).

In ***Figure 9***, a comparison of the reflectivity of the conical tapered chamber and a traditionally implemented chamber at 400 MHz shows a slight difference in back wall reflectivity (180°), but this is related to differences in absorber treatment between the chambers. For the traditional chamber, one can see a large variation in reflectivity for the horizontal polarization as the direction changes from 15° to 60° on either side of the source antenna. These variations are not seen in the conical tapered chamber.

The chamber is configured with

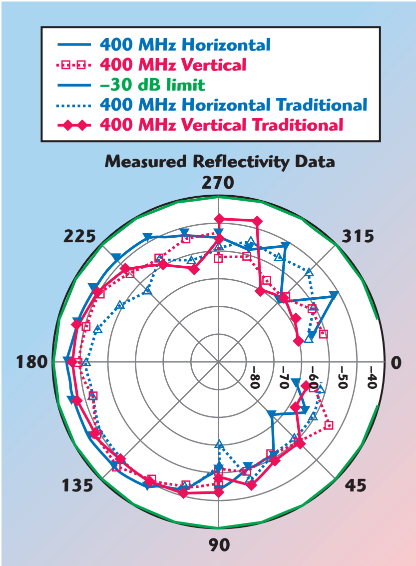

▲ *Fig. 9 Comparison with a traditional chamber.*

Delta's 4.1/9.5 Mini DIN series of coaxial connectors were developed to meet the growing demands of today's high performance mobile communications systems.

The **4.1/9.5** Mini DIN has an operational frequency range of DC-14 GHz, offers excellent VSWR performance and Low Passive Intermodulation (Low PIM) >165 dBc, making it ideally suited for use in **Base Stations, Distributed Antenna Systems (DAS)** and **Small Cell** applications.

Features
- IEC standardization
- 30% smaller and lighter compared to 7/16
- Reduced center to center spacing
- Albaloy Plate

Benefits
- Global standard interface
- Increased package density
- LOW PIM: >165 dBc

Get your copy of our new **4.1/9.5 Mini Din** catalog, contact Delta today!

DELTA
ELECTRONICS MFG. CORP.
Connect Here.

AS9100/ISO 9001:2008 CERTIFIED
ROHS COMPLIANT

(978) 927-1060 • www.deltarf.com

two ranges, a far field tapered range and a NF-FF planar and spherical range. Figure 3 shows the plan of the chamber with the two ranges. The antenna under test uses the same positioner for both ranges, and the QZ is the same as well. For the spherical range the probe is located between the QZ and the planar scanner on the opposite wall. The planar scanner can be used for testing high gain arrays. These arrays can be positioned at the QZ or closer to the scanner by mounting them on a tripod, depending on the frequency of operation or the size of the scanner.

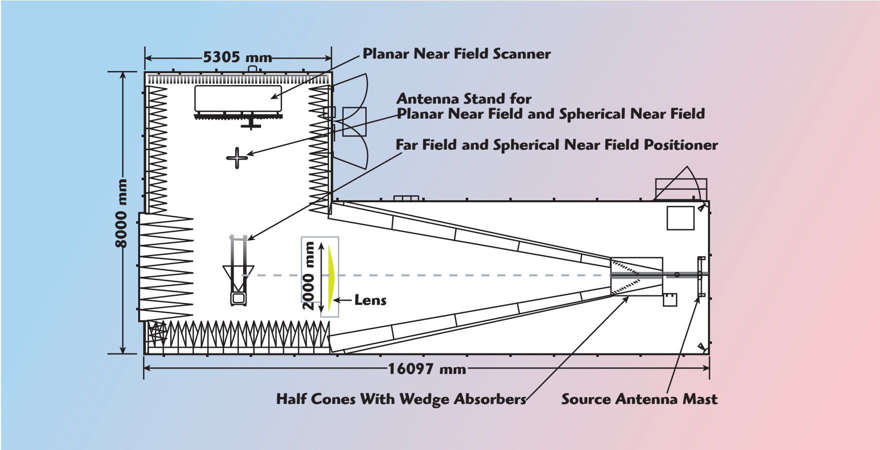

Fig. 10 Placement of lens in tapered chamber.

INCREASING THE QZ SIZE USING AN RF LENS

While the tapered chamber is used to overcome some of the limitations of the standard rectangular chamber for antenna testing at lower frequencies, the size of its quiet zone decreases significantly as frequency increases. For example, the tapered chamber installed at the National University of Singapore (NUS) has a quiet zone of 1.4 m at 500 MHz but only 45 cm at 8 GHz. To increase the quiet zone at the higher frequencies, a custom RF lens is integrated inside the chamber. We are not aware of any other method to increase the quiet zone without physical alterations to the original chamber.

The design of the RF lens is based on the principle of optical refraction to transform a spherical wave from a point source to a planar wave. By precisely controlling the dielectric constant of the lens, the focal length of the lens can be customized based on the lens aperture.

A plano-convex RF lens is integrated into the tapered chamber at NUS (see ***Figure 10***). Its focal length (f) of 10 m is equal to the distance between the source antenna and the end of the chamber's tapered section. The diameter of the lens is chosen to be 2 m in order to cover a large area of the chamber's aperture, while allowing easy mobility of the lens inside the chamber.

The lens has a comparatively high ratio of the size of the planar wave front to the lens diameter (a factor of about 0.7D, where D is the diameter of the lens). Hence, a 2 m diameter lens can produce a 1.4 m plane wave front. The profile $P(x,y)$ of the lens is designed using the following equations from Kraus and Marhefka:[9]

$$x = \frac{r}{\tan\theta_m} - \frac{y}{\tan\theta}, \quad (1)$$

where

$$y = \rho \sin\theta, \quad (2)$$

and

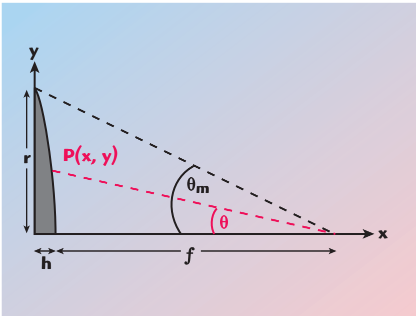

Fig. 11 Lens geometry.

Proven Performance

Choose GORE-FLIGHT™ Microwave Assemblies, 6 Series
for performance that meets the challenges before and after installation.

GORE-FLIGHT™ Microwave Assemblies, 6 Series are ruggedized, lightweight and vapor-sealed airframe assemblies that withstand the challenges of aerospace by maintaining lower insertion loss, more reliable VSWR performance, and consistent impedance of 50 ± 1 Ohms, eliminating insertion loss stack-up issues when routing through airframe bulkheads.

GORE-FLIGHT™ Microwave Assemblies, 6 Series improve system performance with:

- Lowest insertion loss **before and after installation**
- **Lower installed costs** due to fewer failures
- **Increased payload** with weight-saving assembly
- **Faster installation time** due to mechanically robust construction
- **Reduced RF interference** through superior shielding effectiveness
- **Fully qualified in compliance** with MIL-T-81490 requirements

With GORE-FLIGHT™ Microwave Assemblies, 6 Series, a fit-and-forget philosophy is now a reality – providing the most cost-effective solution that ensures mission-critical system performance for military and civil aircraft operators.

GORE
Creative Technologies Worldwide

gore.com/GORE-FLIGHT

LIKE US ON facebook
FOLLOW US ON twitter

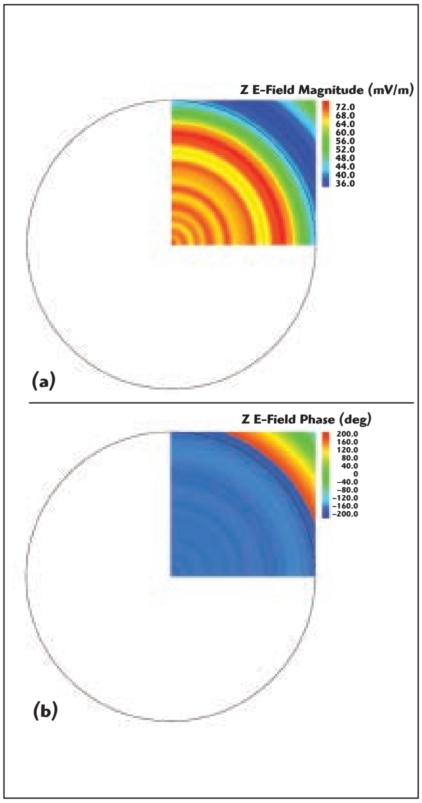

▲ *Fig. 12 Predicted field distribution at 8 GHz, both in magnitude (a) and phase (b).*

$$\rho = \frac{f\left(\sqrt{\varepsilon}-1\right)}{\sqrt{\varepsilon}\cos\theta - 1'} \qquad (3)$$

with

$$h = \frac{r}{\sqrt{\varepsilon}-1}\left(\frac{1}{\sin\theta_m} - \frac{1}{\tan\theta_m}\right) \qquad (4)$$

The variables are defined in ***Figure 11***.

Given its size (2 m), the RF lens cannot be manufactured with traditional dielectric materials due to the difficulty of controlling permittivity throughout the lens to a high degree of accuracy. Furthermore, it would be extremely heavy (~1,000 kg), making installation difficult and requiring a special support structure, potentially causing undesirable diffractions.

To overcome these issues, a new low-loss, lightweight metamaterial manufactured by Matsing Pte Ltd. is used. The material allows the control of the dielectric permittivity to a high degree of accuracy. It has extremely low-loss ($\varepsilon' < 10^{-4}$). Its low density (40 kg/m^3) means that the 2 m lens weighs only 35 kg, making it portable and easily installed. The material is also isotropic and broadband, making the lens suitable for both vertical and horizontal polarizations over a wide range of frequencies.

NUMERICAL ANALYSIS

The performance of the lens is first evaluated using FEKO EM simulation software. A half-wavelength dipole is placed at the focal length of the 2 m lens. The focal length corresponds to the distance (10 m) between the feed and aperture of the tapered chamber. The field is observed at a vertical plane at 2 m (corresponding to the quiet zone region) on the other side of the lens. For simplicity, the lens and the dipole are simulated in free-space without the tapered chamber since the primary aim of the simulation is to ensure that for the given length of the taper, the lens provides

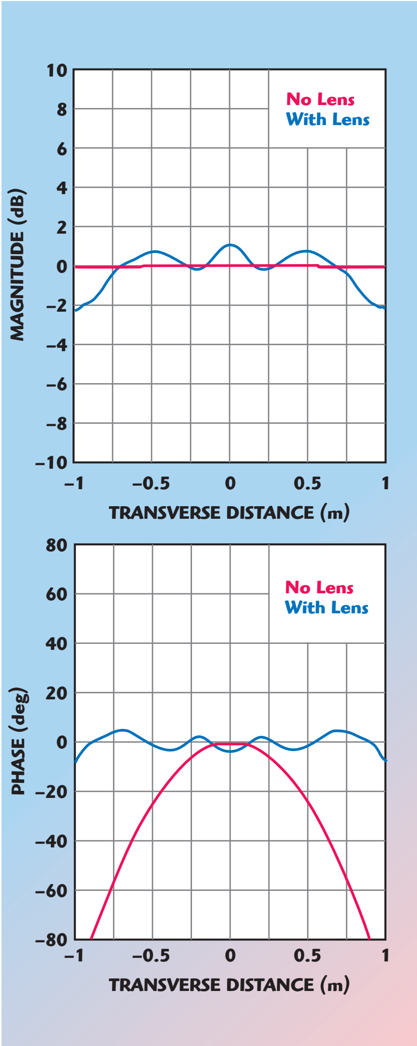

▲ *Fig. 13 Computed field distribution at 2 GHz.*

the best possible illumination. Including the chamber with its absorbers in the simulation model would drastically increase the problem size and complexity beyond the capability of the numerical package at these high frequencies.

Figure 12 shows the predicted fields (for a quadrant) at 8 GHz. The circles in the plots represent the outline of the 2 m lens. Cuts of the fields along the lens diameter are shown in ***Figures 13*** and ***14*** for 2 and 8 GHz, respectively. The fields of the dipole in the absence of the lens are superimposed in the figures for reference. For ease of comparison, the magnitudes are normalized to their respective mean values – the phase without the lens is normalized to its peak value and the phase with the lens is normalized to its mean value. From these figures, it is observed that the field with the lens deviates slightly from the dipole field due mainly to diffraction from the lens. However, the lens significantly reduces the large phase variation of the dipole field, producing a reasonably good plane wave in the vicinity of the quiet zone of the tapered chamber.

MEASURED PERFORMANCE

The lens is installed at the aperture of the tapered chamber as shown in ***Figure 15*** using a special frame made from low reflection material to easily place and hold it. For the field measurement of the quiet zone, a simple linear scanner is set up as shown in ***Figure 16***. A broadband dual-ridged horn is used as the probe antenna. The field is measured along an axis transverse to the lens axis at about 2 m separation. The lens is then removed and the measurement repeated.

The results at 2 and 8 GHz are shown in ***Figures 17*** and ***18***, respectively. The magnitudes and phases are "normalized" in the same manner as the numerical results. Note that the transverse distance in these figures, unlike that of Figures 13 and 14 is relative to the start of the measurement position at 0 m. The plots show that the lens has indeed improved the phase significantly without ad-

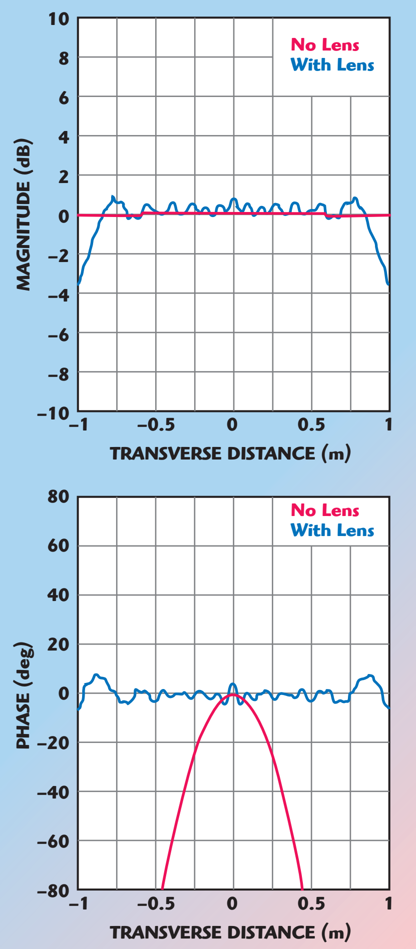

▲ *Fig. 14 Computed field distribution at 8 GHz.*

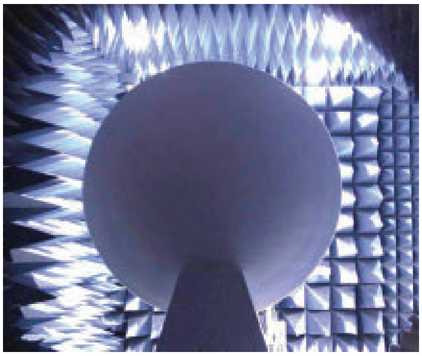

▲ *Fig. 15 View of the lens from the source antenna.*

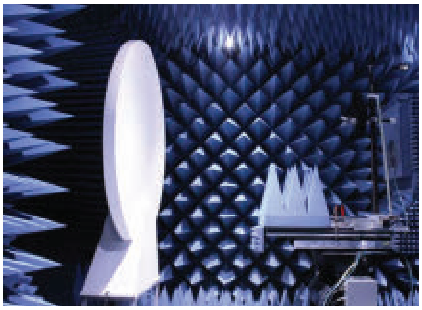

▲ *Fig. 16 The QZ scanned with the lens in place at the end of the taper section.*

30-DAY FREE TRIAL

Take advantage of a free 30-day trial of a Millimeter Wave Radio Link from HXI!

Includes our E-Band and 60 GHz Radio Links
and
Our 60 GHz HD-SDI Wireless Transport System *

*Note: Installation is not included in offer

We Don't Build Our Radio...
We Don't Build Their Radio
HXI Builds YOUR Radio!

Customizable Features/Services:

- Range Optimization
- Ridiculously Low Latency (<2 nS)
- Analog Versions
- Antennas & Mounting
- Alignment Tools
- Niche Applications
- Installation/Alignment Training on our Outdoor Range
- Range Calculations & Site Installation Recommendations
- Consulting Services For Single Link & Multiple Hop Installations

We Also Offer:

- E-Band Interference Testing Tool
- Bench-Top Link Test & Qualification Equipment

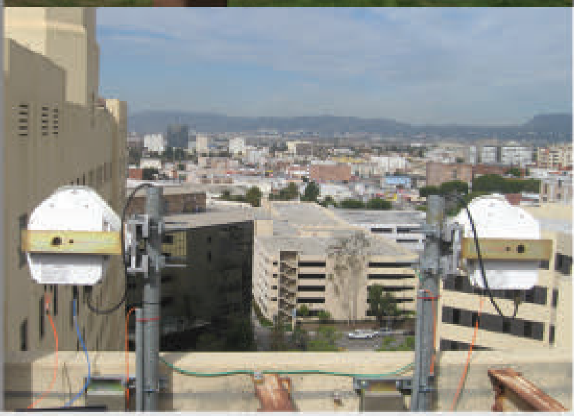

Yes, we have standard radios in E-Band and at 60 GHz, but aren't there times when the standard just won't do? When you need a radio for a unique purpose, choose HXI to configure your link.

12 Lancaster County Road
Harvard, MA 01451
978-772-7774
sales@hxi.com
www.hxi.com

hxi Millimeter Wave Products
A Wholly-Owned Subsidiary of Renaissance Electronics & Communications, LLC

hxi Millimeter Wave Products

Earle Stewart
HXI Business Development Manager
978-772-7774 ext.221
estewart@hxi.com
www.hxi.com

We also offer custom-designed radio links, configured to your requirements

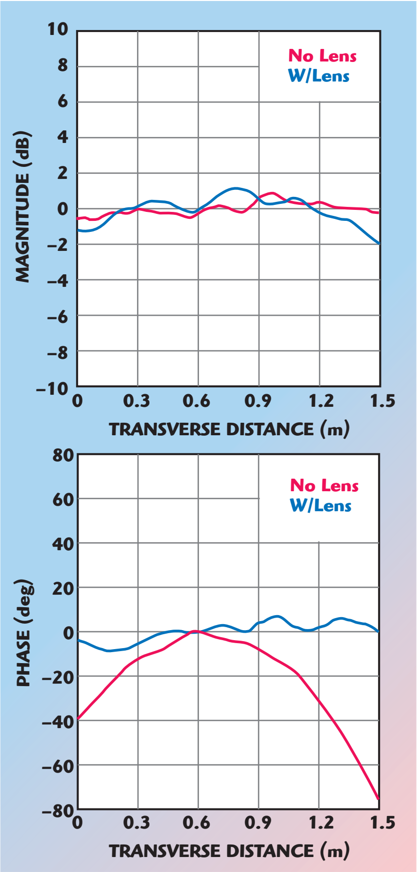

▲ *Fig. 17 Measured field distribution at 2 GHz.*

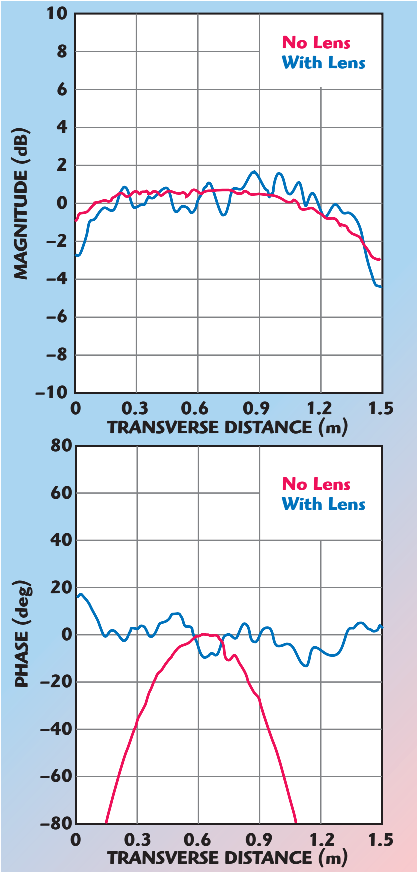

▲ *Fig. 18 Measured field distribution at 8 GHz.*

versely affecting the amplitude. The size of the quiet zone for ±10° phase variation with and without the lens is summarized in ***Table 1***, demonstrating that the lens has significantly improved the phase performance of the tapered chamber. Measurements are also done from 500 MHz to 1 GHz to confirm that the lens does not affect the original quiet zone of the chamber at low frequency.

CONCLUSION

This article introduces a new approach to manufacturing tapered anechoic chambers that provides good QZ reflectivity results over wide frequency ranges. Additionally, it appears to allow the use of lower directivity antennas than the ones used in traditional chambers. A lower directivity antenna provides smaller amplitude tapers across the QZ, reducing errors during gain measurements. With the addition of an RF lens, the phase of the chamber's quiet zone at higher frequencies (2 to 10 GHz) is significantly improved. The lens provides a quick and easy way to enhance the perfor-

TABLE I

SIZE OF QUIET ZONE (IN CM) FOR ±10° PHASE VARIATION WITH AND WITHOUT LENS

f (GHz)	2	4	6	8	10
Without lens	95	65	55	45	40
With lens	140	140	140	140	140

mance of the tapered chamber. Its light-weight construction enables easy user installation. The NUS tapered chamber with an RF lens is now capable of far field measurement of relatively large antennas from 0.3 MHz to 10 GHz. ■

References

1. W.H. Emerson and H.B. Sefton, "An Improved Design for Indoor Ranges," *Proceedings of the IEEE*, Vol. 53, No. 8, August 1965, pp. 1079-1081.
2. H. King, F. Shimabukuro and J. Wong, "Characteristics of a Tapered Anechoic Chamber," *IEEE Transactions on Antennas and Propagation*, Vol. 15, No. 3, May 1967, pp. 488-490.
3. L. H. Hemming, *Electromagnetic Anechoic Chambers: A Fundamental Design and Specification Guide*, Wiley-Interscience, John Wiley and Sons and IEEE Press, Piscataway, N.J., 2002.
4. V. Rodriguez, "Using Tapered Chambers to Test Antennas," *Evaluation Engineering*, Vol. 43, No. 5, May 2004, pp. 62-68.
5. V. Rodriguez and J. Hansen, "Evaluate Antenna Measurement Methods," *Microwaves and RF*, October 2010, pp. 61-67.
6. R.E. Hiatt, E.F. Knott and T.B.A. Senior, "A Study of VHF Absorbers and Anechoic Rooms," *Technical Report 5391-1-F*, University of Michigan, February 1963.
7. V. Rodriguez, S. Matitsine, T.T. Chia, P. Lagoiski, L. Matytsine, M. Matytsine and P.K. Tan, "A Cone Shaped Tapered Chamber for Antenna Measurements Both in Near Field and Far Field in the 200 MHz to 18 GHz Frequency Range and Extension of the Quiet Zone using an RF Lens," *Journal of the Applied Computational Electromagnetic Society*, Vol 28, No. 12, December 2013, pp. 1162-1170.
8. ETS-Lindgren horn, www.ets-lindgren.com/pdf/3164-05.pdf.
9. J.D. Kraus, R.J. Marhefka, *Antennas for All Applications*, 3rd edition, McGraw-Hill, 2001.

Vicente Rodriguez *attended Ole Miss, in Oxford Miss., where he received his B.S.E.E in 1994, his M.S. in 1996 and Ph.D. in 1999. Dr. Rodriguez joined ETS-Lindgren as an RF and Electromagnetics engineer in 2000. In 2004 Dr. Rodriguez became senior principal antenna design engineer, placing him in charge of the development of new antennas. In 2006 Dr. Rodriguez became antenna product manager, placing him in charge of development, marketing and maintenance of the antenna product line. Dr.*

Rodriguez is the author of more than 50 publications and holds patents for hybrid absorber and dual ridge horn antennas.

Serguei Matitsine *graduated with honors from the Moscow Institute of Physics and Technology in 1979 and received his Ph.D. in 1982. From 1982-1984 he held the position of senior researcher at the Institute of Radio-Engineering and Electronics of the Russian Academy of Sciences. From 1984 until 1995 he has held several positions including senior researcher, head of the electromagnetic laboratory and deputy director at the Institute of Theoretical and Applied Electromagnetics of Russian Academy of Sciences. In 1995 Dr. Matitsine joined the research and development group at Singapore Technologies Aerospace as technical director and later moved to the position of chief engineer. Since 2001 Dr. Matitsine has also been working at Temasek Laboratories of the National University of Singapore as an adjunct senior principal research scientist. He is also the chairman and technical director of Matsing Pte. Ltd. His research interests include electromagnetic materials, metamaterials, smart materials, multi-beam antennas, antenna measurement techniques, and most recently, lightweight, large-size RF lenses. He has more than 60 publications in these areas, as well as four patents.*

Tse-Tong Chia *received his B.Eng. degree with first class honors in 1986 from the National University of Singapore, and his M.S. and Ph.D. in 1991 and 1994, respectively, from Ohio State University. He has been with the DSO National Laboratories in Singapore since 1986, where he is currently a distinguished member of the technical staff. Chia was a laboratory head from 1995 until 2010 when he stepped down to focus on research. He is currently also a principal research scientist in the Temasek Laboratories at the National University of Singapore. His research interests include computational methods for electromagnetic scattering and installed antenna performance, as well as the use of lenses for antenna applications.*

Pavel Lagoiski *received his B.S. E.E. from the National University of Singapore in 2010. Since then he has held the position of engineer at Matsing Pte. Ltd. His research interests include antenna measurement system and RF lenses.*

Leo Matytsine *received his B.S. from the University of Southern California in 2009 and his MBA from the Australian Global School of Management in 2013. He has been with Matsing Pte. Ltd. since 2009 and currently holds the position of director. His interests include RF convex lenses and antenna measurement systems.*

Michael Matytsine *received his B.A. from Chapman University in 2006 and his MBA from La Verne University in 2010. He has been with Matsing Pte. Ltd. since 2006 and currently holds the position of director. His interests include Luneburg and convex RF lenses.*

Peng-Khiang Tan *received his degree in electronic and computer engineering from Ngee Ann Polytechnic in 1999 and his Bachelor of Technology in Electronics Engineering (second Class Honors) from the National University of Singapore in 2008. He currently works as a laboratory technologist within the antenna group at the Temasek Laboratories of the National University of Singapore.*

Nonlinear Devices: Optimal Route from Test Bench to Market

Tudor Williams, Randeep Saini and Simon Mathias
Mesuro, UK
Andreas Henkel
Rohde & Schwarz, Munich, Germany

In the fast moving, competitive world of nonlinear design, the ability to turn a new device technology into a final product in the minimum possible time is critical to a company's success. A recent approach, which is gaining momentum, is the use of behavioral models. This combined with advances in the related test and measurement solutions is already showing dramatic reductions in product design cycles. This article looks at tailored measurement/modeling solutions from simple 50 Ω system level testing to full harmonic characterization with arbitrary impedance control required for Waveform Engineering.

Recent years have seen a surge in the interest in behavioral modeling of nonlinear devices, stemming from the release of a number of commercial, off-the-shelf solutions such as the Cardiff Model family. The expectations for such models are high; however, to get the most from them and to accurately simulate device performance, it is essential to fully understand how the model works along with the permitted application space.

THIRD-ORDER PHD MODELS

The Cardiff Model Lite (CML) is a third-order formulation that allows the extension of S-parameters under large signal operation. It is a poly-harmonic distortion (PHD) behavioral model formulation[1] shown in ***Figure 1***. It is based upon the harmonic superposition principle, which describes the large signal 'B' wave (B_{pm}) response, linearized around a large signal operating point (LSOP), in terms of a linear mapping with the other stimulus 'A' waves (A_{qn}).

The DUT is first driven with a fundamental tone, in this case A_{11}. At each fundamental input power (A_{11}), the device is simultaneously perturbated with a small signal tone at each harmonic frequency, A_{qn} – where q denotes the port index and n is the harmonic index. This is accomplished using the second source within a network analyzer.

The phase of this generator is swept with a minimum of six different phases, to allow the model to predict performance correctly. This perturbation process can be completed on both sides of the device, using the circuitry provided within the CML unit. Thus for each harmonic component, the corresponding model parameters, S and T, can be obtained by applying a least-squares fit algorithm to the measured data.

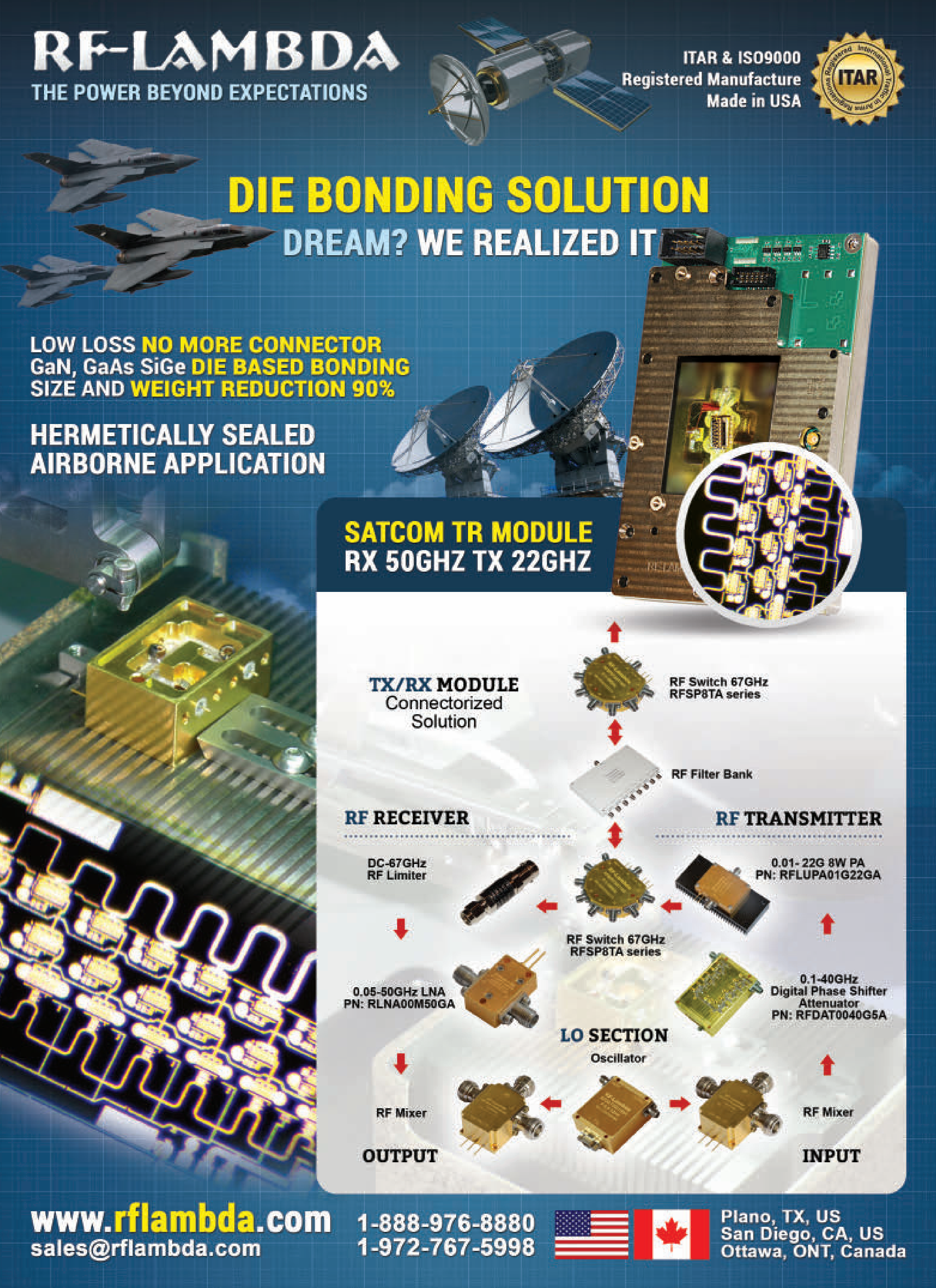

RF-LAMBDA
THE POWER BEYOND EXPECTATIONS
ITAR & ISO9000
Registered Manufacture
Made in USA
ITAR
DIE BONDING SOLUTION
DREAM? WE REALIZED IT
LOW LOSS NO MORE CONNECTOR
GaN, GaAs SiGe DIE BASED BONDING
SIZE AND WEIGHT REDUCTION 90%
HERMETICALLY SEALED
AIRBORNE APPLICATION
SATCOM TR MODULE
RX 50GHZ TX 22GHZ
TX/RX MODULE
Connectorized
Solution
RF Switch 67GHz
RFSP8TA series
RF Filter Bank
RF RECEIVER
RF TRANSMITTER
DC-67GHz
RF Limiter
0.01- 22G 8W PA
PN: RFLUPA01G22GA
RF Switch 67GHz
RFSP8TA series
0.05-50GHz LNA
PN: RLNA00M50GA
0.1-40GHz
Digital Phase Shifter
Attenuator
PN: RFDAT0040G5A
LO SECTION
Oscillator
RF Mixer
RF Mixer
OUTPUT
INPUT
www.rflambda.com
sales@rflambda.com
1-888-976-8880
1-972-767-5998
Plano, TX, US
San Diego, CA, US
Ottawa, ONT, Canada

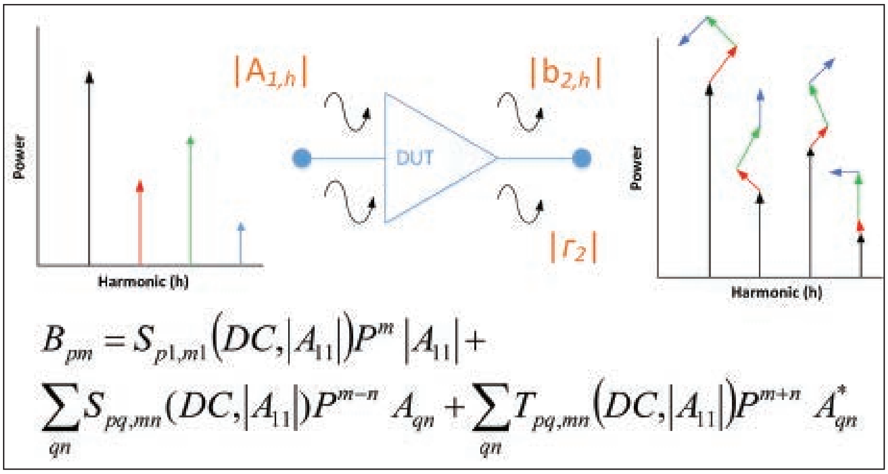

▲ *Fig. 1 PHD model formulation.*

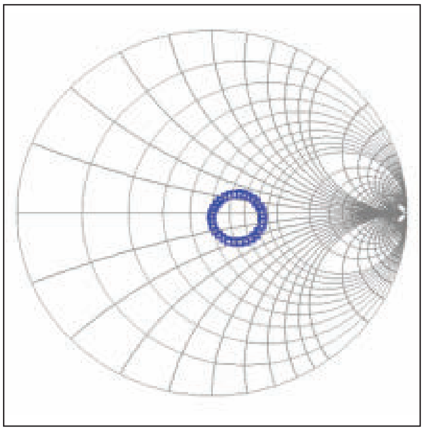

▲ *Fig. 2 Typical impedance sweep using a F0 perturbation tone at the load-side.*

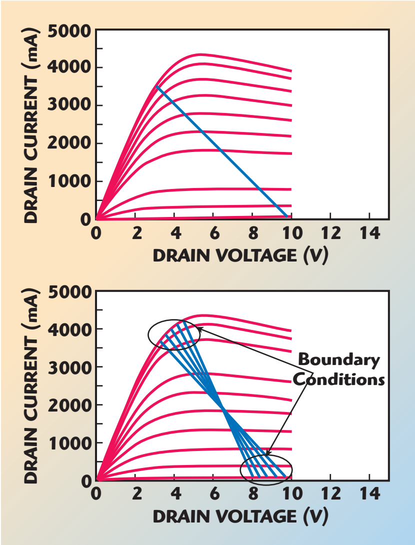

▲ *Fig. 3 Load-lines at 50 Ω and as impedance is swept.*

All third order behavioral models are local models; and as such, only valid for the applied operating conditions such as impedance, bias and temperature. If the measurement is performed correctly, the model will predict device performance to a high degree of accuracy within the measurement space and will extrapolate gracefully.

Note that care must be taken with extrapolation, indeed such models can return completely ambiguous results if the user strays too far from the operating conditions of the measurement. A good way to think of this extrapolation process (in a non-mathematical way) is in the I-V space. The model extraction process for a PHD model uses a small-injected signal with rotating phase at the input and output of the device at the fundamental and harmonic frequencies.

For simplicity, think about the fundamental frequency, the result of this injected signal is a variation in impedance. An example of this load variation or 'load-pull' performed for such a measurement is shown in ***Figure 2***. Think about the I-V curves for a transistor as shown in ***Figure 3*** and the RF load line you would expect when driven in to compression into the system impedance (nominally 50 Ω) as shown on the top of Figure 3. Now spin the load and, of course, the load line will move up and down effectively 'mapping' the device boundaries as shown on the bottom.

If we focus in on the knee region and impose a curve fit using the measured data, the measured data can be accurately modeled. A small extrapolation also does a good job; however, further extrapolation quickly leads to a breakdown of the model.

If used correctly, this model is an excellent way to get nonlinear data into a simulator, and should be

▲ *Fig. 4 Mesuro CML hardware.*

thought of in a similar way to an S-parameter model – if a dense grid is used for frequency and bias, interpolation within the simulator will work well. Typical applications are in system level simulation where a number of 50 Ω components can be cascaded and analyzed in terms of fundamental and harmonic performance. A similar technique can also be used over load impedance, for example to model a power transistor for amplifier design; this is discussed in more detail later in this article.

EXPERIMENTAL SETUP AND MEASUREMENT

The first stage here is to turn the VNA, capable of making only linear measurements, into a nonlinear VNA, capable of measuring the harmonic phase relationships. This can then be used to reconstruct time-domain waveforms. Here a phase reference is required to track the phase relationship as the frequency of the VNA is swept. The Mesuro/Rohde & Schwarz approach employs a conditioned, nonlinear device driven into compression at the fundamental frequency of the measurement. This offers improved harmonic content since the vast majority of the energy is focused at the measured frequencies, improving dynamic range for the initial characterization of the reference device as well as when the reference is used during nonlinear measurements.

For harmonic model extraction, additional hardware is required to route and combine signals to allow the required perturbation measurements at the input and output of the device. The CML unit (shown in ***Figure 4***) integrates the phase reference with this signal conditioning hardware. The unit can be used with four-port R&S ZVA models, and solutions are available covering a range of frequencies up to 67 GHz.

The CML generator software (see ***Figure 5***), offers a suite which provides ease of setup and measurement flexibility to produce the best possible


www.pivotone.com

model. Features include:

- Device pre-characterization measurement allowing the user to understand the key parameters for the extraction.
- Flexibility in the number of phase points.
- Independent control of magnitude of the perturbation tones – with a source-power calibration for each harmonic.
- Post analysis tools showing the actual load perturbations conducted and the ability to verify the model fit against the measured dataset.

LOAD-PULL, WAVEFORM ENGINEERING

Nonlinear devices cannot always be referenced to a 50 Ω impedance environment, and unlike linear S-parameters, it is not possible to transform data measured at one impedance to another. The measurement space required to capture the required design information, therefore, increases dramatically as the impedance space around the device must now be controlled.

Importantly the same 'building blocks' from the Cardiff Model Lite system can be re-used to realize a more capable system. Through the implementation of additional signal sources and a multiplexer, it is possible to create a system allowing the required impedance control at fundamental and harmonic frequencies. Then through variation of bias and impedance the waveform can be engineered to provide detailed insight into the DUT or optimize performance (Waveform Engineering). A schematic of an open loop active harmonic load-pull system is shown in ***Figure 6***.

Open-loop active load-pull[2] is an alternative to passive load-pull techniques,[3] whereby the means of synthesizing the magnitude and phase of the reflected signal, 'a2' has been replaced by a phase-synchronized signal source(s). Note that for each controllable harmonic, an independent source is required.

Recent advances in VNA architectures fit perfectly with this approach. New four source VNA's have direct digital synthesis (DDS) based sources, which is useful in a number of ways. Firstly, there are enough sources to drive the device while performing fundamental, second and third harmonic load-pull simultaneously. In addition, DDS sources do not drift in relative phase over time between multiple sources.

In a DDS synthesizer, shown in schematic form in ***Figure 7***, the tuning word defines the gradient of the phase change and by this the DDS frequency. The phase values are reconverted into digital amplitude val-

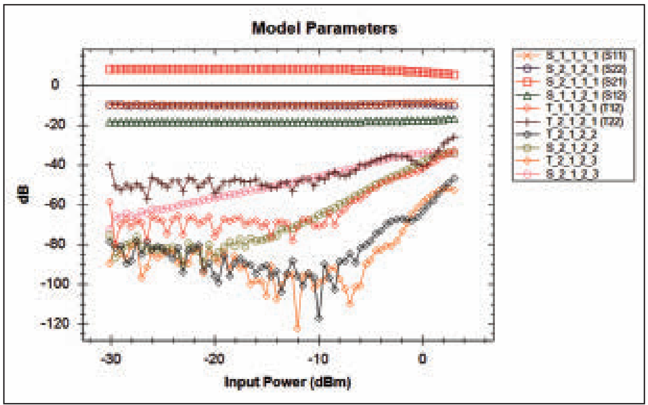

Fig. 5 Extracted model parameters.

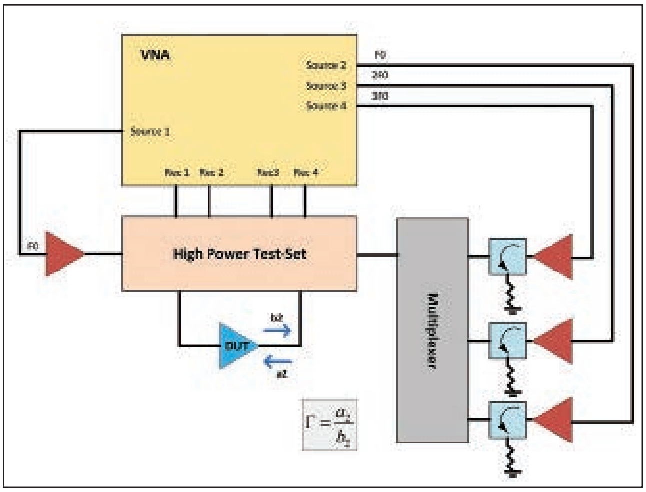

Fig. 6 Schematic of open loop harmonic load-pull.

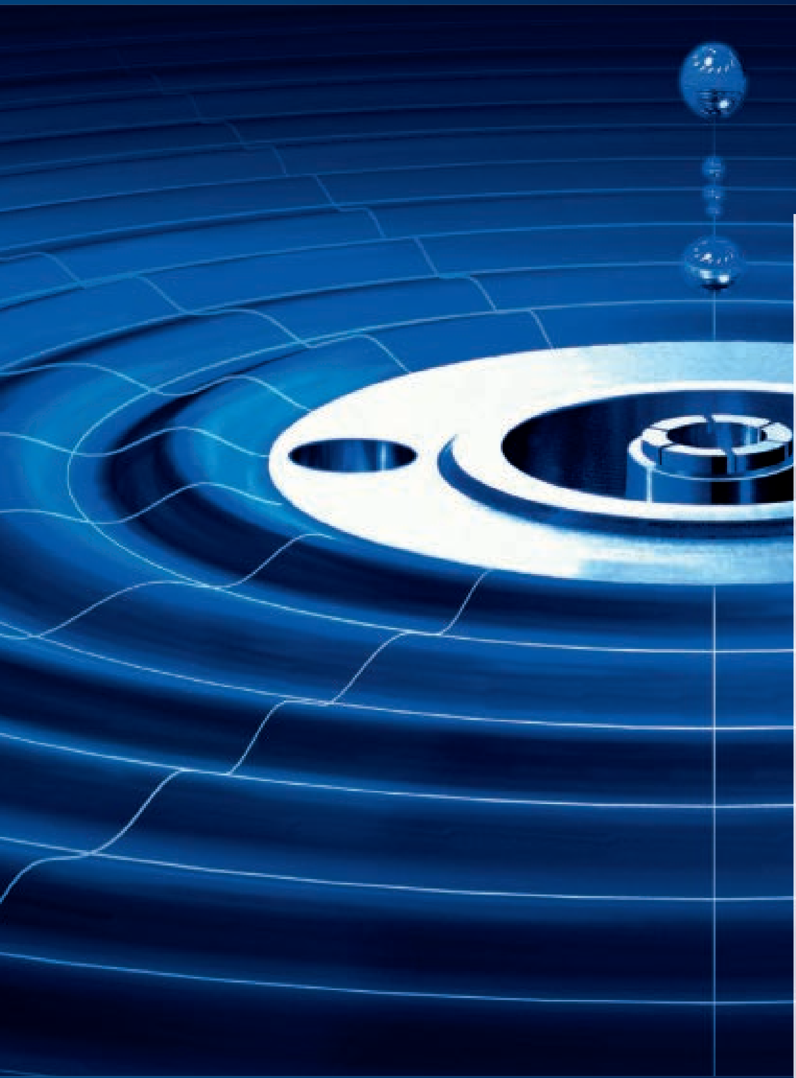

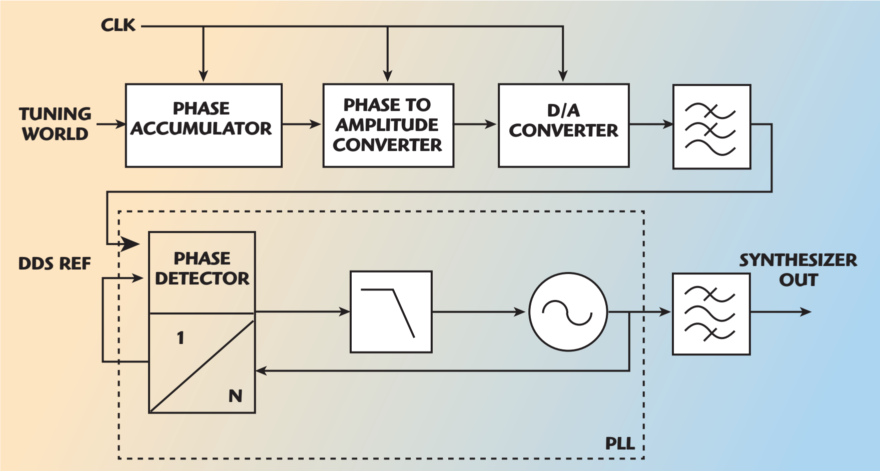

Fig. 7 Schematic of a DDS based signal source.

ues by the sine wave lookup table, e.g., from 0 to 65536 for 16 bit. A sine wave is created via a D/A converter; an anti-aliasing low pass filter is then used. This sine wave is used as a reference signal for a phase detector. The Phase Locked Loop (PLL) then locks the VCO's phase to the reference signal. This allows the setting of the VCO frequency by the DDS reference signal.

Such sources have many advantages over analog designs employing PLL, including improved phase noise, better frequency agility and precise control of the output phase and frequency. As the down-conversion local oscillator and all internal sources are driven from the same digital clock in this setup, there is no drift evident in the measured signals.

This was demonstrated in[4] over a 24-hour period. There are two main benefits. Firstly, it allows for active load-pull at much higher frequencies where the drift between sources locked using analog PLL makes an active load-pull approach unpractical. In this solution, active load-pull at frequencies up to 60 GHz have been demonstrated. Secondly, as the LO is also locked to the signal generators, constant phase relationships from sweep to sweep are achieved resulting in time invariant waveform reconstruction. This means that a phase reference is only required during calibration, thus allowing all sources in the VNA to be used during active harmonic load-pull.

ACTIVE LOAD-PULL AND WAVEFORM ENGINEERING

There are numerous benefits to the active load-pull approach described here, including the ability to control impedance anywhere, inside and outside of the Smith chart; reduced system footprint and perhaps most importantly speed. A recent paper[5] showed that using the same measurement instrument and setup; the speed of a 100-point load grid could be reduced by a factor of 7, from 4.5 minutes to only 41 seconds.

A patented quasi-closed loop architecture was also presented, showing where measurement speed is of the essence, such as in production environments. This architecture maintains the system stability of the open loop approach while offering further speed improvements; the same load-pull test is reduced to just 18.5 seconds.

The system can also be used to measure and engineer the terminal time-domain voltage and current waveforms. This approach can provide valuable insight to the designer. There are two main application spaces for Waveform Engineering.[6] The first is on the process development side, where Waveform Engineering can be used to identify the root cause of process issues.[7] The second application is optimization of device performance, allowing for the best possible design without the need for an iterative design approach.[8,9]

CASE STUDY – DEVICE DEGRADATION

This case study[7] looks at the use of Waveform Engineering to analyze a GaN HFET device that was suffering degradation in the field. Here a combination of RF and DC measurements were used to analyze the un-

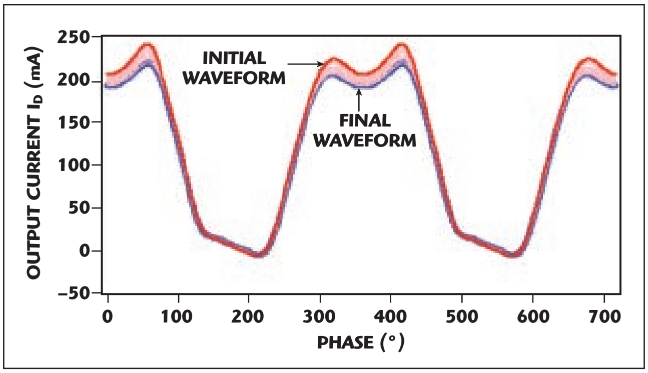

▲ *Fig. 8 Output current waveforms showing degradation.*

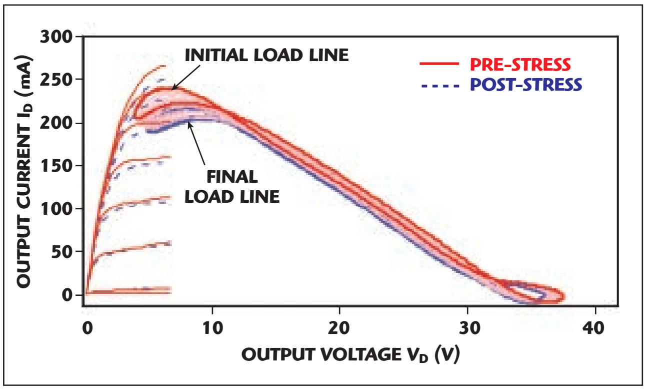

▲ *Fig. 9 RF load-line and DC I-V analysis pre and post stress.*

derlying cause of the problem. ***Figure 8*** illustrates the degradation observed in the output current waveforms (100 waveforms overlaid) with the original waveform shown in red and the final waveform shown in blue.

There is a clear reduction in peak current, causing a drop in output power and efficiency. Next a stress test was applied. To do this DC and RF measurements were conducted first at turn on and then after 90 minutes. DC I-V's with overlaid RF load-lines (created by plotting the output voltage against output current) are shown in ***Figure 9***; again red is the starting condition. The degradation can be seen both in the RF load-lines and the DC I-V's after stress testing.

Using Waveform Engineering it is possible to excite only part of the I-V space of the device. For example, by biasing the device at a low drain voltage with high quiescent current, then limiting the drive power, it is possible to excite only the high current region of the I-V space. Conversely, by biasing at a higher drain voltage and low quiescent current it is possible to excite only the high voltage region of the I-V space.

Although the RF remains unchanged pre/post stress in both cases if we look at the DC I-V's it is clear that the device degradation is caused by high electric field in the high voltage region rather than thermal effect caused by high current. Armed with this additional information the process team could target their efforts and solve the issue in a timely manner.

CARDIFF MODEL+

Having shown how useful the Waveform Engineering can be, this section looks at how to move the design process back to the simulator by means of a more advanced behavioral model. While behavioral modeling techniques such as X-Parameters™ can be created to cover impedance, this requires the creation of a number of nonlinear models – one for each impedance point. Interpolation is then conducted within the simulator.

In contrast, the Cardiff Model+ formulation, which is also a descendent of the PHD model formulation, extends the order of the formulation such that a single model can be used to fit an entire impedance space.[10] This reduces the file size of the model.

CASE STUDY – CARDIFF MODEL+

This case study shows the process and results of modeling a 0.5 W PHEMT device at 9 GHz. In this case the model is for a fixed set of harmonic impedances, but these can also be included in the formulation if required. Once the load-pull has been completed the process of creating a model is simple: load the data into the model generator software, select the appropriate model type (in this case fundamental only) and export the model. The model can be exported in a format suitable for use in either ADS or Microwave Office®.


GREAT SERVICE ISN'T EXPENSIVE...
...IT'S PRICELESS.
EXCELLENT SERVICE
EXCELLENT DELIVERY
EXCELLENT QUALITY
RF COAXIAL RELAYS
SMA, N AND PCB LAUNCH
STANDARD AND CUSTOM DESIGNS
RELCOMM TECHNOLOGIES, INC.
• Mission Critical Communications:
- Security, Safety and Intelligence
- Commercial Telecom Infrastructure
- Military Defense Fixed, Mobile & Shipboard
• Instrumentation:
-Test and Measurement
RF Relay Store.com is the answer to your urgent small quantity needs.
RF Coaxial Relays available from Stock at www.rfrelaystore.com
sales@relcommtech.com • www.relcommtech.com • 410-749-4488
EXCELLENCE BY DESIGN

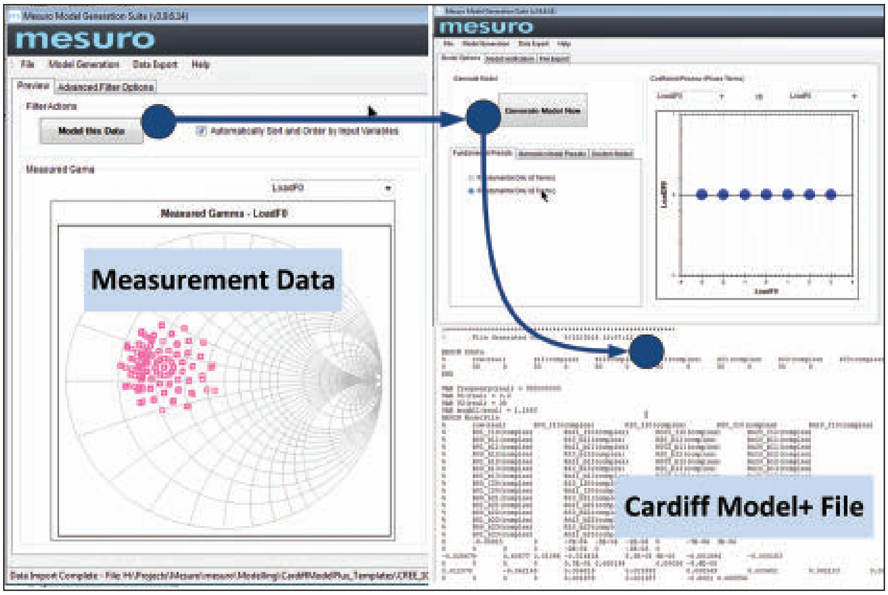

Fig. 10 Model generator software.

Once the process is completed it is possible to verify the results directly in the model generator. The exported model can be used within the CAD environment, see ***Figure 10***, and can be used to look at traditional power and efficiency analysis as well as performing Waveform Engineering.

CONCLUSION

This article has shown how advances in VNA technology can be combined with advances in nonlinear measurement solutions to ease the design process for new device technologies and modules integrating nonlinear devices. A simple behavioral model has been introduced and discussed along with its limitations as a local model. More advanced measurement systems building upon recent advances in VNA technology were also introduced showing how active load-pull can be used to improve the capability of load-pull benches.

Waveform Engineering was introduced with case studies in process development and high power amplifier design. A more advanced behavioral modeling formulation was also introduced, allowing a user to move the Waveform Engineering approach fully into a simulation environment. ■

References

1. J. Verspecht and D. E. Root, "Polyharmonic Distortion Modeling," *IEEE Microwave Magazine 1527-3342/06*, June 2006.
2. Y. Takayama, "A New Load-Pull Characterization Method for Microwave Power Transistors," *MTT-S International Microwave Symposium Digest 1976*, Volume 76, Issue 1, pp. 218–220.
3. Technical Data Sheet 4T-070 Maury Microwave. "High-Gamma Automated Tuners (HGTTM)."
4. A. Aldoumani, P.J. Tasker. R.S. Saini, J.W. Bell, T. Williams and J. Lees, "Operation and Calibration of a VNA-based Large Signal RF I-V Waveform Measurement System without using a Harmonic Phase Reference Standard," *81st ARFTG Microwave Measurement Conference*, June 7, 2013.
5. T. Williams, B. Wee, R. Saini, S. Mathias and M. VandenBossche, "A Digital, PXI-Based Active Load-Pull Tuner to Maximise Throughput of a Load-Pull Test Bench," *83rd ARFTG Microwave Measurement Conference*, June 6, 2014.
6. P. Tasker "Practical Waveform Engineering," *IEEE Microwave Magazine*, December 2009.
7. C. J. Roff. "Application of Waveform Engineering to GaN HFET Characterization and Class F Design," PhD Thesis, University of Wales Cardiff, January 2009.
8. M. Iwata et al., "First Pass Design of a High Power 145 W, High Efficiency Class J Amplifier using Waveform Engineering," *IEEE Radio and Wireless Week 2013*.
9. P. Wright, J. Lees, J. Benedikt, P.J. Tasker, S.C. Cripps, "A Methodology for Realizing High Efficiency Class-J in a Linear and Broad-band PA," *IEEE Transactions on Microwave Theory and Techniques*, Vol. 57, No 12, December 2009.
10. S.P. Woodington. R.S. Saini, D. Williams, J. Lees, J. Benedikt and P.J. Tasker, "Behavioral Model Analysis of Active Harmonic Load-pull Measurements," *Microwave Symposium Digest*, 2010.

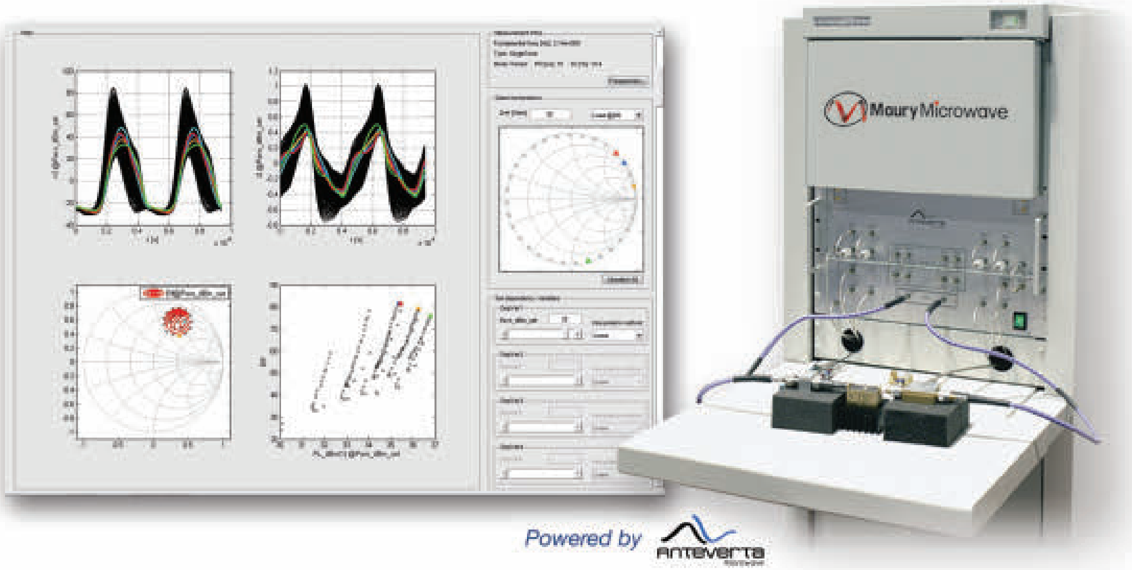
Maury Microwave

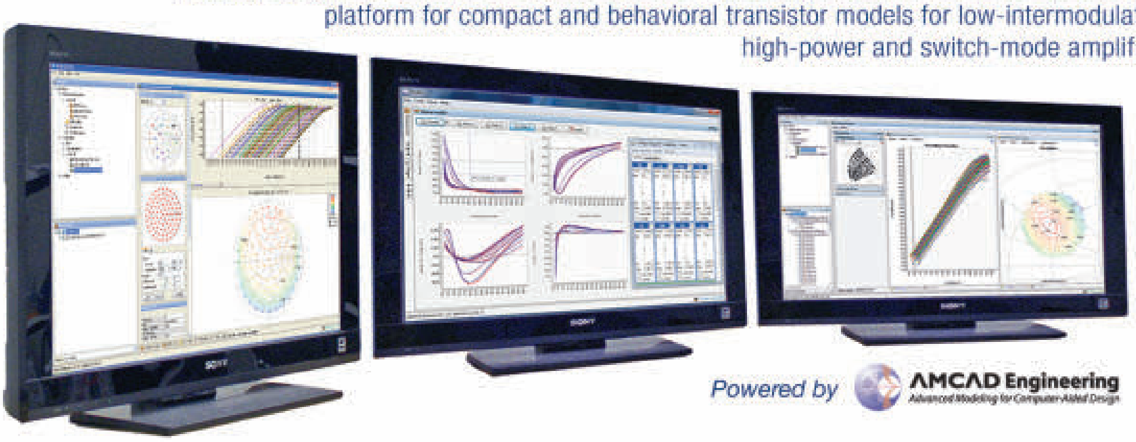

Intelligent Integration

Once Again, CMOS Wins

Peregrine Semiconductor, San Diego, CA

The path to intelligent integration began over 25 years ago when it was first demonstrated that silicon on insulator (SOI) could be mass-produced for the RF industry. RF experts know when silicon reaches the performance of the exotic technologies used to meet RF performance needs – silicon wins! Fast-forward to today and we are seeing unprecedented RF integration – yielding smaller footprints, better reliability, increased power efficiency and configurability. Cellular phone manufacturers can use one RF front-end solution that can accommodate all 40, and growing, LTE bands. We call that technology the UltraCMOS® Global 1. It helps RF engineers face the challenge of designing and tuning products to work in all of these bands and accommodate the 5,000-fold increase in operating states.

The need for intelligent integration is not only in the cellular realm. Aerospace products also need this level of integration. Just look at active electronically scanned array (AESA) antennas, also known as phased-array antennas. These antennas have a large number of individual active elements, each of which requires its own RF signal processing (typically phase and amplitude), as well as amplification and signal path switching. These elements are all tightly packed into a small physical area, and there are tough requirements on the size of the solution, as well as power consumption and efficient programming using a serial digital interface.

That's why Peregrine developed the first integrated X-band, CMOS core chip to utilize MMIC design techniques and unlock performance advantages at high frequencies. On a single die, this chip integrates a 7-bit digital phase shifter, a 7-bit digital step attenuator, all signal path switching and a compact digital serial bus interface. This X-band core chip offers a maximum power handling of +18 dBm from 9-10.1 GHz and covers 31.75 dB attenuation range in 0.25 dB steps. The phase shifter offers 358 degrees of phase range with a resolution of 7 degrees. It maintains high attenuation and phase accuracy over frequency and temperature and exhibits low power consumption.

With the integration capability, repeatability and reliability of silicon, Peregrine's IC manufacturing technology utilizes a low-loss insulating substrate that performs as a high performance equivalent to III-V technologies at milimeter-wave frequencies. Hence, Peregrine's UltraCMOS technology solves the challenge of new AESA antenna systems and does so monolithically through intelligent integration – something gallium arsenide (GaAs) technologies could never achieve.

This is but one example of where the industry is rapidly moving. Peregrine also brings intelligent integration into the low frequencies with the True DC switch, the only RF switch to achieve 0 Hz. UltraCMOS technology allows for intelligent integration across the entire frequency spectrum.

For more information visit www.psemi.com/intelligentintegration.

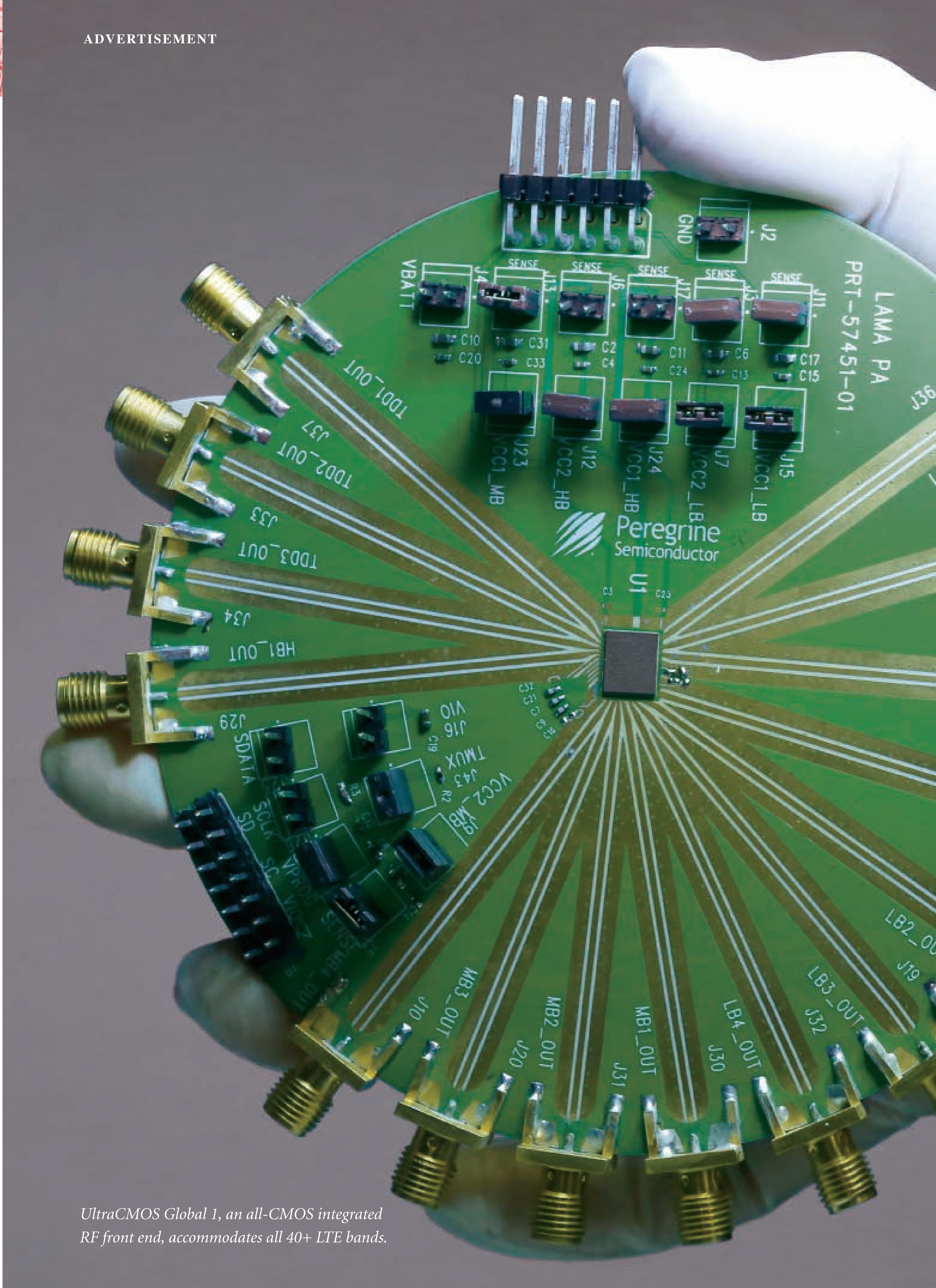

UltraCMOS Global 1, an all-CMOS integrated RF front end, accommodates all 40+ LTE bands.

High Speed Arbitrary Waveform Generator

Keysight Technologies Inc.
formerly Agilent Technologies electronic measurement business
Santa Rosa, Calif.

This is the decade of mobile broadband: seemingly everyone and everything is connected to the Internet, and all need to exchange more and more data. As today's electronic devices become smarter, they contain more functionality, are more highly integrated and manage much greater volumes of data. Enabling access to anything from anywhere—while moving huge amounts of data—is one of today's most daunting challenges.

As electronic devices evolve, so must the instruments used to test them. With the tighter specifications of high speed devices, testing is no longer an option: it's mandatory.

To stay ahead of the curve, today's test instruments must have the following attributes:

- Reach higher frequencies while providing wider bandwidth
- Handle complex modulation techniques needed to cram more data into available bandwidths
- Work with ideal and real-world signals
- Stress devices to their limits
- Provide reliable and repeatable results

FOCUSING ON AWGS

Taking these typical test requirements into consideration, an AWG might seem to be the perfect stimulus device. The M8195A is a new arbitrary waveform generator with the highest combination of sample rate, bandwidth and channel density currently available. It provides up to 65 GSa/s, 20 GHz analog bandwidth and up to four channels in a one-slot AXIe module – simultaneously.

APPLICATIONS

As optical communication data rates move from 100 to 400 Gb/s and 1 Tb/s, they require a very wideband electrical stimulus with a variety of complex modulation formats from QPSK, to any quadrature amplitude modulation (QAM), to orthogonal frequency-division multiplexing (OFDM) at symbol rates up to 32 GBaud (see

Figure 1) and beyond.

In order to drive dual-polarization systems, the M8195A has four independent, precisely synchronized output channels in a single AXIe module. Since all four channels are generated by the same instrument without any external circuitry, precise synchronization down to the femto-second-range can be achieved and maintained.

The M8195A uses digital pre-distortion techniques to achieve a clean signal out-of-the-box and at the device under test. Distortions generated by cables, amplifiers etc. can be compensated by embedding/de-embedding the S-parameters of the respective circuits or by performing an in-situ calibration.

Digital interfaces are facing increasing data throughput as well. Traditionally this has been accomplished by increasing the data rate or by increasing the number of parallel signals. However, at a certain point in time, it is more cost-effective to consider multi-level signaling techniques. Examples are high-speed backplane connections using pulse-amplitude modulation 4 (PAM4) (see ***Figure 2***) or PAM8 modulation formats, but also technologies in the mobile application space such as MIPI C-PHY.

The M8195A is well suited to address these multi-level and multi-channel interfaces using any standard or custom data format. The flexibility of the waveform generation at highest speeds, combined with excellent intrinsic jitter performance (see ***Figure 3***), makes the

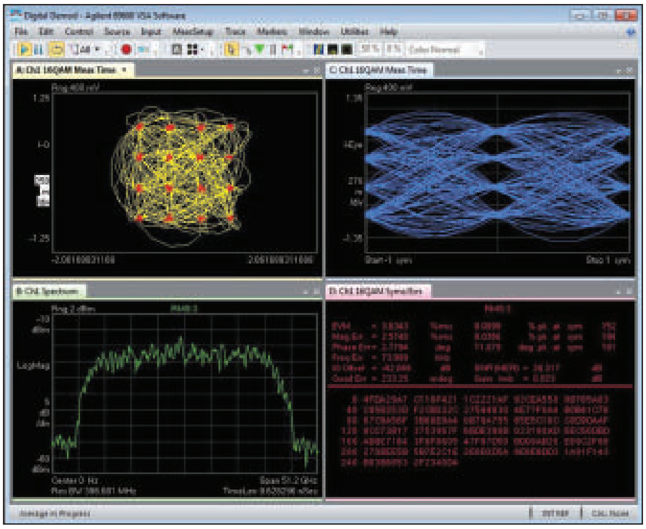

▲ *Fig. 1 16 QAM at 32 GBaud.*

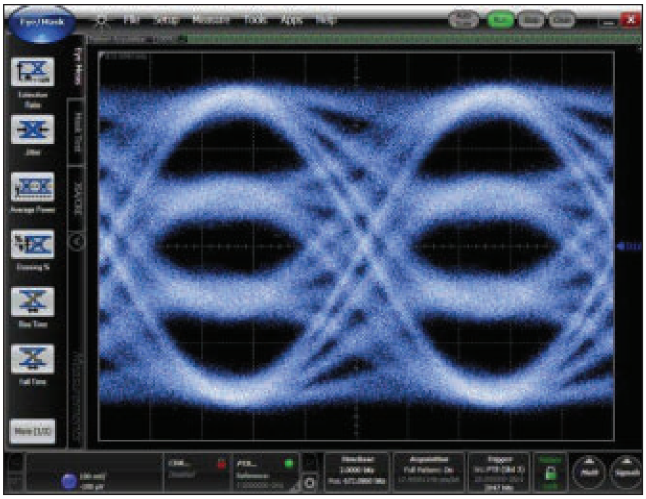

▲ *Fig. 2 PAM 4 signal at 28 GBaud (=56 Gb/s).*

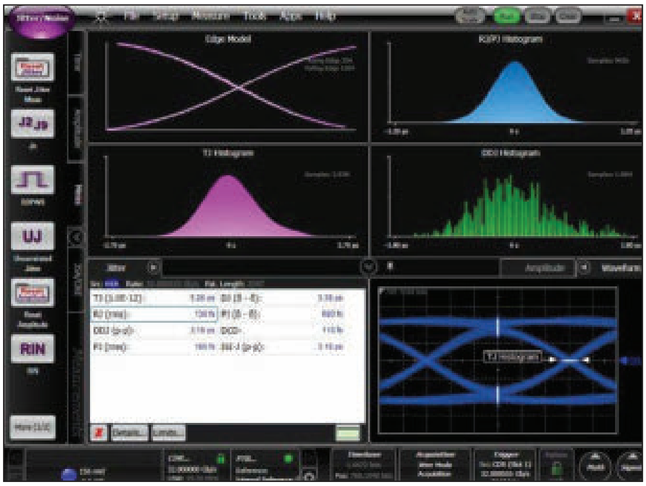

▲ *Fig. 3 32 Gb/s PRBS2^{11}-1 showing 138 fs RJ (rms) generated by the Keysight M8195A.*

M8195A a future proof instrument – independent of which direction the technology is moving.

At data rates of multiple Gb/s, the effect of cables, board traces or connectors have to be taken into account in order to generate the desired signal at the test point of the device under test. The M8195A incorporates digital pre-distortion techniques to generate the desired signal at the device under test. Channels can be embedded / de-embedded with the S-parameters of the respective circuits. With up to four differential output channels per one-slot AXIe module and the ability to synchronize multiple modules, the M8195A is well suited to stimulate multi-lane high speed interfaces in an economic fashion.

Physics, chemistry and electronics research working at the edge of technology, call for precise and configurable pulses down to 100 ps or less for extremely short, yet wideband RF pulses and chirps. Any arbitrary waveform which can be described mathematically can be generated e.g., in Matlab and downloaded to the M8195A.

EW and communications/satcom applications require extremely wide instantaneous bandwidth from DC to the Ku-Band. In addition, jamming requires fast frequency hopping across bands within hundreds of picoseconds.

The M8195A is designed to address these requirements. With built-in frequency and phase calibration, it is straightforward to generate wideband multi-tone signals (see ***Figure 4***) with a flat frequency response up to 20 GHz with the M8195A. Wideband wireless signals with any modulation scheme (e.g., nPSK, nQMA, OFDM, etc.) can be generated directly at carrier frequencies of up to 20 GHz. In many cases, this saves an additional up-conversion stage or enables waveform generation directly at the carrier frequency.

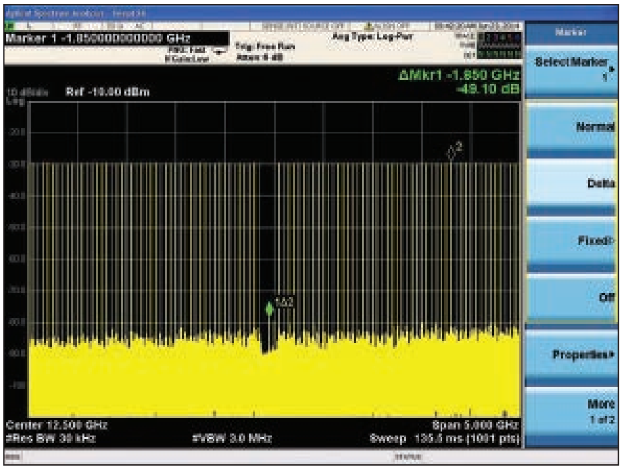

▲ *Fig. 4 Multi-tone signal from 10 to 15 GHz.*

M8195A AT A GLANCE

As devices and interfaces become faster and more complex, the M8195A AWG gives you the versatility to create the signals you need for digital applications, optical and electrical communication, advanced research, wideband radar and satcom. The M8195A gives you the possibility to test where you have never been able to test before in speed, in bandwidth and in channel density.

Key features of the M8195A:
- Sample rate up to 65 GSa/s
- Analog bandwidth to 20 GHz
- 1, 2 or 4 channels in one slot AXIe module

New technologies make it possible to adapt to evolving test requirements. This is especially true with next-generation arbitrary waveform generators, such as the M8195A that offer wide bandwidth and high resolution. These technologies enable the creation of precise time-domain signals and provide the flexibility to address many applications typically covered by function or pulse generators. In the frequency-domain, AWGs have been used to generate baseband signals. Now, they are also moving into RF applications, not only due to high sampling rates and analog bandwidths, but also high signal quality in terms of spurious free dynamic range (SFDR) and phase noise performance.

VENDORVIEW

Keysight Technologies Inc.
(formerly Agilent Technologies electronic measurement business)
Santa Rosa, Calif.
www.keysight.com/find/M8195A

Millimeter-Wave Full Waveguide Band Mixers

SAGE Millimeter Inc.
Torrance, Calif.

Broadband or full waveguide devices are always desirable and required for many system integrations, such as fiber optics, EW and instrumentation applications. Many broadband devices operating from tens of MHz to 50 GHz were developed and have become available in the industry in recent years. However, the broadband devices in high millimeter-wave bands are still under development and their availability is limited. Among these devices, the full waveguide band frequency sources with +13 dBm or higher power output that are required to drive the standard balanced mixers in V-, E-, and W-Bands are still very expensive and difficult to manufacture.

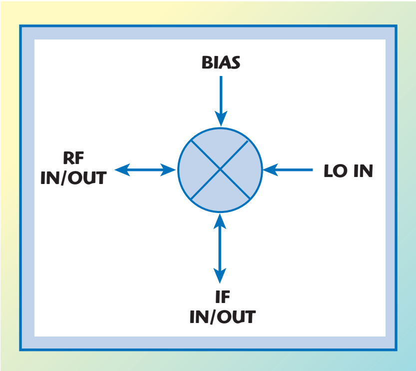

▲ *Fig. 1 Mixer schematic.*

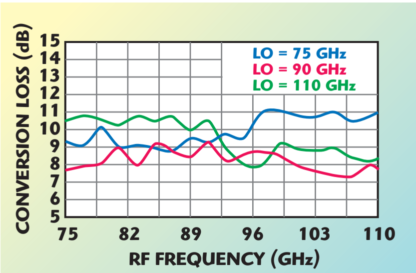

▲ *Fig. 2 Conversion loss vs. RF frequency.*

SAGE Millimeter has introduced a series of full waveguide band externally biased mixers in V- (50 to 75 GHz), E- (60 to 90 GHz), and W-Bands (75 to 110 GHz). These mixers implement high performance GaAs Schottky diodes, a balanced structure and proprietary circuit design to yield full waveguide operation with extreme broadband IF bandwidth. The mixers only require nominal 0 to +5 dBm local oscillator (LO) power and +5 V DC bias. Due to its balanced configuration, these mixers offer low conversion loss and noise figure, less harmonic products and high port-to-port isolations. The IF bandwidth coverage of the mixers is DC to 25 GHz for V-Band and up to DC to 40 GHz for W-Band. The typical input P1dB of these mixers is -5 to 0 dBm. The required 0 to +5 dBm LO driving power for these mixers is readily available from SAGE Millimeter's low cost SFP series passive multipliers.

While these mixers are designed and manufactured for double sideband operation, they can be reconfigured as single sided mixers by adding proper SAGE Millimeter SWF series high performance waveguide filters to form either upper sideband (USB) or lower sideband (LSB) mixers. In the meantime, they can also be used as up-converters for various transmitting or up-converting system applications. ***Figure 1*** shows the circuit schematic of the mixers.

The conversion loss of the mixer in a given bandwidth of operation is the key specification for any mixer product. ***Figure 2*** shows the conversion losses of the W-Band mixer with local oscillator frequency at 75, 90 and 110 GHz while the RF sweeps from 75 to 110 GHz. When LO is set at 75 GHz, the mixer operates as an upper sideband (USB) mixer. When the LO is at 94 GHz, the mixer operates as both an upper and a lower sideband (LSB) mixer. Finally, when the LO is at 110 GHz, the mixer operates as a low sideband (LSB) mixer. The external bias of the mixer is +5 V DC/0.8 mA while the LO power is +3 dBm. The plot shows that the mixer exhibits good conversion

TABLE I

SPECIFICATIONS OF SFB SERIAL EXTERNALLY BIASED MIXERS

Extender Model Number	*SFB-15-E2*	*SFB-12-E2*	*SFB-10-E2*
RF Frequency Range (GHz)	50 to 75	60 to 90	75 to 110
LO Frequency Range (GHz)	50 to 75	60 to 90	75 to 110
LO Power (dBm)	0 to +5	0 to +5	0 to +5
IF Frequency Range (GHz)	DC to 25	DC to 30	DC to 35
Conversion Loss (dB, Typical)	11	12	13
RF and LO Waveguide Size	WR-15	WR-12	WR-10
RF and LO Waveguide Flange	UG385/U	UG387/U	UG387/U-M
IF Port Connector	K(F)	K(F)	K(F)
DC Bias (VDC/mA, Typical)	+5/1	+5/1	+5/1
DC Bias Port Connector	SMA(F)	SMA(F)	SMA(F)
Size (L" × W" × H")	1.16 × 0.75 × 0.75	1.16 × 0.75 × 0.75	1.16 × 0.75 × 0.75
Weight (Oz)	1	1	1

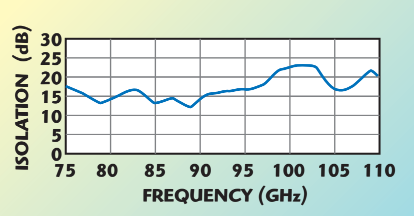

▲ *Fig. 3 RF to LO port isolation.*

losses across DC to 35 GHz IF bandwidth while RF swept is from 75 to 110 GHz.

Figure 3 shows the RF port to LO port isolation. Due to the waveguide cut off nature, the IF to LO and IF to RF port isolation is infinite, while the RF and LO leakage at IF port is relatively high – which can be improved by adding an external lowpass filter (LPF). ***Table 1*** shows the main electrical and interface specifications of the featured full waveguide band externally biased mixers.

Although the mixers' RF and LO ports are equipped with standard waveguides, SAGE Millimeter's SWC series waveguide to coax adapters can be used to convert the interface to 1.85 or 1 mm coaxial interface. In addition, SAGE Millimeter also offers non-biased full waveguide bandwidth balanced mixers to cover the 18 to 140 GHz frequency range.

VENDORVIEW

SAGE Millimeter Inc.
Torrance, Calif.
(424) 757-0168
info@sagemillimeter.com
www.sagemillimeter.com

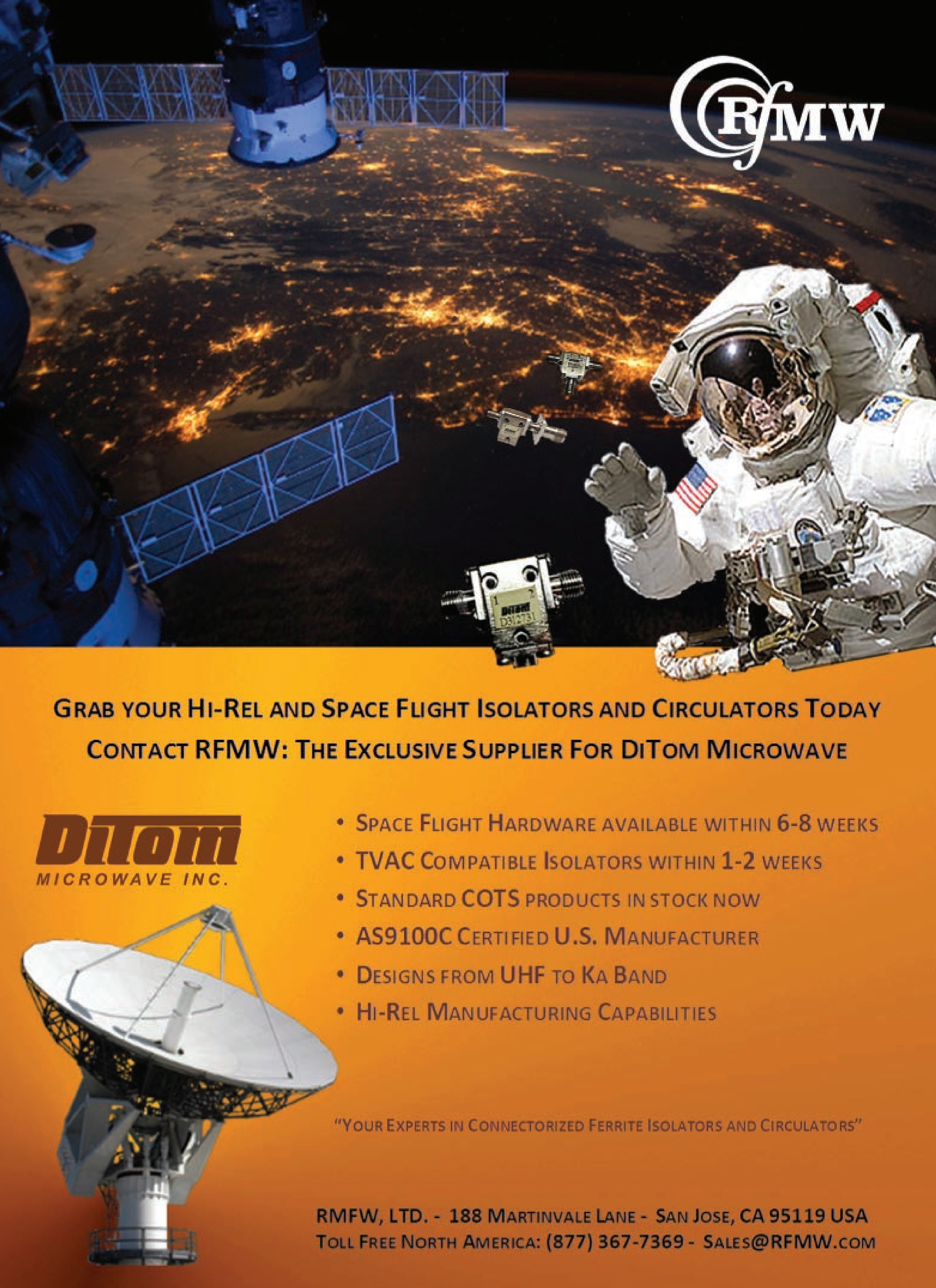
RFMW
GRAB YOUR HI-REL AND SPACE FLIGHT ISOLATORS AND CIRCULATORS TODAY
CONTACT RFMW: THE EXCLUSIVE SUPPLIER FOR DITOM MICROWAVE
DiTom
MICROWAVE INC.
• SPACE FLIGHT HARDWARE AVAILABLE WITHIN 6-8 WEEKS
• TVAC COMPATIBLE ISOLATORS WITHIN 1-2 WEEKS
• STANDARD COTS PRODUCTS IN STOCK NOW
• AS9100C CERTIFIED U.S. MANUFACTURER
• DESIGNS FROM UHF TO KA BAND
• HI-REL MANUFACTURING CAPABILITIES
"YOUR EXPERTS IN CONNECTORIZED FERRITE ISOLATORS AND CIRCULATORS"
RMFW, LTD. - 188 MARTINVALE LANE - SAN JOSE, CA 95119 USA
TOLL FREE NORTH AMERICA: (877) 367-7369 - SALES@RFMW.COM

Transient Analysis and VCO Testing

Anapico Ltd.
Glattbrugg, Switzerland

Anapico has enhanced the APPH series of fully automated signal source analyzers offering a measurement capability up to 26 GHz. Besides the additive and absolute phase noise measurements from 0.1 Hz to 50 MHz offsets, additional measurement capability has been added such as transient analysis, RF spectrum monitoring and VCO characterization, making the APPH a very versatile signal source analyzer.

The instrument is simple to use and offers high accuracy and reproducibility, allied to good measurement speed. It provides high dynamic range with low system noise floors, while at the same time offering attractive cost of ownership for labs and production environments.

Two models are available, which are application dependant – the APPH6040 covers the 5 MHz to 7 GHz range while the APPH20G goes from 5 MHz to 26 GHz. The instruments are Ethernet, USB or GPIB controlled and 'plug-and-play' with any standard computer. The entire instrument is enclosed in a compact, fanless 3U 19 inch chassis and weighs 4.5 kg.

Developing the product on a fully integrated, low power platform has avoided fan cooling, further eliminating spurious signals and ground and power line loops. In fact, using an external battery this unit can be operated anywhere without need for AC power.

Available options include dual programmable low noise power supplies up to 15 V and 500 mA current, an ultra low close to carrier phase noise option of the internal reference synthesizer and a GPIB communication interface. Since the APPH series uses PC, laptop or tablets as the control unit, it does not incorporate displays, which minimizes costs while increasing reliability.

FREQUENCY AND PHASE TRANSIENT MEASUREMENTS

With the enhanced firmware, the APPH works like a high performance modulation domain analyzer – providing a view of frequency or time interval measurements over time. This way of seeing data is intuitive, enabling frequency switching, jitter or modulation to be viewed directly. The APPH also adds the time dimension to frequency counter results. Therefore, frequency variations can be seen directly without the dead-time between measurements traditionally found in frequency counters.

In effect, the APPH becomes a 'frequency oscilloscope' – measuring carrier frequencies

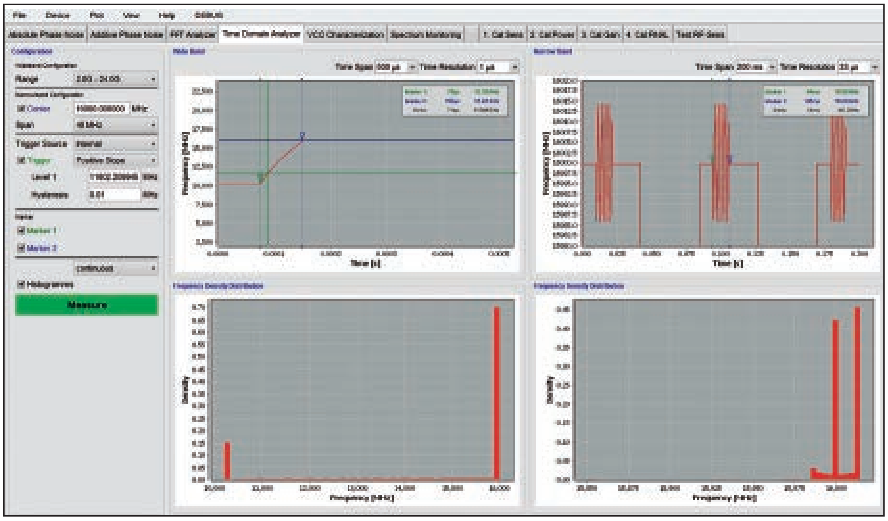

▲ *Fig. 1 APPH time domain measurement.*

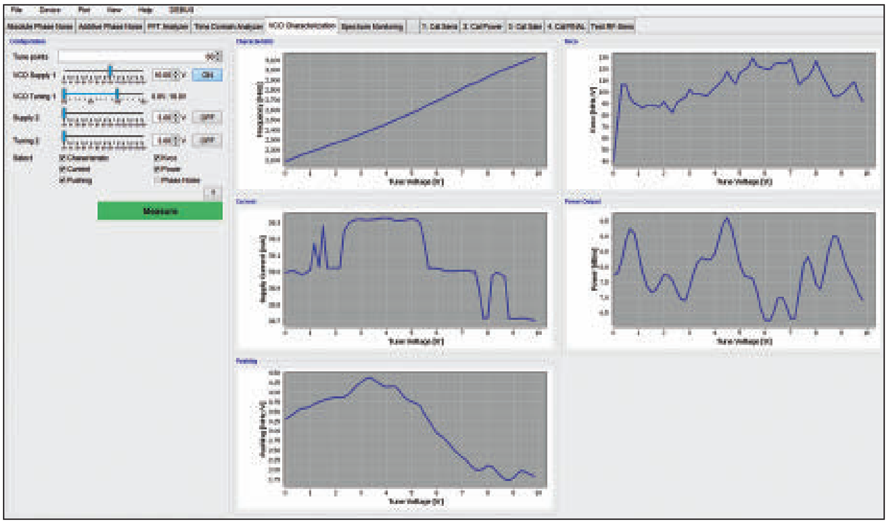

▲ *Fig. 2 APPH VCO characterization example.*

versus time up to 26 GHz as fast as every 16 ns. Through continuous sampling of the carrier frequency, modulation can be recovered and carrier dynamics analyzed.

The APPH's transient measurement supports two modes, a narrowband and a wideband mode, both running synchronously. The wideband mode can be used to observe wide frequency span transients up to 20 GHz bandwidth. The narrowband mode is used to determine frequency transients with fine frequency resolution. With a time resolution down to 16 ns and a continuous time span up to several hours, a large number of applications can be covered. These include: measuring the frequency droop on individual channels in frequency hopping systems; analyzing chirp radar performance; measuring pulse jitter and viewing the distribution histogram; calibrating frequency sweep signals; and calibrating intentional modulation (FM or FSK).

Further applications consist of: analyzing PLLs and frequency locked-loops; discovering phase jumps in synchronization clocks; detecting missing periods from rotational encoders; measuring frequency settling times of VCOs; and characterizing start-up/warm-up of oscillators. A very powerful trigger system enables the selection of the trigger mode, source, polarity and hysteresis, and pre-trigger delay, the same as established digital sampling oscilloscopes provide.

MEASUREMENT EXAMPLE

A screenshot of a time domain measurement is shown in ***Figure 1***. Via the GUI interface, switching between the various measurements such as phase or amplitude noise, FFT analyzer, transient measurement, etc., can be done by just changing the respective tab at the top.

The GUI is configured to trigger on a frequency transient of a fast wideband synthesizer (APSYN420D) switching from approximately 10 to 16 GHz. In the upper left window, the wideband transient can be observed, showing a switching transient of approximately 20 microseconds. In the upper right window the 'zoomed-in' narrowband measurement, taken over a much longer time span, reveals details of the frequency modulation on top of the 16 GHz carrier. The lower windows have been configured to provide the frequency distribution over the measurement time span.

VCO CHARACTERIZATION

In order to characterize a VCO, at least two (low noise) DC sources and one signal analyzer are needed, which can measure power, frequency and phase noise. With its four independent programmable DC voltages to supply and control the device under test (DUT), the APPH can automatically characterize the VCO versus tuning voltage for the following parameters: frequency, tuning sensitivity, output power, current consumption, supply pushing and SSB phase noise. ***Figure 2*** shows a typical measurement of a wideband VCO taken with the APPH SSA. The desired VCO parameters are captured in a single sweep.

In summary, the Anapico APPH signal source analyzer has been extended with new measurement capabilities. Besides the powerful phase noise measurements (additive and absolute), other measurements are supported such as a transient time domain measurement mode, an FFT analyzer, a real time spectrum monitor and a VCO characterization tab. These independent measurement capabilities are easily used by a single intuitive graphical user interface. For production testing (ATE), a remote SCPI based programming language is supported with throughput optimized measurement times.

Anapico Ltd.
Glattbrugg, Switzerland
+41 44 515 55 01
sales@anapico.com
www.anapico.com

Procedure for how to use the N, TNC and 7/16 Push-On male. Push-On Connectors mate with any standard female connector of the same connector style.

1. Convert your standard Assembly into a Push-On Assembly using the Nf to Nm Push-On Adapter.

2. Put your fingers firmly onto the knurls of the "Lock Nut".

3. Push "Lock Nut" forward and engage the Push-On end of the Adapter with the mating female. Back nut must be released.

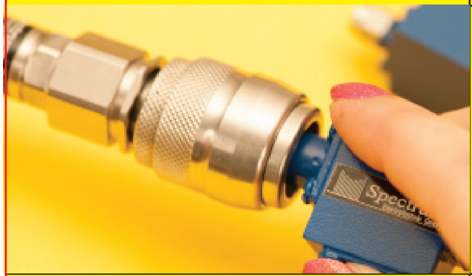

4. The Connection has been completed, easy and fast. The connector has been locked on safely.

5 . To unlock (when "Back Nut" is in unlocked mode) push the "Lock Nut" forward and stop reverse movement by setting your fingers onto the "Back Nut".

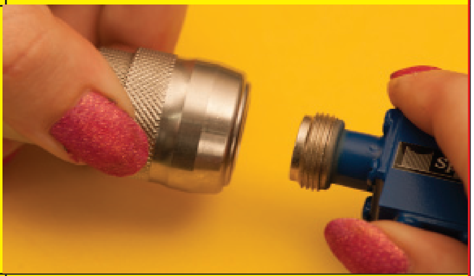

6. Keep fingers on "Back Nut" to ensure that "Lock Nut" cannot slide back and pull the connector off.

Procedure for how to use the SMA male and SMA female Push-On connectors. SMA Push-On Connectors mate with any standard connector of the same but opposite connector style.

1. Convert your standard cable assembly into a Push-On Assembly by threadening the standard female side of the adapter onto the male connector of the assembly.

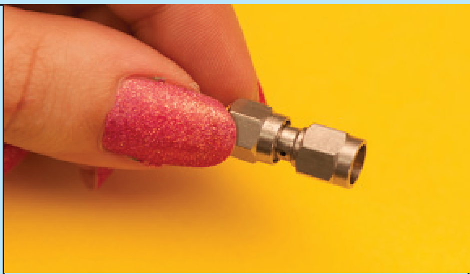

2. Your standard SMA male cable assembly is converted into an SMA male Push-On Assembly.

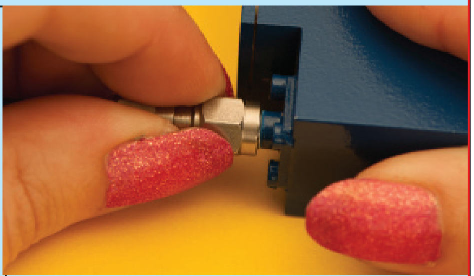

3. Just slide the Push-On SMA male Connector onto any standard SMA female. The connection is securely completed in seconds.

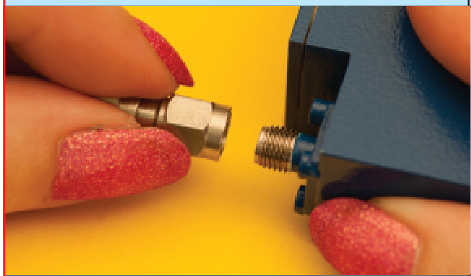

4. To disconnect, just pull the connector off.

Spectrum
Elektrotechnik GmbH

Please contact us at:
www.spectrum-et.com
Email: sales@spectrum-et.com
Phone: +49-89-3548-040
Fax: +49-89-3548-0490

Spectrum
Elektrotechnik GmbH

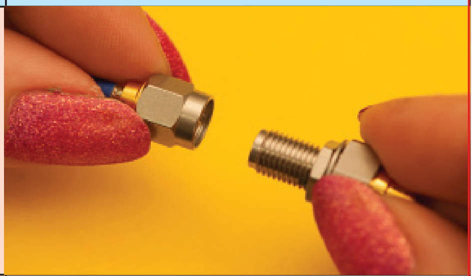

1. Convert your standard cable assembly into a Push-On Assembly by threadening the standard female side of the adapter onto the male connector of the assembly.

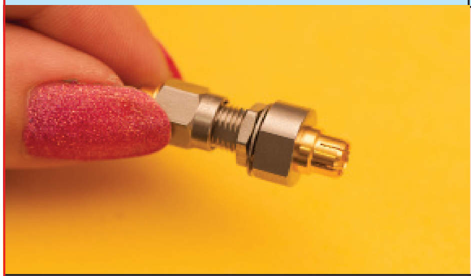

2. Your standard SMA male cable assembly is converted to a Push-On SMA female Cable Assembly.

3. Just slide the Push-On SMA female Connector onto any standard SMA male. The connection is securely done in seconds.

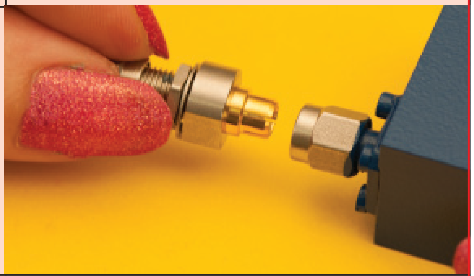

4. To disconnect, just pull the connector off.

Low PIM Cable Jumpers

Pasternack has released a new series of low PIM cable jumpers with 0.163" and 0.276" hand-formable coax cables. They have a low smoke, zero halogen jacket material with PIM specifications of -150 and -160 dBc depending on the model. They are 100 percent RF and PIM tested and available in 4.1/9.5 mini DIN, 7/16 DIN, Type N and SMA combinations. The 4.1/9.5 mini DIN, 7/16 DIN and Type N meet the -160 dBc PIM specification while the SMA versions meet the -150 dBc PIM specification.

The 4.1/9.5 mini DIN cables are designed for DC to 3 GHz with a maximum VSWR of 1.2:1. The 7/16 DIN cables also operate from DC to 3 GHz with a maximum VSWR of 1.15:1. The Type N cables operate from DC to 6 GHz with maximum VSWR of 1.15:1 to 1.25:1. The SMA cables operate from DC to 6 GHz with a maximum VSWR of 1.15:1.

All cables are RoHS compliant with RF shielding of -100 dB and a maximum input power of 440 W. The operating temperature range is -55° to +125°C. The cables are available in standard 100 and 200 cm lengths from stock.

Pasternack is a global supplier of RF and microwave components supported by a growing list of 19 international distributors who service customers in more than 35 countries. Through their partnerships, Pasternack aims to be the most recognized and trusted provider of urgently needed RF/microwave components and assemblies.

VENDORVIEW

Pasternack
Irvine, Calif.
(866) 727-8376
www.pasternack.com

Exceptional Phase Noise Performance

Dielectric Resonator Oscillator

DRO100 & DRO1024

10 GHz **10.24 GHz**

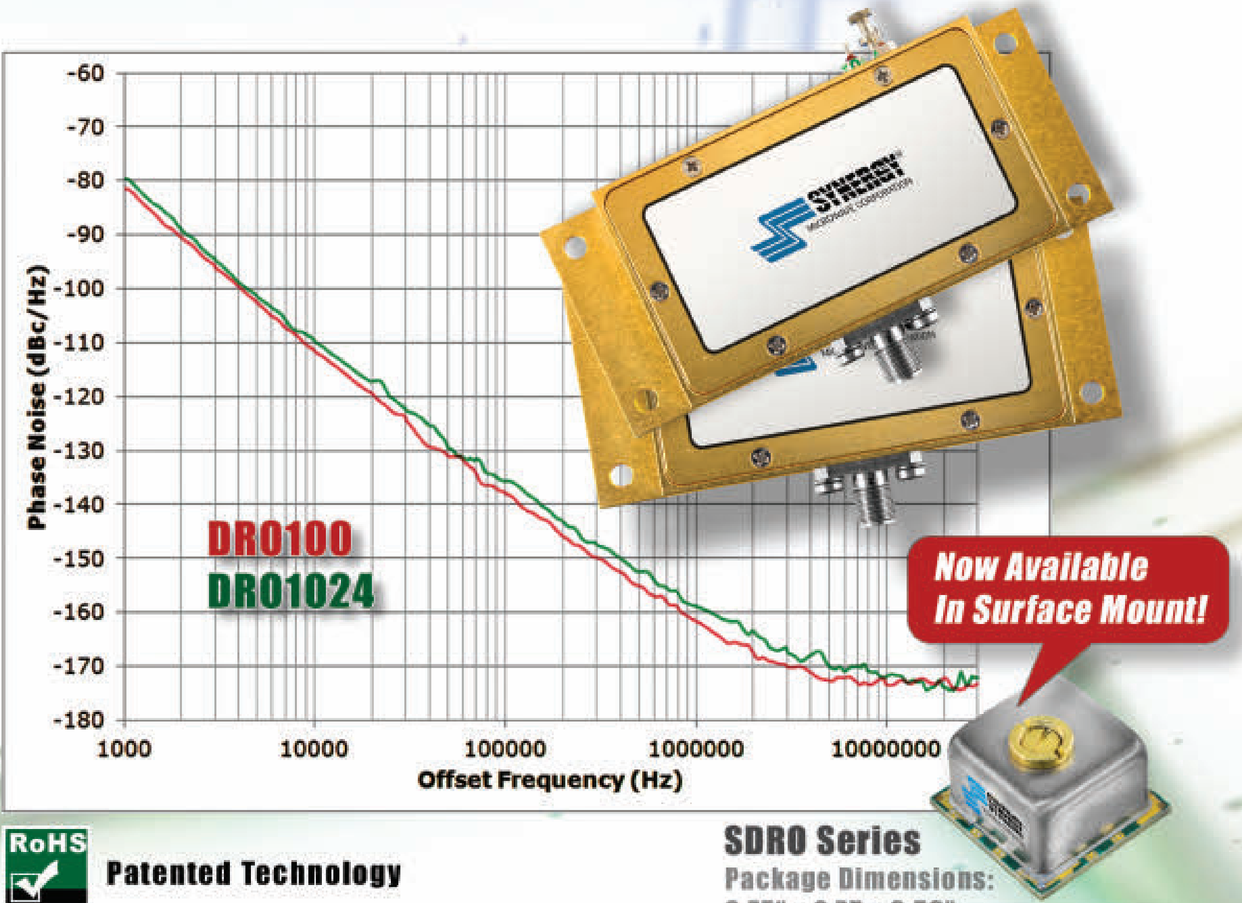

RoHS **Patented Technology**

SDRO Series
Package Dimensions:
0.75" x 0.75 x 0.53"

Call Factory For Your Specific Requirement

SYNERGY® MICROWAVE CORPORATION

Phone: (973) 881-8800 | Fax: (973) 881-8361
E-mail: sales@synergymwave.com
Web: WWW.SYNERGYMWAVE.COM
Mail: 201 McLean Boulevard, Paterson, NJ 07504

Four-Channel 20 GHz Sampling Oscilloscope

The PicoScope 9341 sampling oscilloscope offers 20 GHz bandwidth on four channels for engineers who need to characterize performance of multi-lane gigabit transmission systems and check for channel-to-channel interference and compatibility. The 9300 can perform eye-diagram analysis such as eye-width, eye-height, rise and fall-time, jitter and extinction-ratio testing. In addition, pattern lock triggering derived from bit rate, pattern length, and trigger divide ratio can build up an eye pattern from a specified group of bits in a sequence which helps to isolate data dependent errors and sources of cross-channel crosstalk.

Eye Line mode uses the pattern lock feature to establish a pattern sync trigger, and then uses that trigger to walk through each bit of the data pattern which can be averaged for a precision view of specific bit trajectories. This allows pattern dependent effects to be investigated. For example, the trace leading to a mask violation can be captured and displayed.

The scopes quickly measure more than 30 fundamental parameters used to characterize non-return-to-zero (NRZ) signals and return-to-zero (RZ) signals. Up to 10 parameters can be measured simultaneously, with comprehensive statistics also shown. For clarity the measurement points and levels used to generate each parameter can be automatically annotated on the trace.

Mask testing can be used to give a visual indication of deviations from a standard waveform. A library of built-in and custom masks can be automatically generated and modified using the graphical editor. A specified margin can be added to any mask to enable stress-testing. Mask testing can also be used as the basis for automated testing and statistical analysis, with capability to count or to take action on mask violations.

The display can be grey-scaled or color-graded to aid in analyzing noise and jitter in eye diagrams. There is also a statistical display showing a failure count for both the original mask and the margin.

Pico Technology
St Neots, UK
+44 1480 396 395
www.picotech.com

UP TO **100 Watt**

AMPLIFIERS

NOW! **100 kHz to 18 GHz**

from $995 ea. qty. (1-9)

High-powered performance across wide frequency ranges. These class A/AB linear amplifiers have set a standard throughout the RF & microwave industry. Rugged and reliable, they feature over-voltage and over-temperature protection, including the ability to withstand opens and shorts! And they're all in stock, whether with a heat sink/fan (for design labs and test benches), or without (for quick integration into customer assemblies). Go to minicircuits.com, where it's easy to select the models that meet your needs, including new features like TTL-controlled RF output. Place an order today, and you can have them in your hands as soon as tomorrow—or if you need a custom model, just give us a call for an engineer-to-engineer discussion of your requirements!

Model	Frequency (MHz)	Gain (dB)	Pout @ Comp. 1 dB (W)	Pout @ Comp. 3 dB (W)	$ Price (Qty. 1-9)
ZVE-3W-83+	2000-8000	35	2	3	1295
ZVE-3W-183+	5900-18000	35	2	3	1295
NEW ZHL-4W-422+	500-4200	25	3	4	1570
NEW ZHL-5W-422+	500-4200	25	3	5	1670
ZHL-5W-2G+	800-2000	45	5	6	995
ZHL-5W-1	5-500	44	8	11	1020
ZHL-10W-2G	800-2000	43	10	13	1295
• ZHL-16W-43+	1800-4000	45	13	16	1595
• ZHL-20W-13+	20-1000	50	13	20	1395
• ZHL-20W-13SW+	20-1000	50	13	20	1445
LZY-22+	0.1-200	43	16	32	1495
ZHL-30W-262+	2300-2550	50	20	32	1995
ZHL-30W-252+	700-2500	50	25	40	2995
LZY-2+	500-1000	47	32	38	2195
LZY-1+	20-512	42	37	50	1995
• ZHL-50W-52+	50-500	50	40	63	1395
• ZHL-100W-52+	50-500	50	63	79	1995
• ZHL-100W-GAN+	20-500	42	79	100	2395
ZHL-100W-13+	800-1000	50	79	100	2195
ZHL-100W-352+	3000-3500	50	100	100	3595
ZHL-100W-43+	3500-4000	50	100	100	3595
LZY-5+	0.4-5	52.5	100	100	1995

Listed performance data typical, see minicircuits.com for more details.

• Protected under U.S. Patent 7,348,854

Mini-Circuits®

www.minicircuits.com P.O. Box 350166, Brooklyn, NY 11235-0003 (718) 934-4500 sales@minicircuits.com

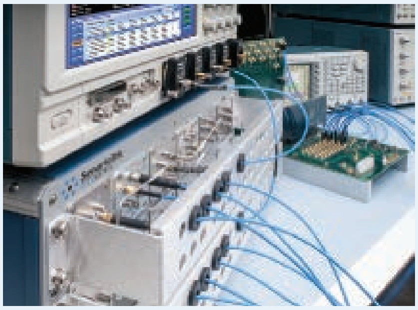

Multi-Lane, Single Connection Signal Integrity Measurements

Frequencies of high speed serial standards continue to climb and the difficulty of meeting the design requirements has grown accordingly. Test instrumentation is readily available for testing a single four-lane path, however changing connections introduces error and repeatability issues.

The FlexMatrix Differential Series offers dual one by 4, 8, 16 and 32 port solutions to speed time-to-market for products using the latest standards such as PCI Express Gen 3, IEEE 1394, USB 3.0, SATA, SerDes, InfiniBand and Gigabit Ethernet (10 GbE and 100 GbE). The Differential Series minimizes path delay skew between differential pairs, including delay matching for transceiver measurements as low as 2 picoseconds at the DUT interface. Test engineers can perform multi-lane testing with a single connection. Complete test plans may be automated and suspected problems may be checked without changing any connections.

SenarioTek strives to ensure their equipment performs better than the extremes of the test environment. Most importantly, their switch matrix helps to ensure that station-to-station test results are consistent and correlate to make it easier for the engineers to evaluate results. FlexMatrix offers excellent cycle-to-cycle insertion loss magnitude and delay repeatability, lowering test system calibration uncertainty for longer periods of time. Each switch matrix contains on-board internal memory providing the ability to conveniently de-embed the nominal amplitude and delay of each differential pair. The Differential Series tight phase/delay matching produces results with the lowest uncertainty and repeatability to allow developers to verify their most challenging designs.

SenarioTek's FlexMatrix RF Switch Matrix Family delivers off-the-shelf performance from DC up to 40 GHz. FlexMatrix offers test engineers a high performance RF switching capability over the broadest range of standard input and output configurations for applications such as radar, military communications, consumer wireless and signal integrity.

VENDORVIEW

SenarioTek
Santa Rosa, Calif.
www.senariotek.com

CatalogUpdate

EMC & RF Testing Catalog

VENDORVIEW

AR has completed another revision of their sought-after full line product catalog. Many new products have been included and various sections were updated to provide you with the information required to make your equipment research more in-depth. The catalog is easy to use, with "find-it-fast" charts and color coding to help get right to whatever you need for RF & EMC testing. Please contact your local AR sales associate for a hard copy or visit AR's website for a free download, either in full or by section.

AR RF/Microwave Instrumentation
www.arworld.us

Oscillators Brochure

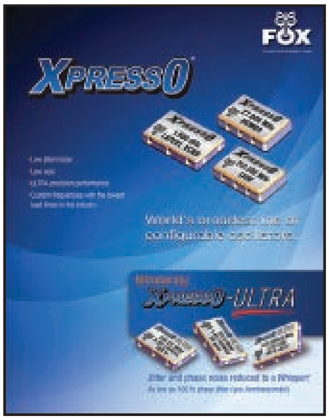

Fox's latest brochure now provides data on the new ultra precision oscillators, including typical phase noise, jitter and a model description selection guide. The guide helps users determine the model number appropriate for their application by choosing between available options for output, package size, voltage as well as stabilities, operating temperature range and frequency. The end result is a semi-custom oscillator optimized to the user's specifications without trade-offs. The literature also features a comparison of XpressO-ULTRA and the original XpressO oscillator performance to help determine which product family is most appropriate for the customer's application.

Fox Electronics
www.foxonline.com

LTE and LTE-Advanced Poster

VENDORVIEW

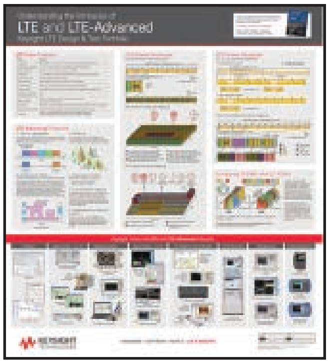

Keysight's new "Understanding the Intricacies of LTE and LTE-Advanced" poster provides insight into the latest 3GPP LTE standards and test measurement information for engineers developing products with LTE and LTE-Advanced. Information is provided on the major features of both LTE and LTE-A as well as FDD and TDD frame structures, and a comparison of OFDMA and SC-FDMA. For the new Keysight LTE/LTE-Advanced Poster, visit www.Keysight.com/find/LTE-Insight.

Keysight Technologies Inc.
www.keysight.com

Low PIM Components Catalog

VENDORVIEW

MECA's new 12-page catalog features an extensive line of low PIM RF/microwave components with industry leading performance including RF loads, attenuators, directional couplers, power splitters, divider/tappers, adapters, jumpers and D.A.S. equipment. MECA's low PIM loads are considered a benchmark for the industry and are currently the only terminations capable of handling full rated power at +85°C. Visit www.e-meca.com/pdfs/MECA_catalogo-2014.pdf to download your copy.

MECA Electronics Inc.
www.e-MECA.com

SATCOM Product Guide

VENDORVIEW

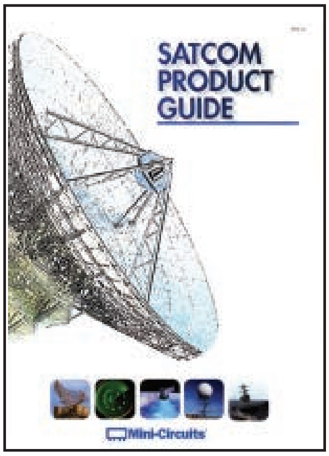

Mini-Circuits has released a new SATCOM product guide in print and for download from their website. This 32-page guide features a full survey of components and assemblies for satellite and earth station systems. With selected products from over 20 different product types to 40 GHz, the guide provides key performance parameters for each product and serves as a handy reference for engineers evaluating parts for their design needs.

Mini-Circuits
www.minicircuits.com

Test & Measurement Catalog

VENDORVIEW

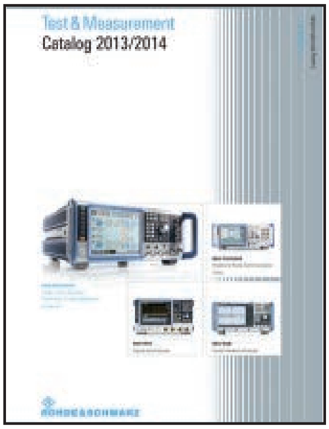

The 2013/14 Rohde & Schwarz test & measurement catalog is over 200 pages of information about Rohde & Schwarz test & measurement instruments, systems and software. It includes a short description and photos of each product, important specifications and ordering information. You can download this catalog as a pdf from the Rohde & Schwarz website or email customer support at customersupport@rohde-schwarz.com (use order number: PD 5213.7590.42).

Rohde & Schwarz GmbH & Co. KG
www.rohde-schwarz.com

EDI CON
2015
Electronic Design Innovation Conference
电子设计创新会议
April 14-16, 2015
China National Convention Center • Beijing, China
Where the Experts Speak...
Three full days of peer-reviewed, industry-focused technical papers, workshops, expert panels and guest keynotes on market and technology trends in China and beyond.
RF, Microwave, High Speed Digital & EMC/EMI Design
Exhibition
• Test & Measurement Equipment
• Test Solutions
• EDA/CAD Software
• Components, Modules
• Subsystems
• RFICs & MMICs
• Cables/Connectors
• Materials
• Semiconductor Foundries
• Manufacturing Services
Host Sponsor:
KEYSIGHT TECHNOLOGIES
Diamond Sponsor:
ROHDE&SCHWARZ
Corporate Sponsor:
NATIONAL INSTRUMENTS
Gold Sponsors:
Anritsu envision : ensure
CETC 41st
CST
RichardsonRFPD An Arrow Company
Mini-Circuits ISO 9001 ISO 14001 AS 9100
ARROW RF & Power
Organized by:
horizon house
ACT
Microwave Journal
www.EDICONCHINA.com
Exhibition Spaces Available

Components

Filters

3H Communication Systems announced its new micro and nano thin filter product lines. These filters are now available from 50 MHz to 6 GHz with bandwidths up to 100 percent. The micro-thin and nano-thin products offer low insertion loss and 60 dB ultimate rejection. The micro-thin height is specified at 0.09" and the nano-thin height is specified at 0.08".

3H Communication Systems
www.3hcomm.com

High Temperature MLCCs

AVX Corp. has introduced a new series of high temperature MLCCs rated at an industry leading 250°C. Designed to accommodate the rapidly emerging military and commercial market demands for capacitors capable of high-reliability, long lifetime performance at operating temperatures in excess of the current 125°C requirement, the new AT series capacitors exhibit high current handling capabilities, high volumetric efficiency, high insulation resistance, and extremely low ESR and ESL.

AVX Corp.
www.avx.com

Low, Medium and High Power Attenuators

Fairview Microwave Inc. announced its new family of 25, 50 and 100 W attenuators with operating frequencies up to 18 GHz depending on the configuration. There are a total of 236 new part numbers in this attenuator. Attenuation options include 3, 6, 10, 20, 30, 40, 50 and 60 dB models for most connector styles. These attenuators can be ordered with in-series connector configurations including SMA, TNC, Type-N and 7/16 DIN.

Fairview Microwave Inc.
www.fairviewmicrowave.com

Digitally Controlled PIN Diode I&Q Vector Modulator

Model M2L-42A-5JJ is a digitally controlled PIN diode I&Q vector modulator that operates from 4.4 to 5 GHz with a dynamic range of 20 dB and 360 degrees. The amplitude balance is ±1 dB with a phase vs. frequency of ±7 degrees. This unit features an insertion loss of less than 11 dB with a 1.80:1 VSWR in 50 Ohms. The supply voltage accommodates up to ±12 to ±15 VDC at ±100 mA.

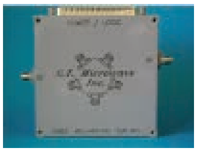

G.T. Microwave Inc.
www.gtmicrowave.com

X-Band High Power Limiter

Herotek offers a new X-Band high power limiter with high power protection 100 W CW and 1 kW peak (1 microsec pulse width). Model LS0812PP100A operates from 8 to 12 GHz. It is ideal for radar application. The limiter has maximum insertion loss of 2 dB, maximum VSWR of 2:1, typical limiting threshold is +4 dBm, max input peak (1 microsec pulse width) is 1,000 W. Typical leakage power at 1 W CW input is +6 dBm, at 25 W CW input, +10 dBm, and at 100 W CW input, +13 dBm.

Herotek Inc.
www.herotek.com

Compact Low PIM Loads

VENDORVIEW

MECA's new compact low PIM (-160 dBc typ.) 50 W loads offer extended power handling capabilities. These loads feature industry leading PIM performance of -155 dBc min. all while handling full rated power to 85°C. All of the terminations cover 0.698 to 2.7 GHz frequency bands in 7/16 DIN, Type N & 4.1/9.5 (mini-DIN) connectors, VSWR = 1.10:1 typ/1.20:1 min. All in a compact package of 6" × 2.25". Made in the U.S. and 36-month warranty.

MECA Electronics Inc.
www.e-meca.com

C-Band High Power Polarizer

The C-Band polarizer has been developed for use in high power TWTA based radar systems. This highly integrated solution, delivers less than 1 dB insertion loss; a peak power handling of 60 kW and average power of 1.5 kW. The manufacturer's expertise and proven heritage in ferrite switches and phase shifters is the key that allows the radar to be switched between linear horizontal or vertical and circular polarisations in less than 2 µs.

MESL Microwave Ltd.
www.meslmicrowave.com

Switches

VENDORVIEW

Mini-Circuits' switches operate up to 6 GHz and offer extremely fast switching times (<10 ns) up to medium power levels. Supplied in both MMIC and PIN diode based designs, with and without internal TTL/CMOS drivers, these products are offered in connectorized and surface mount packages.

Mini-Circuits
www.mini-circuits.com

F Attenuators

VENDORVIEW

Pasternack Enterprises Inc. announced its expanded line of 75 Ohm F attenuators. This new line of F-type attenuators is perfect for broadcast, HDTV and satcom applications in the L and S microwave bands up to 3 GHz. They are

available in 1 to 10 dB values in 1 dB steps, as well as 16 and 20 dB values. These F 75 Ohm fixed attenuators are widely used in the broadcast industry for signal leveling and to attenuate strong input signals.

Pasternack Enterprises Inc.
www.pasternack.com

Indoor Broadband Quadruplexer

Pivotone's indoor broadband quadruplexer combines 700, 850, PCS and AWS. Designed for high power DAS or POI systems, LTE can be added to existing sites while providing a low insertion loss and a high degree of isolation (minimum 50 dB) between systems. PIM is guaranteed to be lower than -153 dBc.

Pivotone Communication Technologies
www.pivotone.com

Drop-in Circulator

VENDORVIEW

Renaissance's new 3G2BG circulator is a wideband drop-in circulator designed for CW and pulsed applications such as wireless infrastructures, radar, military communication radios and general purpose duplexing applications. Operating over 690 to 1100 MHz, this circulator comes in a compact size of ~ 2"× 2" × 0.6". It is capable of withstanding 350 W of CW power levels.

Renaissance Electronics & Communications LLC
www.rec-usa.com

6 GHz Fast Switching DSA

VENDORVIEW

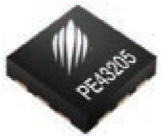

RFMW Ltd. announced design and sales support for Peregrine Semiconductor's two-bit, fast-switching digital step attenuator (DSA). The PE43205 offers 29 ns switching time when transitioning between 6, 12 or 18 dB of attenuation. Specified from 35 MHz to 6 GHz, the PE43205 offers IIP3 of 61 dBm for highly linear, wide dynamic range circuits. In addition, the Peregrine PE43205 offers an extended temperature range of +105°C to support passive/convection cooling in wireless infrastructure, small cell and land mobile radio applications.

RFMW Ltd.
www.rfmw.com

16-Bit, Dual ADC

VENDORVIEW

Richardson RFPD Inc. announced the availability and full design support capabilities for a new dual, 16-bit analog-to-digital converter with sampling speeds of up to 310 MSPS from Analog

Devices Inc. The AD9652 is designed to support demanding, high speed signal processing applications that require exceptional dynamic range over a wide input frequency range (up to 465 MHz). A low noise floor and a large signal spurious-free dynamic range (SFDR) performance allows low level signals to be resolved in the presence of large signals.
Richardson RFPD/Arrow RF & Power
www.richardsonrfpd.com

Ultra Wideband Frequency Synthesizer

The LFSW35105-50 is a surface mount synthesizer operating between 350 and 1050 MHz with a step size of 500 kHz. Phase noise performance is optimized to -95 dBc/Hz at 1 kHz offset and -103 dBc/Hz at 10 kHz offset with a settling time of 10 msec. Bias requirement is +5 V at 175 mA maximum and spurious-free output power is +10 dBm minimum.
Synergy Microwave Corp.
www.synergymwave.com

DC to 32 GHz Attenuators

Looking for qualified M3933/30 (DC to 32 GHz) attenuators? SV Microwave has been approved by DLA as the only QPL source for these components. SV has the precision, quality and performance using 2.92 mm connectors for DC through 32 GHz. Values range from 0.5 to 30 dB with low VSWR and flat attenuation.
SV Microwave
www.svmicrowave.com

Millimeter-Wave Transmitter Module

Vubiq Networks announced a fully integrated 60 GHz radio transmitter module. Small and lightweight, the unit features a patented chip

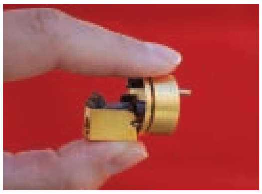

to waveguide transition that is compatible with WR-15 and UG-385/U waveguide flange interfaces. The waveguide modules operate within the V-Band of RF spectrum, between the license free frequencies of 57 to 64 GHz, and cover the IEEE 802.11ad and 802.11aj channels. The modules support up to 1.8 GHz modulation bandwidth, with an I/Q signaling interface for baseband modulation, and also support non-coherent modulation techniques.
Vubiq Inc.
www.vubiq.com

Low Noise Voltage Regulator

The LNVR module is a low noise voltage regulator designed to provide excellent power supply spurious rejection when clean DC voltage is required for modules used in low noise applications. This module features low nV/Root-Hz performance, multiple output tabs and can handle current loads up to 1 A. The compact modular package is designed for use in subsystems and instruments as well as bench top applications.
Wenzel Associates Inc.
www.wenzel.com

Fixed Frequency Synthesizer

Z-Communications Inc. announced a new RoHS compliant fixed frequency synthesizer model SFS10625E-LF. It is a single

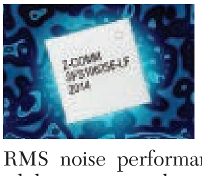

frequency PLL solution pre-programmed to operate at 10.625 GHz. This device utilizes ceramic resonator topology to achieve integrated RMS noise performance of better than 0.4° while consuming less than 500 mW of power. The SFS10625E-LF is designed to operate over the temperature range of -30° to +70°C and delivers +3 dBm of output power into a 50 Ω load.
Z-Communications Inc.
www.zcomm.com

Cables and Connectors

Coaxial to Waveguide Adapters

RLC Electronics offers coaxial to waveguide adapters in a variety of configurations for your specific application. RLC offers both broadband adapters (whose excellent electrical specs are maintained over the entire adapter bandwidth) and also narrow band adapters (whose enhanced performance are provided over a specific band of the adapters' bandwidth). Computer design and the latest in RF techniques coupled with precision assembly ensure optimal electrical performance in the recommended frequency ranges. Options are available from WR229 (3.3 to 4.9 GHz) to WR22 (33 to 50 GHz).
RLC Electronics Inc.
www.rlcelectronics.com

2.9 In Series Adapter

This 2.9 in series adapter #370SF-40RAD is precision stainless steel 2.9 mm male/2.9 mm female with a 90 degree radius right angle and VSWR 1.30:1 maximum, VSWR from DC to 40 GHz.
United Microwave Products
www.unitedmicrowave.com

Amplifiers

Amplifier

The Model 177Ka provides 750 W peak power at duty cycles up to 10 percent from 34 to 36 GHz. Particular emphasis has been placed

on the generation of the output RF pulse shape. The RF output pulse width tracks the input 5 V video pulse. Internal power supplies are DC to DC converter designs operating at 50 kHz with fast loop response times to that output level variations are minimal for any PRF including a non-periodic or burst type PRF.

Applied Systems Engineering Inc.
www.applsys.com

Single Band AR Amplifier

VENDORVIEW

Model 200S1G6 is a self-contained, air cooled, broadband, solid-state amplifier designed for applications where instantaneous bandwidth,

high gain and linearity are required. The unit, when used with a sweep generator, will provide a minimum of 200 W of RF power from 0.7 to 6 GHz in a single amplifier and can be used in many RF applications such as: RF susceptibility testing, antenna/component testing and communication testing.

AR RF/Microwave Instrumentation
www.arww-rfmicro.com

GaN Power Amplifier

VENDORVIEW

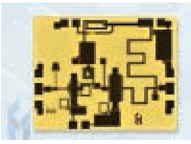

Custom MMIC announced the addition of the CMD216, a new 14 to 18 GHz GaN power amplifier in die form to its expanding product line. The CMD216 delivers 16 dB of flat gain across the entire 14 to 18 GHz bandwidth, an output 1 dB compression point of +37 dBm and a saturated output power of +38 dBm. The CMD216 requires a bias of Vdd = 28 V, 550 mA, and Vgg = -3.4 V.

Custom MMIC
www.custommmic.com

K-Band Linear Power Amplifier

Ducommun Inc.'s power amplifier model AHP-22092825-01 with single supply operates in the 18 to 26.5 GHz frequency range. It provides a minimum 25 dB gain with a minimum output power at 1 dB gain compression of +28 dBm and 2:1 maximum VSWR. The amplifier has an integrated voltage regulator and operates at +12 V DC and draws 1.0 A current, typical. It utilizes K (f) connectors and measures has a dimension of 2"(L) × 1.3"(W) × 0.6"(H).

Ducommun Inc.
www.ducommun.com

26 to 40 GHz Low Noise/High Gain Amplifier

MITEQ's new model JS5-26004000-32-18P is a state-of-the-art 26 to 40 GHz low noise high gain amplifier with only 3.2 dB maximum noise

figure and +18 dBm minimum P1dB. This model has a gain of 32 dB minimum in a small hermetically sealed package with field replaceable K-connectors. MIL-883 screening is also available. This model is also available as RoHS compliant, along with different options such as low gain, noise figure and power output.

MITEQ Inc.
www.miteq.com

Low Noise Amplifier

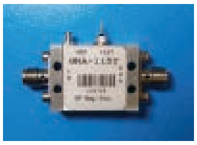

RF Bay Inc. GNA-115T is 0.4 dB noise figure, 19 dB gain, low noise amplifier that operates in a frequency range from 400 to 2000 MHz. The +21 dBm P1dB and +36 dBm IP3 makes GNA-115T a driver amplifier for many applications. Operating at 9 to 15 V at 80 mA, the unit measured at 1.00" × 0.75" × 0.45" with SMA female connectors on both sides. Visit the company's website for over 100 different models of low noise amplifiers.

RF Bay Inc.
www.rfbayinc.com

Low Noise Broadband Amplifiers

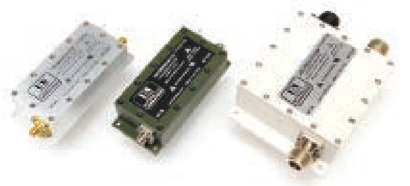

The USLN low noise broadband amplifier series cover bandwidths of more than 11 octaves from the HF spectrum up to S-Band, providing outstanding flatness, sub-dB noise figure, typical P1dB of 20 dBm and a supply voltage range from 7 to 28 V. They feature non-destructive reverse polarity and overvoltage protection, and their current consumption is inversely proportional to the supply voltage for continuous maximum efficiency. All models meet all specifications from -40° through 85°C, and the outdoor option is IP65 compliant.

US Microwave Laboratories
www.usmicrolabs.com

3 W GSM Frequency Power Amplifier

Model AHP0195-26-3235 is a PHEMT based power amplifier offering 32 dB of linear gain and 35 dBm minimum output power at 1 dB

gain compression point over the frequency range from 1.7 to 2.2 GHz with excellent gain flatness and VSWR. The amplifier has built-in DC voltage regulator and requires a single +12 V DC power supply. The package size of the amplifier without heatsink is 2.08" × 1.25" × 0.5".

Wenteq Microwave Corp.
www.wenteq.com

Packaging

Circuit Boards

Twin Industries MicroAmp MB series circuit boards are designed for rapid prototyping of many different low and high frequency circuit

2015 IEEE SYMPOSIUM ON ELECTROMAGNETIC COMPATIBILITY & SIGNAL INTEGRITY

CALL FOR PAPERS

EMC&SI 2015

Silicon Valley • March 15-21, 2015

PAPER TOPICS OF INTEREST

Topics include and are not limited to the following technical areas.

Preliminary Full Paper Manuscript Due By October 19, 2014

Theme Topic I
Signal & Power Integrity (TC10)

- Interconnects
  - Interconnect design and optimization;
  - Interconnect modeling and extraction;
  - Channel analysis
- Power Distribution Network and Decoupling
  - PDN Design, analysis, simulation, modeling and measurement techniques
  - PDN optimization
- Chip-level SI and PI
  - On-chip and off-chip high-speed signaling techniques;
  - 3-D IC, TSV, and Multi-Chip Modules
- Tools and methodologies
  - Jitter/Noise/Crosstalk/BER;
  - De-embedding methodologies
  - TD and FD measurement techniques
  - Embedded test
- Simulation and modeling techniques
  - High-frequency and electromagnetic simulation techniques
  - Simulation and measurement correlation
  - Advanced simulation tools/algorithms
  - Device modeling and characterization
- System co-design
  - SI/PI for chip/package/board/connector / cable co-design
  - SI/PI co-analysis
  - System-level SI/PI/EMI co-design

Theme Topic II
EMC for Emerging Technologies (TC11, SCs)

- Wireless EMC
- Radio-Frequency Interference
- Smart Grid EMC
- Nano-Materials and Silicon Photonics
- Unmanned Aircraft Systems EMC
- Power Electronics EMC

ALL ACCEPTED PAPERS will be Submitted for Posting to IEEE Xplore. Authors of accepted papers will be invited to submit an extended version of their symposium paper for possible publication in a special issue of the IEEE Transactions on Electromagnetic Compatibility.

Theme Topic III
Space EMC

EMC Management (TC1)
- Personnel & Laboratory Accreditation
- EMC Education
- Legal Issues

EMC Measurements (TC2)
- Test Instrumentation & Facilities
- Measurement Techniques
- Standards and Regulations

EM Environment (TC3)
- EM Signal Environment
- Atmospheric & Man-Made Noise

EM Interference (TC4)
- Shielding, Gasketing & Filtering
- Cables and Connectors
- Circuit & System EMC Analysis
- Grounding

High Power Electromagnetics (TC5)
- ESD & Transients
- EMP, IEMI & Lightning
- Information Leakage

Spectrum Management (TC6)
- Spectrum Management
- Spectrum Monitoring

Low Frequency EMC (TC7)
- Power Quality and Conducted EMC
- Power Electronics

Computational Electromagnetics (TC9)
- Computer Modeling Methods
- Tools and Techniques
- Validation Methods
- Statistical Analysis

For More Information Visit www.emc2015usa.emcss.org

Technical Paper Chair: Prof. Chuck Bunting • *charles.bunting@okstate.edu*
Technical Program Chair: Prof. Jun Fan • *jun.fan@ieee.org*

functions. Boards are available for many popular MMIC amplifiers, filters, frequency dividers, multipliers, VCOs, passive circuits and op-amps. Using standard surface-mount components, functional circuits are easily attainable with these easy-to-assemble boards. Boards conform to the MicroAmp MH series of connectorized housings. They may be used as a single or dual-cascaded circuit.

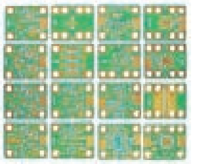

Twin Industries
www.twinind.com

Test Equipment

Configurable Frequency Synthesizers

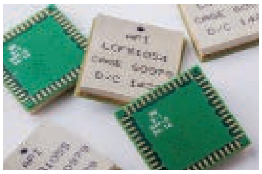

API Technologies Corp. announced the launch of configurable frequency synthesizers (Models LCFS-X), the newest addition to the company's line of standard RF/microwave products. Offering superior phase noise performance as low as -92 dBc/Hz at 100 kHz offset, the synthesizers are ideally suited for a variety of applications including SIGINT/electronic warfare (EW), SATCOM, Doppler radar and telecommunication systems. The compact surface mount packaging and affordable price point make these synthesizers an ideal solution for unmanned systems applications.

API Technologies Corp.
www.apitech.com

0.5 to 18 GHz Tuner

The P518B500 wideband tuner provides instantaneous bandwidth of 500 MHz over the 0.5 to 18 GHz band. The 1U rack mount system tunes the input range to a main output band of 750 to 1250 MHz (optionally 950 to 1450 MHz). Auxiliary outputs are at 900 MHz (200 MHz bandwidth), 120/160 MHz and 21.4 MHz, and are simultaneously accessible, synchronous and without frequency inversion. The P518B500 operates by simple command set via USB, Ethernet or serial interface.

diminuSys
www.diminusys.com

Power Sensor

LadyBug Technologies' new LB5908L power sensor measures RF power at frequencies from 9 kHz to 8 GHz, making it ideal for source calibration and EMC testing applications. It has excellent sensitivity and measures from -60 to +20 dBm. It has three interfaces. Customers can connect to the sensor using USBTMC, USB HID, or the optional SPI/IIC interface. It has a built-in real-time clock and measurement storage. Once programmed, it can make and store over 100 million measurements with no computer or power meter connected.

LadyBug Technologies
www.ladybug-tech.com

Engineering Probe Systems

MPI Corp. introduced a wide range of engineering probe systems addressing the specific requirements of various market segments and applications such as device characterization for modeling, failure analysis, design verification, IC engineering, wafer level reliability as well as special requirements for MEMS, high power, RF and mmW device testing. The TS series modular design concept allows a unique upgrade path towards reduced cost of ownership.

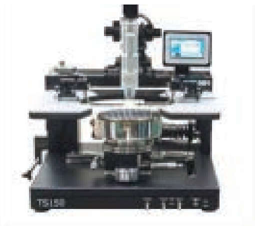

MPI Corp.
www.mpi-corporation.com

Ethernet Microcontroller Test Box

VENDORVIEW

PMI model no. PL-MCU-ENET-TTL-MAH is an ethernet microcontroller test box that allows for an ethernet command to be sent up to 18 parallel TTL output bits. This controller can be used with many PMI products that require parallel digital commands, such as switches, attenuators, phase shifters and IQ modulators.

Planar Monolithics Industries Inc.
www.pmi-rf.com

Wideband Transcorder

The WBT provides complete RF recording and playback at 50 MHz (2 × 25 MHz) bandwidth tunable from 50 MHz to 6 GHz. At less than 10 lbs and 70 W, this portable solution records to solid state devices and costs far less than other products. Using the industry standard VRT file format (VITA-49), the WBT is fully contained in a single box, so there's no need for a separate spectrum analyzer to digitize the signal, or a signal generator to play it back at RF.

QRC Technologies
www.qrctech.com

Broadband 90° Quadrature Hybrid

Response Microwave Inc. announced the availability of its new broadband 3 dB, 90° quadrature hybrid for use in automated test

MICRO-ADS

and production applications. The new RMHY3.18000Sf covers the 2 to 18 GHz band offering typical electrical performance of 1.5 dB insertion loss, VSWR of 1.50:1, minimum isolation of 16 dB. Average power handling is 50 W and the unit is operational over the -55° to +85°C range. Mechanical package is 1.93" × 1.00" × 0.43", plus passivated stainless SMA female connectors.

Response Microwave Inc.
www.responsemicrowave.com

F-Band Scalar Network Analyzer Extender

VENDORVIEW

Model STN-SF908-00-P2 is an F-Band scalar network analyzer extender that covers the frequency range from 90 to 140 GHz. It offers an alternative way of allowing users to achieve millimeter wave scalar measurement in a low cost approach without losing any of the functionalities and features that the industry standard models have to offer. The scalar network analyzer extender utilizes a x9 frequency extender (STE-SF908-00-S1) to extend the measurement range from 10 to 15.56 GHz to 90 to 140 GHz.

SAGE Millimeter Inc.
www.sagemillimeter.com

Custom Switch Matrix Solutions

VENDORVIEW

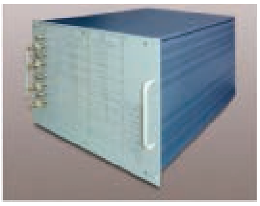

Senario Tek's build to print custom switch matrix solutions offer the ability to design from concept and to reverse engineering (obsolescence, upgrades, etc.), redesign existing products and prototyping.

Senario Tek
www.senariotek.com

2014 Asia-Pacific Microwave Conference

http://www.apmc2014.org/

APMC 2014

November 4-7, 2014, Sendai International Center, Sendai, Japan

APMC 2014
Nov. 4-7 Sendai Japan

The 2014 Asia-Pacific Microwave Conference (APMC 2014) will be held at the Sendai International Center, Sendai, Japan, on November 4-7, 2014. As you may know, Sendai is one of the historic sites for microwave & antenna engineering and is the birthplace of Yagi-Uda antenna. You will feel a touch of inspiration from Sendai and the microwave & antenna heritages.

This conference is organized and sponsored by The Institute of Electronics, Information and Communication Engineers (IEICE) of Japan, and will be supported by Ministry of Internal Affairs and Communications. It will be cooperatively sponsored by IEEE MTT-S, IEEE AP-S, EuMA, URSI, IEEE MTT-S Japan/Kansai/Nagoya Chapters, IEEE Sendai Section, IEICE Technical Committee on Microwaves, IEICE Technical Committee on Electronics Simulation Technology, IEICE Technical Committee on Microwave Photonics, Japan Institute of Electronics Packaging, Japan Society of Electromagnetic Wave Energy Applications, IEEJ Investigative Committee on Innovative Electromagnetic Technologies and Their Applied Developments.

The APMC2014 is the largest microwave conference in Asia-Pacific region, bringing together international researchers, engineers, and students to showcase the most advanced research and development in microwave technologies. Sixty-five technical sessions, both oral and poster, which include various Special Sessions, are organized. In addition, the technical program will be supplemented by 5 workshops, 3 short courses, one Rump session, 2 Student design competitions, and one Technical Tour.

Those who intend to participate in the 2014 Asia-Pacific Microwave Conference (APMC 2014), including the speakers, session chairs, committee members, etc., are requested to register for the "Conference" (from November 5 to 7, 2014) and/or the "Workshops/ Short Courses" (on November 4, 2014). Pre-Registration (Early Bird & Advanced) is available on the APMC 2014 website from August 8 to October 24, 2014. For those who cannot register beforehand, On-Site-Registration is available at the Registration Desk at the Conference venue from November 3 to 7, 2014.

Beautiful sceneries around Sendai

Yagi-Uda Antenna

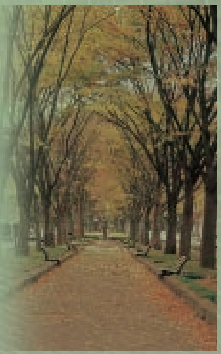

> Matsushima

Matsushima, a small bay dotted with more than 260 islands beautifully covered with evergreens, is one of Japan's celebrated Three Views. Japanese poems "Haiku" have been composed at Matsushima, since ancient times. "Matsushima is the most scenic place in Japan," wrote Matsuo Basho, the greatest master of "Haiku".

> Okama Crater of Zao Mountain

The kettle-shaped Crater Lake known as Okama is a part of the Zao mountain range in the Tohkoku region. Hikers will enjoy the beautiful scenic splendor of the volcanic peaks. The mountains change their colors in Autumn, like wearing beautiful kimono of autumn leaves.

LOCATION OF SENDAI

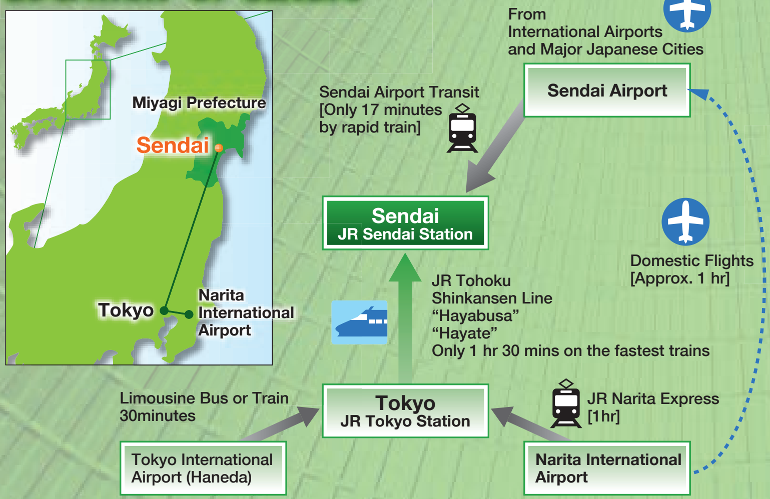

SENDAI

Sendai is one of the largest cities in Japan, and is the political and economic center in the Tohoku (northeast) region. It is also well known as the City of Trees, where the Japanese Zelkova trees on the streets are in harmony with the view of the modern city. Sendai area is home to many natural sites of beautiful scenery, such as the Hirose River, running through the central Sendai, Akiu Great Falls, famous as one of Japan's three most beautiful waterfalls, and Matsushima, known as one of the Three Views of Japan.

For the microwave community, a lot of important technologies and innovative inventions have been produced in Sendai. The Yagi-Uda antenna, which is one of the most famous antennas, was invented by Dr. Hidetsugu Yagi and Dr. Shintaro Uda, both with Tohoku University, Sendai, in 1925.

The conference site and the city center of Sendai have recovered from the East Japan Great Earthquake on March 11, 2011. Sendai is 100 kilometers away from the nuclear power plant in Fukushima. The intensity of radiation is the same level as before the disaster.

CONTACT

For further information, please contact:
Prof. Noriharu Suematsu
Chair, APMC 2014 Steering Committee
c/o APMC 2014 Secretariat,
Real Communications Corp.
3F Shinmatsudo S bldg., 1-409
Shinmatsudo, Matsudo 270-0034, Japan
Phone: +81-47-309-3616,
Fax: +81-47-309-3617
E-mail: mweapmc@io.ocn.ne.jp
http://www.apmc2014.org/

MTTS EuMA European Microwave Association URSI Ministry of Internal Affairs and Communications

Electronic Warfare Receivers and Receiving Systems

Richard A. Poisel

Receiver systems are considered the core of electronic warfare (EW) intercept systems. They are a key element critical to the overall system performance. This book considers the major components of receiver systems and the receivers used in them.

Electronic Warfare Receivers and Receiving Systems provides system design engineers with techniques for the design and development of EW receivers for modern modulations (spread spectrum) in addition to receivers for older, common modulation formats. Each major component of the system such as the amplifiers, mixers, converters, filters, etc., is considered in detail. Design information is included as well as performance trade-offs of various components. Major factors that influence the functioning of the modules are identified and discussed. Key performance parameters are identified as well as a variety of approaches to achieving design goals.

At 800 pages this is a large volume that covers all aspects of EW receivers and receiving systems, making it an ideal resource on the subject. It is appropriate for students and engineers as a reference piece or as a comprehensive overview of these systems. This book is also useful for a focused study of any components within the receiver chain. Each major function is covered in depth. Overall, *Electronic Warfare Receivers and Receiving Systems* is a quality learning reference tool.

To order this book, contact:

Artech House
685 Canton St., Norwood, MA 02062
(800) 225-9977
or
16 Sussex St., London, SW1V 4RW, UK
+44 (0) 20 7596 8750
800 pages, $179 hardcover or ebook
ISBN: 978-1-60807-842-4

Advertising Index

Advertisers in blue are enabled with the layar app

Sales Representatives

Microwave Journal
Frequency Matters.

Eastern and Central Time Zones
Chuck Boyd
Northeast Reg. Sales Mgr.
(New England, New York, Eastern Canada)
685 Canton Street
Norwood, MA 02062
Tel: (781) 619-1942
FAX: (781) 769-5037
cboyd@mwjournal.com

Michael Hallman
Eastern Reg. Sales Mgr.
(Mid-Atlantic, Southeast, Midwest)
4 Valley View Court
Middletown, MD 21769
Tel: (301) 371-8830
FAX: (301) 371-8832
mhallman@mwjournal.com

Pacific and Mountain Time Zones
Brian Landy
Western Reg. Sales Mgr.
(CA, AZ, OR, WA, ID, NV, UT, NM, CO, WY, MT, ND, SD, NE & Western Canada)
144 Segre Place
Santa Cruz, CA 95060
Tel: (831) 426-4143
FAX: (831) 515-5444
blandy@mwjournal.com

International Sales
Richard Vaughan
International Sales Manager
16 Sussex Street
London SW1V 4RW, England
Tel: +44 207 596 8742
FAX: +44 207 596 8749
rvaughan@horizonhouse.co.uk

Germany, Austria, and Switzerland (German-speaking)
WMS.Werbe- und Media Service
Brigitte Beranek
Gerhart-Hauptmann-Street 33,
D-72574 Bad Urach
Germany
Tel: +49 7125 407 31 18
FAX: +49 7125 407 31 08
bberanek@horizonhouse.com

Israel
Liat Heiblum
Oreet International Media
15 Kineret Street
51201 Bene-Berak, Israel
Tel: +972 3 570 6527
FAX: +972 3 570 6526
liat@oreet-marcom.com

Korea
Young-Seoh Chinn
JES Media International
2nd Floor, ANA Bldg.
257-1, Myungil-Dong
Kangdong-Gu
Seoul, 134-070 Korea
Tel: +82 2 481-3411
FAX: +82 2 481-3414
yschinn@horizonhouse.com

Japan
Katsuhiro Ishii
Ace Media Service Inc.
12-6, 4-Chome,
Nishiiko, Adachi-Ku
Tokyo 121-0824, Japan
Tel: +81 3 5691 3335
FAX: +81 3 5691 3336
amskatsu@dream.com

China
Michael Tsui
ACT International
Tel: 86-755-25988571
Tel: 86-21-62511200
FAX: 86-10-58607751
michaelT@actintl.com.hk

Hong Kong
Mark Mak
ACT International
Tel: 852-28386298
markm@actintl.com.hk

Ed Kiessling
Traffic Manager/Inside Sales
685 Canton Street
Norwood, MA 02062
Tel: (781) 619-1963
FAX: (781) 769-6178
ekiessling@mwjournal.com

MicrowaveJournal's

STEM Works

UAV [yu-a-ve]

UAV is an acronym for Unmanned Aerial Vehicle. A UAV is an aircraft with no pilot on board. UAVs can be remotely controlled aircraft (flown by pilots in ground control stations); alternatively, they can be made autonomous through the use of pre-programmed flight plans or more complex control systems. UAVs were first developed for military applications and are widely employed in roles such as reconnaissance, surveillance and attack.

1792 The earliest UAVs take the form of balloons. In France, the Montgolfier brothers are the first to experiment with balloons and send unmanned aerostats aloft in preparation for manned flight. During the American Civil War of 1861-1865, the Union Army launches unmanned balloons containing incendiary devices to start fires on the Confederate side of the battle lines.

1918 The Kettering Aerial Torpedo is built by the Dayton-Wright Airplane Co. with Orville Wright acting as an aeronautical consultant and Elmer Ambrose Sperry as the control and guidance system designer. Once launched, a small onboard gyroscope guides the aircraft to its destination using a pneumatic/vacuum system, an electric system and an aneroid barometer/altimeter.

1942 A TV-controlled Interstate BQ-4/TDR aircraft carrying an onboard camera is successfully guided into a target ship from a control aircraft 50 km (30 miles) away.

Source: DoD photo by Capt. Jane E. Campbell, U.S. Navy. (Released)

1951 The Ryan Firebee UAV is designed to be a jet-powered gunnery target. It develops into a capable unmanned surveillance system in the 1960s. As the AQM-34, it flies more than 34,000 ISR sorties over Southeast Asia during the Vietnam War.

1989 Abraham Karem at General Atomics introduces the Gnat 750. Equipped with video cameras, it flies reconnaissance missions over Bosnia while being controlled by ground personnel in nearby Albania. The Gnat 750 is the precursor to the well-known RQ-1/MQ-1 Predator and its variants.

1998 The Northrop Grumman RQ-4 Global Hawk initially designed by Ryan Aeronautical provides a broad (high altitude) overview and persistent surveillance using high resolution synthetic aperture radar (SAR) and long-range electro-optical/infrared (EO/IR) sensors.

2012 The FAA Modernization and Reform Act of 2012 sets a deadline of September 30, 2015 for the agency to establish regulations allowing the use of commercial UAVs in U.S. airspace.

2014 BP wins the first Federal approval to fly unmanned aerial vehicles over U.S. land for commercial purposes. UAV maker AeroVironment uses its aircraft to survey BP pipelines, roads and equipment near Alaska's Prudhoe Bay.

Scan page using layar app

WERLATONE®

Absorptive Filters

Low Pass | High Pass | Band Pass

Model AF9350

Model AF9349

Model AF9313

NON-Reflective!

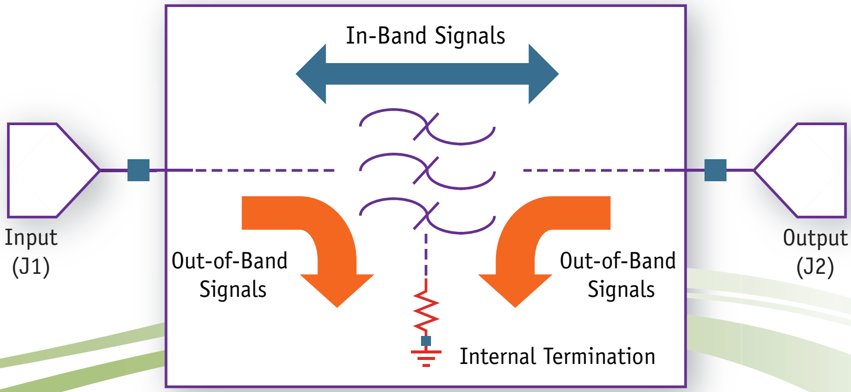

* Input / Output Characteristic Impedance: 50 Ω

Out-of-Band Signals are NOT reflected back to the source.

- Out-of-Band signals are **internally terminated.**
- Electrical Specifications are less susceptible to temperature change.
- Reduces the dependency of the system on the length of interconnecting cable between two non-perfect components.

Werlatone Absorptive Filters Eliminate:

- Instability of power amplifiers at out-of-band frequencies.
- Excessive In-Band ripples due to out-of-band reflected energies.
- False trigger of power detector circuitry due to reflected harmonics.
- Potential damage to power amplifiers due to reflection of high power out-of-band energies.

Model	Frequency (MHz)			Power (W CW)		Insertion Loss(dB)	Rejection(dB)	VSWR	
	Pass Band	3dB Corner	Stop Band	Pass Band	Stop Band	Pass Band	Stop Band	Pass Band	Stop Band
AF9673	1-2.7	3.5	3.9-32	1,200	150	0.4	50	1.40:1	1.40:1
AF9438	1-30	32	50-380	5,000	250	0.5	50	1.30:1	1.60:1
AF9349	10-150	200	270-1500	500	25	0.4	50	1.35:1	1.60:1
AF9255	10-170	220	300-1500	50	10	0.6	50	1.25:1	1.60:1
AF9187	10-490	620	850-3000	100	10	0.5	45	1.40:1	1.90:1
AF9350	10-500	540	750-3000	400	25	0.5	45	1.25:1	1.60:1
AF9960	10-500	540	750-3000	600	25	0.5	45	1.25:1	1.60:1
AF9680	10-520	540	1040-3000	160	10	0.6	60	1.25:1	1.60:1
AF9313	10-870	1340	1700-4000	100	10	0.6	53	1.30:1	1.60:1

* Specifications are for reference only and subject to change without notice.